CENTER for BIOLOGICAL DIVERSITY Because life is good.

February 5, 2015

Jeanine Townsend, Clerk to the Board
State Water Resources Control Board
P.O. Box 100
Sacramento, CA 95812-2000
commentletters@waterboards.ca.gov

Re: Comment Letter—303(d) List portion of the 2012 California Integrated Report

The State Water Resources Control Board has failed to adequately consider ocean acidification in its water quality assessment. The proposed Integrated Report is devoid of any mention of ocean acidification. This runs counter to EPA's recommendations and the requirements of the Clean Water Act.

California has failed to identify waters impaired by ocean acidification, and data submitted by the Center was not evaluated by the State Water Board. California waters are especially vulnerable to ocean acidification, and scientists have already documented corrosive waters and biological impacts off the California coast.

Ocean acidification is caused by increasing carbon dioxide (CO_2) emissions and land use changes. Seawater absorbs CO_2, causing a chemical reaction that reduces seawater pH and makes the oceans more acidic. Anthropogenic sources of carbon dioxide have caused a thirty percent increase in ocean acidity globally. While carbon emissions are the main driver of ocean acidification, regional factors also have significant effects. These local contributions include agricultural runoff, erosion, polluted stormwater, river discharges and local emissions of nitrogen oxides, and sulfur oxides.

Acidified ocean waters seriously harm marine wildlife and the entire ocean ecosystem. When CO_2 concentrations in seawater increase, the availability of carbonate ions decreases, making it more difficult for marine organisms to form, build, and maintain the calcium carbonate shells and skeletons required for their survival. As seawater becomes more corrosive, it can kill fish eggs and inhibit the development of, and essentially dissolve, the shells of small crustaceans, baby shellfish, and other tiny creatures at the base of the food web. Ocean acidification also harms and stresses fish, squid, and other animals that do not build shells. Not only does ocean acidification directly threaten various types of marine animals, it also has implications for the broader marine environment and food web.

In previous comments, the Center has provided significant information and supporting materials about the impacts of ocean acidification on the California coast. As shown in the record for this draft integrated report, on February 27, 2007, the Center for Biological Diversity submitted scientific information supporting the inclusion of ocean waters on California's 303(d) list to each of the coastal regional water boards. I was informed that the regional board deferred action on ocean acidification to the State Water Resources Control Board. On June 11, 2008; February 4, 2009, May 28, 2010; August 27, 2010, and April 16, 2014 the Center submitted additional information and comments on ocean acidification for consideration in the water quality assessment. Those comments are incorporated here by reference and are available upon request. Since then, it has become more apparent that ocean acidification poses a serious threat to seawater quality with adverse effects on marine life.

The State Water Resources Control Board must solicit and evaluate data on ocean acidification for its water quality assessment, and it should identify water segments that are violating water quality standards -- including designated uses, numeric, and narrative criteria — as threatened or impaired.

1. California Must Evaluate its Own Data and Solicit it from Research Organizations

California has an independent duty to evaluate ocean acidification during its water quality assessment (Environmental Protection Agency 2010). Specifically, EPA directed states to evaluate ocean acidification data for their 2012 integrated reports (Environmental Protection Agency 2010). The Clean Water Act provides that states must "evaluate all existing and readily available water quality-related data and information to develop the list." 40 C.F.R. § 130.7(b)(5); *see also Sierra Club v. Leavitt*, 488 F.3d 904 (11th Cir. 2007). Beyond reviewing the information submitted by the Center, California must also evaluate pH, biological information, and other monitoring data that is available to it and seek out ocean acidification data from state, federal, and academic research institutions. EPA's 2010 memo and Integrated Report Guidance discussed several sources, including the National Oceanic and Atmospheric Administration data (EPA 2010: 7-9; EPA Guidance 30-31). There are now several sources for high resolution ocean acidification data. California must obtain and evaluate data from research institutions, including but not limited to:

- CEDEN, California's Water Quality Repository http://www.ceden.org/
- BCO-DMO, Biological and Chemical Oceanography Data Management Office http://www.bco-dmo.org/data
- California Current Long Term Ecosystem Monitoring http://oceaninformatics.ucsd.edu/datazoo/data/ccelter/datasets
- PMEL NOAA http://www.pmel.noaa.gov/
- National Ocean Data Center http://www.nodc.noaa.gov/
- Integrated Ocean Observing System http://www.ioos.noaa.gov/
- Central & Northern California Ocean Observing System http://www.cencoos.org/
- Monterey Bay Aquarium Research Institute
- Scripps Institution of Oceanography
- West Coast Ocean Acidification and Hypoxia Science Panel http://westcoastoah.org
- California Current Acidification Network http://c-can.msi.ucsb.edu/

For example, the enclosed dataset from the Santa Barbara Channel long term ecological research site must be evaluated (Hoffmann 2014) (available at http://sbc.lternet.edu//data/index.html).

California has failed to meet the Clean Water Act's requirements to evaluate all readily accessible data and information on ocean acidification. To correct its integrated report and 303(d) list, the Board needs to obtain and evaluate all relevant parameters of ocean acidification data available from these sources that serve as clearinghouses for ocean acidification data, especially those that are specific to California's waters.

2. California Should List Ocean Waters as Impaired

The State Water Board must evaluate whether any of California's ocean waters must be included on the 303(d) list because current measures are not stringent enough to prevent ocean acidification and achieve water quality standards. 33 U.S.C. § 1313(d).

The Clean Water Act requires that California protect the water quality for designated uses of its waters. California's Ocean Plan defines the designated uses of ocean waters:

> The beneficial uses of the ocean waters of the State that shall be protected include industrial water supply; water contact and non-contact recreation, including aesthetic enjoyment; navigation; commercial and sport fishing; mariculture; preservation and enhancement of designated Areas of Special Biological Significance (ASBS); rare and endangered species; marine habitat; fish migration; fish spawning and shellfish harvesting.

California Ocean Plan at 3 (2012). These uses are not being attained by ocean waters off California due to ocean acidification.

California must consider ocean acidification data in light of designated uses and applicable standards. The standards for chemical and biological characteristics require that:

- The pH shall not be changed at any time more than 0.2 units from that which occurs naturally.
- Marine communities, including vertebrate, invertebrate, and plant species, shall not be degraded.
- The natural taste, odor, and color of fish, shellfish, or other marine resources used for human consumption shall not be altered.[1]
- The concentration of organic materials in fish, shellfish or other marine resources used for human consumption shall not bioaccumulate to levels that are harmful to human health.

[1] There are also indications that the taste of shellfish is adversely impacted by ocean acidification (Dupont et al. 2014).

Ocean plan at 6 & 10. Finally, California's antidegradation policy requires the maintenance of existing high quality. Resolution 68-16. Ocean acidification is causing violations of these standards in certain waters of California.

While the state has failed to evaluate ocean acidification data, the Center's prior submissions indicate water quality problems and violations of the above standards that warrant listing. Without repeating former comments, I will urge the state to evaluate the Center's submissions as well as publicly available monitoring data on ocean acidification. Moreover, this comment focuses on new scientific data that underscores the fact that these standards are already not being attained.

Shellfish in the California Current large marine ecosystem have experienced massive mortality during this water quality assessment period. Hatcheries and natural shellfish have experienced reproduction failures from California to Washington (Feely et al. 2012). A new study by Waldbusser et al. identified aragonite saturation as the factor causing limited growth and mortality for shellfish (Waldbusser & Hales 2014). Pacific oyster larvae in hatcheries in the Pacific Northwest experienced massive mortality due to ocean acidification (Barton et al. 2012). The Waldbusser follow-up study identifies saturation state as the principal cause of the adverse biological impacts (Waldbusser & Hales 2014). Notably, California already experiences levels of aragonite undersaturation that have been linked to harmful effects in shellfish (Feely et al. 2008; Gruber et al. 2012; Hauri et al. 2013). Such conditions in experiments caused a forty percent increase in deformities and death of rare northern abalone (Crim et al. 2011). Another study of Olympia oysters, a foundation species along the coast, showed that ocean acidification stunted their growth (Hettinger et al. 2012). California mussels also grew thinner and weaker shells that are more vulnerable to mortality, predation, and desiccation (Gaylord et al. 2011).

Off of California's coast, scientists have documented harmful biological consequences in marine communities of plankton. In a recent study of pteropods in the California Current (Bednaršek et al. 2014), scientists found 53% of onshore individuals and 24% of offshore individuals to have severe dissolution damage that was correlated positively with the percentage of undersaturated water with respect to aragonite (*id*.). Further, scientists estimate that shell damage due to ocean acidification has doubled in near shore habitats since pre-industrial conditions and will triple by 2050 (*id*.). Because pteropods form the base of the foodweb, providing food for many species of fish, a decline in pteropods could have far-reaching ecosystem impacts.

Additionally, ocean acidification has likely increased the toxicity of harmful algal blooms in Southern California that have both caused objectionable aquatic growth and concentrated toxins in seafood that are harmful to human health. The toxicity of harmful algal blooms increases with ocean acidification. Ocean acidification conditions can increase toxins as much as five-fold in harmful algae that can poison marine mammals and even cause paralytic shellfish poisoning in people (Fu et al. 2012; Avery O Tatters et al. 2013; Tatters et al. 2012; Avery O. Tatters et al. 2013). The neurotoxin domoic acid in diatom *Pseudo-nitzschia* increased with acidification as did the toxicity of *Alexandrium catenella* (Id.). A -0.5pH change caused toxin production in the diatoms to increase 4.2-fold and a -0.3pH unit change increased the toxicity 2.5-fold (Tatters et al. 2012). The experiments done in these studies were at levels of CO_2 that

are already occurring in California, and the increase in the toxicity of harmful algal blooms in Southern California may be consistent with ocean acidification (Id.) Already, these harmful algal blooms have been related to mass mortalities of fish and marine mammals and these studies suggest that the damage will become much worse.

While these are a few new studies highlighted, the body of science previously submitted plus the data sets recommended herein provide ample information on ocean acidification for California to evaluate against its water quality standards. A failure to do so undermines the intent and provisions of the Clean Water Act.

* * *

In conclusion, California must thoroughly evaluate ocean acidification data and identify undersaturated waters and others that are not meeting water quality standards as threatened or impaired. It is imperative that the state take action now on ocean acidification to address this important water quality problem before it has devastating consequences on its fisheries and ecosystems.

Sincerely,

/s/ Miyoko Sakashita
Miyoko Sakashita
miyoko@biologicaldiversity.org

enclosure

Barton, A. et al., 2012. The Pacific oyster, Crassostrea gigas, shows negative correlation to naturally elevated carbon dioxide levels: Implications for near-term ocean acidification effects. *Limnology and Oceanography*, 57(3), pp.698–710.

Bednaršek, N. et al., 2014. Limacina helicina shell dissolution as an indicator of declining habitat suitability owing to ocean acidification in the California Current Ecosystem Limacina helicina shell dissolution as an indicator of declining habitat suitability owing to ocean acidi. *Proc. R. Soc. B*, 281, p.20140123.

Crim, R.N., Sunday, J.M. & Harley, C.D.G., 2011. Elevated seawater CO2 concentrations impair larval development and reduce larval survival in endangered northern abalone (Haliotis kamtschatkana). *Journal of Experimental Marine Biology and Ecology*, 400(1-2), pp.272–277.

Dupont, S. et al., 2014. First Evidence of Altered Sensory Quality in a Shellfish Exposed to Decreased pH Relevant to Ocean Acidification. *Journal of Shellfish Research*, 33(3), pp.857–861.

Environmental Protection Agency, 2010. Memo: Integrated reporting and listing decisions related to ocean acidification.

Feely, R.A. et al., 2008. Evidence for upwelling of corrosive “acidified” water onto the continental shelf. *Science*, 320(5882), pp.1490–2.

Feely, R.A., Klinger, T. & Newton, J.A., 2012. *Scientific Summary of Ocean Acidification in Washington State Marine Waters*,

Fu, F., Tatters, A. & Hutchins, D., 2012. Global change and the future of harmful algal blooms in the ocean. *Marine Ecology Progress Series*, 470, pp.207–233.

Gaylord, B. et al., 2011. Functional impacts of ocean acidification in an ecologically critical foundation species. *The Journal of experimental biology*, 214(Pt 15), pp.2586–94.

Gruber, N. et al., 2012. Rapid progression of ocean acidification in the California Current System. *Science (New York, N.Y.)*, 337(6091), pp.220–3.

Hauri, C. et al., 2013. The intensity, duration, and severity of low aragonite saturation state events on the California continental shelf. *Geophysical Research Letters*, 40(13), pp.3424–3428.

Hettinger, A., Sanford, E. & Hill, T., 2012. Persistent carry-over effects of planktonic exposure to ocean acidification in the Olympia oyster. *Ecology*, In press.

Hofmann, G. E. , C. Blanchette, U. Passow, L. Washburn, J. Lunden, E. Rivest and L. Kapsenberg. 2014. SBC LTER: pH time series: Water-sample pH and CO2 system chemistry, ongoing since 2011. Santa Barbara Coastal LTER. knb-lter-sbc.75.1 (http://metacat.lternet.edu/knb/metacat/knb-lter-sbc.75.1/lter).

Tatters, A.O. et al., 2013. diatom community to acidification and warming Short- and long-term conditioning of a temperate marine diatom community to acidification and warming.

Tatters, A.O. et al., 2013. High CO2 promotes the production of paralytic shellfish poisoning toxins by Alexandrium catenella from Southern California waters. *Harmful Algae*, 30, pp.37–43.

Tatters, A.O., Fu, F.-X. & Hutchins, D. a, 2012. High CO2 and silicate limitation synergistically increase the toxicity of Pseudo-nitzschia fraudulenta. *PloS one*, 7(2), p.e32116.

Waldbusser, G. & Hales, B., 2014. Saturation-state sensitivity of marine bivalve larvae to ocean acidification. *Nature Climate Change*, (December).

Site	Time_stam	Latitude_N	Longitude_	Salinity_CC	Temperatu	Pressure_d	Total_P_CC	Total_Si_C
ALE	2011-07-2	-120.29	34.4618	33.2	25	0	0	0
ALE	2011-07-2	-120.29	34.4618	33.2	25	0	0	0
PUR	2011-07-2	-120.627	34.7265	33.1	25	0	0	0
LOL	2011-08-3	-120.609	34.7188	33.2	25	0	0	0
PUR	2011-09-1	-120.627	34.7265	33.1	25	0	0	0
LOL	2011-06-0	-120.609	34.7188	34.1	25	0	0	0
PUR	2011-09-2	-120.627	34.7265	33.4	25	0	0	0
ALE	2011-09-2	-120.29	34.4618	33.2	25	0	0	0
ALE	2011-10-1	-120.29	34.4618	33	25	0	0	0
LOL	2011-10-2	-120.609	34.7188	33.1	25	0	0	0
LOL	2011-10-2	-120.609	34.7188	33.1	25	0	0	0
ALE	2011-10-2	-120.29	34.4618	33.3	25	0	0	0
PUR	2011-10-2	-120.627	34.7265	33.2	25	0	0	0
ALE	2011-11-2	-120.29	34.4618	33.1	25	0	0	0
PUR	2011-11-2	-120.627	34.7265	33.2	25	0	0	0
LOL	2011-12-1	-120.609	34.7188	33.3	25	0	0	0
LOL	2011-12-0	-120.609	34.7188	33.1	25.4	0	0	0
PUR	2012-04-2	-120.627	34.7265	33.4	25.6	0	0	0
LOL	2012-03-0	-120.609	34.7188	33.5	25.3	0	0	0
ALE	2012-02-0	-120.29	34.4618	33	25.37	0	0	0
LOL	2012-02-2	-120.609	34.7188	33.4	25.43	0	0	0
LOL	2012-05-0	-120.609	34.7188	33.5	25.4	0	0	0
MKO	2012-06-0	-119.73	34.3932	33.3	25.3	0	0	0
LOL	2012-06-2	-120.609	34.7188	33.3	25.37	0	0	0
ALE	2012-06-2	-120.29	34.4618	33.2	25.37	0	0	0
ALE	2012-04-2	-120.29	34.4618	33.4	25	0	0	0
PUR	2012-06-1	-120.627	34.7265	33.2	25.07	0	0	0
MKO	2012-06-2	-119.73	34.3932	33.1	25.1	0	0	0
LOL	2012-01-2	-120.609	34.7188	33.1	25.3	0	0	0
LOL	2012-07-0	-120.609	34.7188	33.4	25.43	0	0	0
PUR	2012-08-1	-120.627	34.7265	33.3	25.33	0	0	0
LOL	2012-08-0	-120.609	34.7188	33.3	25.03	0	0	0
MKO	2012-08-0	-119.73	34.3932	33.2	25	0	0	0
ALE	2012-08-1	-120.29	34.4618	33.2	25.17	0	0	0
LOL	2012-08-3	-120.609	34.7188	33.3	25.4	0	0	0
ARQ	2012-10-1	-120.12	34.465	33.1	25.7	0	0	0
ARQ	2013-01-1	-120.12	34.465	33.2	25.8	0	0	0
RZR	2013-01-2	-120.278	34.4672	32.1	25.9	0	0	0
MKO	2012-02-1	-119.73	34.3932	33.1	25.4	0	0	0
MKO	2013-01-2	-119.73	34.3932	33.2	25.7	0	0	0
PUR	2012-09-2	-120.627	34.7265	33	25.6	0	0	0
PUR	2012-11-0	-120.627	34.7265	33.2	25.5	0	0	0
LOL	2012-10-1	-120.609	34.7188	33	25.1	0	0	0
LOL	2012-12-1	-120.609	34.7188	33.2	25	0	0	0
LOL	2012-12-1	-120.609	34.7188	33.1	25.1	0	0	0
ALE	2012-10-1	-120.29	34.4618	33	25.5	0	0	0

LOL	2013-02-0	-120.609	34.7188	33.1	25.1	0	0	0
LOL	2013-02-0	-120.609	34.7188	33	25.2	0	0	0
RZR	2013-01-2	-120.278	34.4672	32.9	25.6	0	0	0
RZR	2013-02-1	-120.278	34.4672	33.1	25.2	0	0	0
RZR	2013-02-1	-120.278	34.4672	33.1	25.1	0	0	0
RZR	2013-02-2	-120.278	34.4672	33.2	25.07	0	0	0
RZR	2013-02-2	-120.278	34.4672	33.2	25.27	0	0	0
ALE	2013-03-2	-120.29	34.4618	33.2	25.17	0	0	0
LOL	2013-02-2	-120.609	34.7188	33.2	25.23	0	0	0
LOL	2013-02-2	-120.609	34.7188	33.3	25.23	0	0	0
ARQ	2013-04-0	-120.12	34.465	33.2	25.5	0	0	0
MKO	2013-04-0	-119.73	34.3932	33	25.4	0	0	0
ALE	2013-03-2	-120.29	34.4618	33.2	25.5	0	0	0
RZR	2013-04-0	-120.278	34.4672	33.3	25.4	0	0	0
RZR	2013-04-0	-120.278	34.4672	33.3	25.4	0	0	0
LOL	2013-04-0	-120.609	34.7188	33.3	25.3	0	0	0
LOL	2013-04-0	-120.609	34.7188	33.3	25.3	0	0	0
ALE	2013-04-2	-120.29	34.4618	33.3	25.2	0	0	0
RZR	2013-04-2	-120.278	34.4672	33.5	25.4	0	0	0
LOL	2013-04-3	-120.609	34.7188	33.5	25.4	0	0	0
LOL	2013-04-3	-120.609	34.7188	33.4	25.2	0	0	0
MKO	2013-05-0	-119.73	34.3932	33.2	25.3	0	0	0
MKO	2013-05-0	-119.73	34.3932	33.3	25.7	0	0	0
ARQ	2013-05-0	-120.12	34.465	33.3	25.7	0	0	0
ARQ	2013-06-1	-120.12	34.465	33.1	26.2	0	0	0
ALE	2013-06-1	-120.29	34.4618	33.3	25.93	0	0	0
LOL	2013-05-2	-120.609	34.7188	33.1	25.33	0	0	0
LOL	2013-06-2	-120.609	34.7188	33.4	25.3	0	0	0
LOL	2013-06-2	-120.609	34.7188	33.3	25.4	0	0	0
ARQ	2013-07-1	-120.12	34.465	33	25.3	0	0	0
MKO	2013-07-1	-119.73	34.3932	33.1	25.27	0	0	0
COP	2013-07-2	-119.878	34.4067	33	25.17	0	0	0
LOL	2013-07-2	-120.609	34.7188	33.1	25.3	0	0	0
MKO	2013-08-0	-119.73	34.3932	33.2	24.97	0	0	0
MKO	2013-08-0	-119.73	34.3932	33.2	25.23	0	0	0
ARQ	2013-08-0	-120.12	34.465	33.3	25.17	0	0	0
RZR	2013-08-2	-120.278	34.4672	33.2	25.1	0	0	0
RZR	2013-08-2	-120.278	34.4672	33.3	24.97	0	0	0
PUR	2013-08-2	-120.627	34.7265	33.3	25.53	0	0	0
ALE	2013-08-2	-120.29	34.4618	33.2	25.43	0	0	0
COP	2013-08-2	-119.878	34.4067	33	25.3	0	0	0
LOL	2013-08-2	-120.609	34.7188	33.3	24.93	0	0	0
LOL	2013-08-2	-120.609	34.7188	33.2	25.17	0	0	0
LOL	2013-05-2	-120.609	34.7188	33.4	25.03	0	0	0
LOL	2013-05-2	-120.609	34.7188	33.3	25.2	0	0	0
LOL	2013-10-0	-120.609	34.7188	33.1	25.1	0	0	0
LOL	2013-10-0	-120.609	34.7188	33.3	25.1	0	0	0

COP	2013-10-0	-119.878	34.4067	33.2	25.17	0	0	0
COP	2013-10-0	-119.878	34.4067	33.1	25.3	0	0	0
ARQ	2013-10-1	-120.12	34.465	33.1	25.07	0	0	0
MKO	2013-10-1	-119.73	34.3932	33.1	25.23	0	0	0
ALE	2013-10-1	-120.29	34.4618	33.1	25.17	0	0	0
PUR	2013-10-1	-120.627	34.7265	33.1	25.23	0	0	0
RMC	2013-10-1	-121.073	35.5224	33.3	25.37	0	0	0
RMC	2013-10-1	-121.073	35.5224	33.1	25.3	0	0	0
LOL	2013-11-0	-120.609	34.7188	33.1	25.3	0	0	0
LOL	2013-11-0	-120.609	34.7188	33.1	25.2	0	0	0
MKO	2013-11-0	-119.73	34.3932	33.2	25.2	0	0	0
MKO	2013-11-0	-119.73	34.3932	33.2	25.23	0	0	0
ARQ	2013-11-0	-120.12	34.465	33.1	25.27	0	0	0
ARQ	2013-11-0	-120.12	34.465	33.1	25.3	0	0	0
MKO	2013-12-0	-119.73	34.3932	33.2	25.17	0	0	0
ARQ	2013-12-0	-120.12	34.465	33.2	25.1	0	0	0
MKO	2013-12-0	-119.73	34.3932	33.2	25.13	0	0	0
LOL	2013-12-1	-120.609	34.7188	33.2	25.17	0	0	0
LOL	2013-12-1	-120.609	34.7188	33.1	25.1	0	0	0
MKO	2014-01-0	-119.73	34.3932	33.1	25.17	0	0	0
ARQ	2014-02-0	-120.12	34.465	33	25.13	0	0	0
MKO	2014-02-0	-119.73	34.3932	33.2	25.13	0	0	0
LOL	2014-02-1	-120.609	34.7188	33.2	25.33	0	0	0
LOL	2014-02-1	-120.609	34.7188	33.1	25.27	0	0	0
MKO	2014-02-1	-119.73	34.3932	32.9	25.02	0	0	0
MKO	2014-02-1	-119.73	34.3932	32.9	25.01	0	0	0
ARQ	2014-03-1	-120.12	34.465	32.8	24.98	0	0	0
MKO	2014-03-1	-119.73	34.3932	32.8	25.01	0	0	0
LOL	2014-03-2	-120.609	34.7188	33.2	25.02	0	0	0
LOL	2014-03-2	-120.609	34.7188	33.2	25.02	0	0	0
MKO	2014-04-1	-119.73	34.3932	33.1	25.03	0	0	0
ARQ	2014-04-1	-120.12	34.465	33.1	25.03	0	0	0
LOL	2014-04-2	-120.609	34.7188	33.5	25.1	0	0	0
LOL	2014-04-2	-120.609	34.7188	33.5	25.1	0	0	0
MKO	2014-04-1	-119.73	34.3932	33.3	24.8	0	0	0
LOL	2014-05-2	-120.609	34.7188	33.3	24.8	0	0	0
LOL	2014-05-2	-120.609	34.7188	33.2	24.6	0	0	0
ARQ	2014-06-0	-120.12	34.465	33.3	24.9	0	0	0
MKO	2014-06-1	-119.73	34.3932	33.2	24.9	0	0	0
MKO	2014-06-0	-119.73	34.3932	33.2	24.9	0	0	0
LOL	2014-06-1	-120.609	34.7188	33.3	25.2	0	0	0
LOL	2014-06-1	-120.609	34.7188	33.3	25.2	0	0	0
SBH	2012-10-1	-119.685	34.41	33.52	25	0	0	0
SBH	2012-10-2	-119.685	34.41	33.31	25	0	0	0
SBH	2012-11-0	-119.685	34.41	33.55	25	0	0	0
SBH	2012-11-0	-119.685	34.41	33.5	25	0	0	0
SBH	2012-11-1	-119.685	34.41	33.5	25	0	0	0

SBH	2012-11-2	-119.685	34.41	33.4	25	0	0	0
SBH	2012-11-2	-119.685	34.41	33.2	25	0	0	0
SBH	2012-12-0	-119.685	34.41	33.4	25	0	0	0
SBH	2012-12-0	-119.685	34.41	33.4	25	0	0	0
SBH	2012-12-1	-119.685	34.41	33.5	25	0	0	0
SBH	2012-12-1	-119.685	34.41	33.4	25	0	0	0
SBH	2013-01-0	-119.685	34.41	33.48	25	0	0	0
SBH	2013-01-0	-119.685	34.41	33.48	25	0	0	0
SBH	2013-01-0	-119.685	34.41	33.48	25	0	0	0
SBH	2013-01-1	-119.685	34.41	33.5	25	0	0	0
SBH	2013-01-2	-119.685	34.41	33.5	25	0	0	0
SBH	2013-02-0	-119.685	34.41	33.4	25	0	0	0
SBH	2013-02-0	-119.685	34.41	33.4	25	0	0	0
SBH	2013-02-0	-119.685	34.41	33.4	25	0	0	0
SBH	2013-02-1	-119.685	34.41	33.5	25	0	0	0
SBH	2013-02-2	-119.685	34.41	33.5	25	0	0	0
SBH	2013-03-0	-119.685	34.41	33.5	25	0	0	0
SBH	2013-03-0	-119.685	34.41	33.5	25	0	0	0
SBH	2013-03-0	-119.685	34.41	33.5	25	0	0	0
SBH	2013-03-1	-119.685	34.41	33.5	25	0	0	0
SBH	2013-03-1	-119.685	34.41	33.5	25	0	0	0
SBH	2013-03-2	-119.685	34.41	33.5	25	0	0	0
SBH	2013-04-0	-119.685	34.41	33.4	25	0	0	0
SBH	2013-04-0	-119.685	34.41	33.4	25	0	0	0
SBH	2013-04-1	-119.685	34.41	33.7	25	0	0	0
SBH	2013-04-1	-119.685	34.41	33.6	25	0	0	0
SBH	2013-04-2	-119.685	34.41	33.6	25	0	0	0
SBH	2013-05-0	-119.685	34.41	33.6	25	0	0	0
SBH	2013-05-0	-119.685	34.41	33.6	25	0	0	0
SBH	2013-05-1	-119.685	34.41	33.5	25	0	0	0
SBH	2013-05-1	-119.685	34.41	33.5	25	0	0	0
SBH	2013-05-2	-119.685	34.41	33.5	25	0	0	0
SBH	2013-05-3	-119.685	34.41	33.4	25	0	0	0
SBH	2013-06-0	-119.685	34.41	33.4	25	0	0	0
SBH	2013-06-0	-119.685	34.41	33.4	25	0	0	0
SBH	2013-06-1	-119.685	34.41	33.4	25	0	0	0
SBH	2013-06-2	-119.685	34.41	33.5	25	0	0	0
SBH	2013-06-2	-119.685	34.41	33.4	25	0	0	0
SBH	2013-07-0	-119.685	34.41	33.5	25	0	0	0
SBH	2013-07-1	-119.685	34.41	33.3	25	0	0	0
SBH	2013-07-2	-119.685	34.41	33.3	25	0	0	0
SBH	2013-08-0	-119.685	34.41	33.1	25	0	0	0
SBH	2013-08-0	-119.685	34.41	33.1	25	0	0	0
SBH	2013-08-1	-119.685	34.41	33.1	25	0	0	0
SBH	2013-08-2	-119.685	34.41	33.1	25	0	0	0
SBH	2013-08-2	-119.685	34.41	33.1	25	0	0	0
SBH	2013-10-2	-119.685	34.41	33	25	0	0	0

SBH	2013-10-3	-119.685	34.41	32.9	25	0	0	0
SBH	2013-11-0	-119.685	34.41	33.6	25	0	0	0
SBH	2013-11-1	-119.685	34.41	33.6	25	0	0	0
SBH	2013-11-2	-119.685	34.41	33.5	25	0	0	0
SBH	2013-12-0	-119.685	34.41	33.5	25	0	0	0
SBH	2013-12-1	-119.685	34.41	33.5	25	0	0	0
SBH	2014-01-1	-119.685	34.41	33.5	25	0	0	0
SBH	2014-02-0	-119.685	34.41	33.4	25	0	0	0

TA_CO2cal	TCO2_CO2	pH_CO2cal	fCO2_CO2c	pCO2_CO2	TA_CO2cal	TCO2_CO2	pH_CO2cal	fCO2_CO2c
2228.5	-9999	7.96	-9999	-9999	2228.5	1993.7	7.96	494.04
2232.8	-9999	7.929	-9999	-9999	2232.8	2013.1	7.929	538.67
2232.4	-9999	7.896	-9999	-9999	2232.4	2029.2	7.896	589.28
2217.3	-9999	7.742	-9999	-9999	2217.3	2080.5	7.742	877.36
2217.2	-9999	7.959	-9999	-9999	2217.2	1984.3	7.959	493.24
2197.1	-9999	7.535	-9999	-9999	2197.1	2131.5	7.535	1460.85
2227.2	-9999	7.968	-9999	-9999	2227.2	1987	7.968	482.11
2227	-9999	7.949	-9999	-9999	2227	1997.8	7.949	508.76
2229.7	-9999	7.957	-9999	-9999	2229.7	1997.6	7.957	499.32
2138.4	-9999	7.611	-9999	-9999	2138.4	2052.1	7.611	1182.1
2137.4	-9999	7.626	-9999	-9999	2137.4	2046.1	7.626	1137.64
2227.1	-9999	7.91	-9999	-9999	2227.1	2016.3	7.91	565.08
2228.6	-9999	7.877	-9999	-9999	2228.6	2033.8	7.877	618.44
2223.1	-9999	7.915	-9999	-9999	2223.1	2011.5	7.915	557.47
2211.7	-9999	7.858	-9999	-9999	2211.7	2026.5	7.858	645.53
2223.7	-9999	7.719	-9999	-9999	2223.7	2095.2	7.719	933.09
2211	-9999	7.654	-9999	-9999	2211	2105.9	7.654	1098
2255.5	-9999	7.725	-9999	-9999	2255.5	2119.7	7.725	932.55
2190.9	-9999	7.656	-9999	-9999	2190.9	2084.6	7.656	1079.07
2225	-9999	7.833	-9999	-9999	2225	2049	7.833	695.43
2166.9	-9999	7.555	-9999	-9999	2166.9	2095.7	7.555	1378.02
2251.6	-9999	7.254	-9999	-9999	2251.6	2277.2	7.254	2990.8
2244.2	-9999	7.903	-9999	-9999	2244.2	2033.7	7.903	580.46
2187.3	-9999	7.22	-9999	-9999	2187.3	2223.4	7.22	3154.59
2241.7	-9999	7.732	-9999	-9999	2241.7	2105.8	7.732	911.08
2251.5	-9999	7.792	-9999	-9999	2251.5	2091.9	7.792	781.31
2241.9	-9999	7.925	-9999	-9999	2241.9	2023.1	7.925	546.85
2241.3	-9999	7.915	-9999	-9999	2241.3	2027.7	7.915	562.18
2192.5	-9999	7.685	-9999	-9999	2192.5	2077.2	7.685	1005.67
2209.4	-9999	7.245	-9999	-9999	2209.4	2237.3	7.245	3000.47
2246.3	-9999	7.681	-9999	-9999	2246.3	2129.7	7.681	1040.02
2230.2	-9999	7.208	-9999	-9999	2230.2	2272.7	7.208	3305.5
2252.9	-9999	7.884	-9999	-9999	2252.9	2053.4	7.884	613.79
2246.8	-9999	7.936	-9999	-9999	2246.8	2021.5	7.936	531.93
2261.7	-9999	7.151	-9999	-9999	2261.7	2323.9	7.151	3848.3
2236.7	-9999	7.905	-9999	-9999	2236.7	2024.1	7.905	576.34
2241.8	-9999	7.757	-9999	-9999	2241.8	2093.4	7.757	854.51
2146.5	-9999	7.714	-9999	-9999	2146.5	2023.4	7.714	921.66
2227.1	-9999	7.758	-9999	-9999	2227.1	2081.8	7.758	846.73
2236	-9999	7.753	-9999	-9999	2236	2090.2	7.753	861.06
2224.1	-9999	7.732	-9999	-9999	2224.1	2088.7	7.732	905.51
2234.6	-9999	7.886	-9999	-9999	2234.6	2032	7.886	605.49
2199.5	-9999	7.803	-9999	-9999	2199.5	2039.2	7.803	743.58
2188.6	-9999	7.784	-9999	-9999	2188.6	2036.2	7.784	776.18
2219	-9999	7.873	-9999	-9999	2219	2026.5	7.873	622.88
2229.9	-9999	7.901	-9999	-9999	2229.9	2021.7	7.901	581.31

2222.4	-9999	7.762	-9999	-9999	2222.4	2077.4	7.762	835.78
2193.9	-9999	7.827	-9999	-9999	2193.9	2023.2	7.827	696.3
2228.8	-9999	7.78	-9999	-9999	2228.8	2074.3	7.78	801.68
2235.6	-9999	7.776	-9999	-9999	2235.6	2083.7	7.776	810.88
2239.6	-9999	7.8	-9999	-9999	2239.6	2078.1	7.8	762.86
2236.7	-9999	7.793	-9999	-9999	2236.7	2077.9	7.793	775.28
2241.8	-9999	7.839	-9999	-9999	2241.8	2061.8	7.839	688.59
2247.3	-9999	7.92	-9999	-9999	2247.3	2029.8	7.92	555.66
2210.9	-9999	7.709	-9999	-9999	2210.9	2085.9	7.709	952.89
2245	-9999	7.738	-9999	-9999	2245	2107	7.738	897.53
2243.5	-9999	7.876	-9999	-9999	2243.5	2045	7.876	624.51
2250.8	-9999	7.861	-9999	-9999	2250.8	2060.6	7.861	653.3
2239.1	-9999	7.938	-9999	-9999	2239.1	2010.9	7.938	527.11
2259.8	-9999	7.76	-9999	-9999	2259.8	2111.3	7.76	853.71
2248.3	-9999	7.817	-9999	-9999	2248.3	2076.2	7.817	731.49
2178.3	-9999	7.737	-9999	-9999	2178.3	2043	7.737	872.63
2221.6	-9999	7.942	-9999	-9999	2221.6	1993.5	7.942	516.73
2239.2	-9999	7.956	-9999	-9999	2239.2	2003.4	7.956	501.43
2235.7	-9999	7.855	-9999	-9999	2235.7	2046.3	7.855	656.5
2222.3	-9999	7.541	-9999	-9999	2222.3	2154.7	7.541	1463.05
2220.8	-9999	7.703	-9999	-9999	2220.8	2097	7.703	970.68
2237.4	-9999	7.946	-9999	-9999	2237.4	2006.8	7.946	515.36
2241.3	-9999	7.878	-9999	-9999	2241.3	2040.1	7.878	620.04
2243.5	-9999	7.912	-9999	-9999	2243.5	2025.8	7.912	566.29
2240.9	-9999	7.935	-9999	-9999	2240.9	2009.6	7.935	532.21
2245.9	-9999	7.942	-9999	-9999	2245.9	2011.4	7.942	522.42
2236.5	-9999	7.816	-9999	-9999	2236.5	2067	7.816	730.59
2203.8	-9999	7.285	-9999	-9999	2203.8	2219	7.285	2716.44
2249.3	-9999	7.842	-9999	-9999	2249.3	2066.1	7.842	684.98
2233.1	-9999	7.928	-9999	-9999	2233.1	2013	7.928	541.17
2241.7	-9999	7.944	-9999	-9999	2241.7	2012.6	7.944	519.7
2325.6	-9999	7.433	-9999	-9999	2325.6	2295.4	7.433	2005.03
2214.7	-9999	7.36	-9999	-9999	2214.7	2206.9	7.36	2280.33
2240.1	-9999	7.974	-9999	-9999	2240.1	1997.4	7.974	477.98
2242.5	-9999	7.926	-9999	-9999	2242.5	2022	7.926	545.5
2247.4	-9999	7.951	-9999	-9999	2247.4	2013.9	7.951	510.29
2308.4	-9999	7.519	-9999	-9999	2308.4	2249.3	7.519	1607.49
2306.7	-9999	7.512	-9999	-9999	2306.7	2250.2	7.512	1632.72
2245.1	-9999	7.969	-9999	-9999	2245.1	1999.7	7.969	485.06
2253.1	-9999	7.95	-9999	-9999	2253.1	2018.3	7.95	513.42
2299.7	-9999	7.518	-9999	-9999	2299.7	2240.9	7.518	1608.43
2234.2	-9999	7.275	-9999	-9999	2234.2	2254.8	7.275	2818.22
2229.7	-9999	7.825	-9999	-9999	2229.7	2057.1	7.825	710.54
2222.6	-9999	7.335	-9999	-9999	2222.6	2223	7.335	2425
2237.3	-9999	7.746	-9999	-9999	2237.3	2096.6	7.746	876
2225.2	-9999	7.944	-9999	-9999	2225.2	1998.5	7.944	515.77
2134	-9999	7.645	-9999	-9999	2134	2035	7.645	1081.24

2241.7	-9999	7.89	-9999	-9999	2241.7	2039	7.89	600.94
2241	-9999	7.877	-9999	-9999	2241	2044.1	7.877	622.62
2234.8	-9999	7.885	-9999	-9999	2234.8	2036.1	7.885	607.64
2230.4	-9999	7.95	-9999	-9999	2230.4	1999.5	7.95	508.61
2232.6	-9999	7.928	-9999	-9999	2232.6	2012.8	7.928	540.56
2224.7	-9999	7.805	-9999	-9999	2224.7	2061.1	7.805	747.9
2210.6	-9999	8.263	-9999	-9999	2210.6	1791.9	8.263	203.93
2179	-9999	8.171	-9999	-9999	2179	1827.3	8.171	265.35
2234.2	-9999	7.828	-9999	-9999	2234.2	2059.8	7.828	707.05
2156.5	-9999	7.665	-9999	-9999	2156.5	2050.1	7.665	1040.37
2240.2	-9999	7.916	-9999	-9999	2240.2	2024.9	7.916	559.88
2238.5	-9999	7.912	-9999	-9999	2238.5	2025.1	7.912	565.53
2237.8	-9999	7.929	-9999	-9999	2237.8	2016.5	7.929	540.38
2233.8	-9999	7.939	-9999	-9999	2233.8	2007.6	7.939	524.9
2238.7	-9999	7.907	-9999	-9999	2238.7	2028.1	7.907	573.26
2229.9	-9999	7.89	-9999	-9999	2229.9	2028.4	7.89	597.67
2232.6	-9999	7.89	-9999	-9999	2232.6	2030.7	7.89	598.42
2178.8	-9999	7.731	-9999	-9999	2178.8	2046.9	7.731	886.92
2215.8	-9999	7.91	-9999	-9999	2215.8	2006.3	7.91	563.13
2237.4	-9999	7.907	-9999	-9999	2237.4	2027.4	7.907	573.42
2232.7	-9999	7.843	-9999	-9999	2232.7	2053.3	7.843	679.53
2236.4	-9999	7.873	-9999	-9999	2236.4	2042.2	7.873	627.41
2144.5	-9999	7.842	-9999	-9999	2144.5	1968	7.842	652.65
2249.8	-9999	7.943	-9999	-9999	2249.8	2020.7	7.943	523.07
2237.7	-9999	7.879	-9999	-9999	2237.7	2043.1	7.879	619.36
2238.4	-9999	7.853	-9999	-9999	2238.4	2055.6	7.853	663.97
2229.1	-9999	7.914	-9999	-9999	2229.1	2019.5	7.914	562.05
2231.9	-9999	7.917	-9999	-9999	2231.9	2020.5	7.917	558.24
2201.9	-9999	7.814	-9999	-9999	2201.9	2036.3	7.814	721.96
2226.6	-9999	7.838	-9999	-9999	2226.6	2049.3	7.838	685.44
2244	-9999	7.978	-9999	-9999	2244	1999.2	7.978	474.05
2241	-9999	8.053	-9999	-9999	2241	1955.8	8.053	384.15
2226.1	-9999	7.78	-9999	-9999	2226.1	2071.6	7.78	796.38
2179.5	-9999	7.691	-9999	-9999	2179.5	2061.7	7.691	981.11
2228.5	-9999	7.904	-9999	-9999	2228.5	2022	7.904	574.68
2199.3	-9999	7.656	-9999	-9999	2199.3	2096	7.656	1083.45
2210.8	-9999	7.226	-9999	-9999	2210.8	2248.6	7.226	3133.58
2237.8	-9999	7.967	-9999	-9999	2237.8	1998.8	7.967	486.33
2246.7	-9999	7.937	-9999	-9999	2246.7	2022.8	7.937	530.5
2245.8	-9999	7.936	-9999	-9999	2245.8	2022.5	7.936	531.72
2203.7	-9999	7.296	-9999	-9999	2203.7	2216	7.296	2645.38
2208.4	-9999	7.744	-9999	-9999	2208.4	2069.6	7.744	868.92
-9999	2038.6	7.839	-9999	-9999	2217.4	2038.6	7.839	678.94
-9999	2076.1	7.858	-9999	-9999	2264.9	2076.1	7.858	660.9
-9999	2040.7	7.91	-9999	-9999	2254.8	2040.7	7.91	571.1
-9999	2114.1	7.797	-9999	-9999	2277.6	2114.1	7.797	779.71
-9999	2034.1	7.926	-9999	-9999	2255.7	2034.1	7.926	547.37

-9999	2101.1	7.771	-9999	-9999	2252	2101.1	7.771	825.52
-9999	2101.1	7.702	-9999	-9999	2222.7	2101.1	7.702	974.99
-9999	2125.8	7.69	-9999	-9999	2244.4	2125.8	7.69	1014.03
-9999	2125.8	7.69	-9999	-9999	2244.4	2125.8	7.69	1014.03
-9999	2063.4	7.716	-9999	-9999	2190.5	2063.4	7.716	924.62
-9999	2210.1	7.632	-9999	-9999	2309.1	2210.1	7.632	1209.77
-9999	2302.9	7.679	-9999	-9999	2423.5	2302.9	7.679	1127.24
-9999	2090.4	7.81	-9999	-9999	2258.5	2090.4	7.81	747.18
-9999	2090.4	7.81	-9999	-9999	2258.5	2090.4	7.81	747.18
-9999	2090	7.723	-9999	-9999	2220.9	2090	7.723	920.99
-9999	2004	7.744	-9999	-9999	2139.8	2004	7.744	839.75
-9999	2036	7.773	-9999	-9999	2184.7	2036	7.773	796.11
-9999	2036	7.773	-9999	-9999	2184.7	2036	7.773	796.11
-9999	2182	7.768	-9999	-9999	2335.3	2182	7.768	863.53
-9999	2185	7.715	-9999	-9999	2316.3	2185	7.715	981.45
-9999	2186	7.686	-9999	-9999	2305.6	2186	7.686	1052.22
-9999	2210	7.727	-9999	-9999	2347.3	2210	7.727	964.59
-9999	2210	7.727	-9999	-9999	2347.3	2210	7.727	964.59
-9999	2147	7.59	-9999	-9999	2229.6	2147	7.59	1296.94
-9999	2180	7.692	-9999	-9999	2301.8	2180	7.692	1034.45
-9999	2057	7.93	-9999	-9999	2282.5	2057	7.93	548.09
-9999	2131	7.838	-9999	-9999	2314.5	2131	7.838	711.52
-9999	2070	7.795	-9999	-9999	2229.8	2070	7.795	767.55
-9999	2070	7.795	-9999	-9999	2229.8	2070	7.795	767.55
-9999	2200.1	7.585	-9999	-9999	2282.9	2200.1	7.585	1343.52
-9999	2213	7.651	-9999	-9999	2320.1	2213	7.651	1156.98
-9999	2087	7.891	-9999	-9999	2294.8	2087	7.891	611.83
-9999	2121.1	7.808	-9999	-9999	2290.4	2121.1	7.808	761.32
-9999	2121.1	7.808	-9999	-9999	2290.4	2121.1	7.808	761.32
-9999	2033.7	7.924	-9999	-9999	2254.3	2033.7	7.924	549.98
-9999	2090.4	7.825	-9999	-9999	2265.5	2090.4	7.825	720.38
-9999	2097.6	7.78	-9999	-9999	2252.7	2097.6	7.78	806.04
-9999	2120.6	7.875	-9999	-9999	2321.1	2120.6	7.875	647.28
-9999	2135.2	7.84	-9999	-9999	2319.3	2135.2	7.84	709.84
-9999	2135.2	7.84	-9999	-9999	2319.3	2135.2	7.84	709.84
-9999	2106.6	7.859	-9999	-9999	2298.2	2106.6	7.859	668.62
-9999	2004.1	7.977	-9999	-9999	2251.4	2004.1	7.977	475.19
-9999	2024.6	7.954	-9999	-9999	2260	2024.6	7.954	508.63
-9999	2079.2	7.917	-9999	-9999	2299.3	2079.2	7.917	572.09
-9999	2110.8	7.857	-9999	-9999	2301.1	2110.8	7.857	673.62
-9999	2071.4	7.916	-9999	-9999	2289.1	2071.4	7.916	572
-9999	2133.6	7.841	-9999	-9999	2316.3	2133.6	7.841	708.76
-9999	2049.1	7.927	-9999	-9999	2269.6	2049.1	7.927	551.33
-9999	2054.6	7.918	-9999	-9999	2270.9	2054.6	7.918	565.24
-9999	2039.3	7.891	-9999	-9999	2240.7	2039.3	7.891	599.53
-9999	2044.7	7.934	-9999	-9999	2268.7	2044.7	7.934	540.73
-9999	2090.1	7.841	-9999	-9999	2269.7	2090.1	7.841	694.71

-9999	2140.2	7.705	-9999	-9999	2263	2140.2	7.705	987.59
-9999	2073.1	7.858	-9999	-9999	2263.4	2073.1	7.858	658.9
-9999	2073.4	7.871	-9999	-9999	2270.1	2073.4	7.871	638.38
-9999	2041.5	7.884	-9999	-9999	2242.1	2041.5	7.884	609.19
-9999	2052.8	7.871	-9999	-9999	2247.6	2052.8	7.871	632.38
-9999	2071.9	7.843	-9999	-9999	2254.4	2071.9	7.843	683.42
-9999	2057.7	7.857	-9999	-9999	2246	2057.7	7.857	655.96
-9999	2036.3	7.876	-9999	-9999	2231.9	2036.3	7.876	620.01

pCO2_CO2	HCO3_CO2	CO3_CO2c	CO2_CO2c	B_Alk_CO2	OH_CO2cal	P_Alk_CO2	Si_Alk_CO2	Revelle_CC
495.6	1808.25	171.27	14.16	72.42	5.32	0	0	10.76
540.4	1835.78	161.9	15.44	68.3	4.95	0	0	11.15
591.2	1860.55	151.71	16.9	63.85	4.58	0	0	11.6
880.2	1943.9	111.46	25.14	47.27	3.22	0	0	13.68
494.8	1800.45	169.73	14.14	71.99	5.29	0	0	10.78
1465.5	2016.47	73.34	41.67	31.93	2.03	0	0	16.02
483.7	1798.83	174.39	13.8	74.13	5.43	0	0	10.63
510.4	1815.57	167.67	14.58	70.94	5.18	0	0	10.89
500.9	1813.5	169.76	14.32	71.42	5.26	0	0	10.84
1185.9	1936.3	81.91	33.9	35.93	2.38	0	0	15.35
1141.3	1928.96	84.47	32.62	37.07	2.46	0	0	15.16
566.9	1844.08	156.05	16.19	66.14	4.75	0	0	11.36
620.4	1869.79	146.29	17.72	61.8	4.39	0	0	11.82
559.3	1838.83	156.65	15.98	66.22	4.78	0	0	11.34
647.6	1868.14	139.91	18.5	59.55	4.2	0	0	12.05
936.1	1961.54	106.92	26.73	45.3	3.06	0	0	13.99
1101.5	1980.89	93.86	31.17	39.67	2.72	0	0	14.81
935.5	1981.23	112.15	26.3	46.7	3.27	0	0	13.78
1082.5	1960.05	93.87	30.64	40.42	2.73	0	0	14.68
697.6	1894.15	135.05	19.77	56.7	4.08	0	0	12.37
1382.4	1981.35	75.37	39.03	32.69	2.18	0	0	15.86
3000.3	2151.51	40.98	84.72	17.11	1.09	0	0	16.38
582.3	1860.57	156.6	16.5	65.69	4.8	0	0	11.41
3164.6	2097.18	36.72	89.52	15.72	1	0	0	16
914	1968.22	111.75	25.87	46.72	3.25	0	0	13.77
783.8	1943.86	125.66	22.37	52.71	3.62	0	0	12.97
548.6	1845.76	161.7	15.64	67.88	4.93	0	0	11.2
564	1853.21	158.44	16.08	66.36	4.83	0	0	11.34
1008.9	1949.75	98.86	28.62	42.19	2.89	0	0	14.39
3010	2112.98	39.37	84.97	16.71	1.07	0	0	16.27
1043.3	1999.14	101.03	29.54	42.23	2.88	0	0	14.47
3316.1	2142.05	36.04	94.61	15.18	0.94	0	0	15.89
615.8	1885.89	149.95	17.59	62.64	4.46	0	0	11.76
533.6	1840.34	165.95	15.18	69.47	5.11	0	0	11.05
3860.6	2182.14	32.63	109.12	13.5	0.86	0	0	15.18
578.2	1849.9	157.91	16.24	65.98	4.97	0	0	11.33
857.2	1950.32	119.12	24	49.63	3.58	0	0	13.31
924.6	1894.98	102.41	25.97	43.49	3.2	0	0	14.02
849.4	1940.89	116.85	24.04	49.07	3.45	0	0	13.39
863.8	1948.43	117.49	24.25	49.12	3.51	0	0	13.38
908.4	1951.86	111.2	25.59	46.58	3.3	0	0	13.73
607.4	1863.29	151.53	17.14	63.59	4.69	0	0	11.6
746	1893.2	124.76	21.28	53.1	3.72	0	0	12.81
778.7	1894.34	119.64	22.24	51.44	3.54	0	0	13.04
624.9	1864.04	144.68	17.82	61.2	4.38	0	0	11.86
583.2	1850.21	155	16.47	64.91	4.83	0	0	11.44

838.4	1937.05	116.44	23.9	49.12	3.39	0	0	13.41
698.5	1872.43	130.88	19.88	55.81	3.97	0	0	12.45
804.2	1929.18	122.46	22.67	51.09	3.68	0	0	13.09
813.5	1939.74	120.85	23.13	50.64	3.54	0	0	13.2
765.3	1929.72	126.6	21.82	53.01	3.7	0	0	12.89
777.8	1930.92	124.82	22.18	52.46	3.64	0	0	12.97
690.8	1904.33	137.84	19.6	57.73	4.12	0	0	12.29
557.4	1852.91	161.04	15.86	67.39	4.92	0	0	11.25
955.9	1954.01	104.7	27.15	44.44	3.04	0	0	14.08
900.4	1968.38	113.02	25.56	47.34	3.26	0	0	13.7
626.5	1878.08	149.26	17.67	62.37	4.58	0	0	11.74
655.4	1897.54	144.46	18.55	59.94	4.37	0	0	12.02
528.8	1828.42	167.61	14.92	70.24	5.28	0	0	10.95
856.4	1967.54	119.57	24.21	49.68	3.48	0	0	13.37
733.8	1922.29	133.21	20.74	55.67	3.97	0	0	12.55
875.4	1908.56	109.61	24.81	47.32	3.27	0	0	13.6
518.4	1811.92	166.84	14.69	70.75	5.25	0	0	10.89
503	1816.97	172.16	14.29	72.49	5.37	0	0	10.77
658.6	1884.47	143.21	18.6	60.49	4.35	0	0	11.97
1467.7	2038.05	75.16	41.44	31.85	2.11	0	0	16.06
973.8	1965.12	104.24	27.65	44.23	3	0	0	14.14
517	1823.11	169.01	14.66	71	5.29	0	0	10.89
622	1871.73	150.87	17.45	63.16	4.69	0	0	11.65
568.1	1848.68	161.15	15.94	67.42	5.07	0	0	11.21
533.9	1824.91	169.93	14.81	70.62	5.57	0	0	10.86
524.1	1824.91	171.86	14.62	71.73	5.55	0	0	10.8
732.9	1914.78	131.41	20.77	55.01	3.92	0	0	12.61
2725.1	2099.17	42.68	77.18	18.19	1.16	0	0	16.59
687.2	1906.75	139.96	19.42	58.48	4.21	0	0	12.21
542.9	1835.16	162.44	15.41	68.05	5.05	0	0	11.14
521.4	1829.58	168.25	14.8	70.39	5.24	0	0	10.94
2011.4	2176.75	61.35	57.27	24.6	1.6	0	0	17.07
2287.6	2091.8	50.19	64.89	21.16	1.37	0	0	16.95
479.5	1807.13	176.59	13.71	74.3	5.47	0	0	10.62
547.2	1843.65	162.82	15.54	68.25	5.02	0	0	11.15
511.9	1828.25	171.07	14.55	71.77	5.29	0	0	10.84
1612.6	2129.99	73.34	45.95	29.79	1.94	0	0	16.51
1637.9	2131.39	72.06	46.8	29.38	1.89	0	0	16.57
486.6	1807.44	178.56	13.71	74.81	5.7	0	0	10.56
515.1	1831.6	172.17	14.55	71.74	5.4	0	0	10.83
1613.6	2122	73.07	45.8	29.61	1.97	0	0	16.51
2827.2	2132.21	41.71	80.87	17.55	1.09	0	0	16.57
712.8	1903.84	132.96	20.28	56.03	3.95	0	0	12.49
2432.8	2106.09	47.59	69.37	20.16	1.27	0	0	16.88
878.8	1957.24	114.35	24.97	48.07	3.31	0	0	13.58
517.4	1817.63	166.13	14.75	70.13	5.16	0	0	10.96
1084.7	1915.69	88.38	30.89	38.99	2.6	0	0	14.84

602.9	1870.15	151.69	17.15	63.62	4.59	0	0	11.63
624.6	1878.23	148.19	17.72	61.95	4.5	0	0	11.79
609.6	1869.72	149.02	17.39	62.6	4.49	0	0	11.73
510.2	1815.89	169.07	14.5	71.13	5.29	0	0	10.86
542.3	1835.31	162.09	15.43	68.14	5	0	0	11.15
750.3	1912.27	127.5	21.32	53.7	3.79	0	0	12.77
204.6	1496.81	289.34	5.79	124.08	11.06	0	0	7.93
266.2	1575.2	244.56	7.55	105.78	8.86	0	0	8.58
709.3	1905.34	134.29	20.12	56.29	4.02	0	0	12.45
1043.7	1927.41	93	29.68	40.39	2.74	0	0	14.63
561.7	1849.5	159.44	15.96	66.92	4.89	0	0	11.28
567.3	1850.72	158.25	16.11	66.45	4.86	0	0	11.32
542.1	1837.82	163.26	15.39	68.42	5.06	0	0	11.12
526.6	1826.41	166.21	14.94	69.77	5.19	0	0	10.99
575.1	1855.24	156.49	16.36	65.73	4.78	0	0	11.4
599.6	1860.75	150.55	17.09	63.51	4.56	0	0	11.62
600.3	1862.76	150.88	17.09	63.56	4.58	0	0	11.62
889.8	1913.94	107.65	25.31	46.41	3.19	0	0	13.74
564.9	1835.11	155.1	16.11	65.73	4.77	0	0	11.37
575.3	1854.99	156.09	16.37	65.46	4.77	0	0	11.42
681.7	1896.7	137.2	19.43	57.51	4.09	0	0	12.3
629.4	1878.01	146.27	17.92	61.5	4.4	0	0	11.85
654.7	1816.79	132.7	18.55	58.15	4.17	0	0	12.1
524.7	1837.22	168.56	14.9	70.26	5.23	0	0	10.96
621.3	1878.65	146.7	17.77	61.29	4.39	0	0	11.86
666.1	1897.04	139.48	19.05	58.25	4.13	0	0	12.22
563.9	1847.58	155.78	16.15	65.24	4.74	0	0	11.43
560	1847.44	157.02	16.03	65.66	4.78	0	0	11.38
724.3	1887.79	127.85	20.68	54.63	3.81	0	0	12.64
687.6	1894.13	135.57	19.63	57.29	4.02	0	0	12.34
475.6	1807.44	178.2	13.58	74.65	5.54	0	0	10.58
385.4	1740.79	203.99	11.01	85.65	6.59	0	0	9.76
798.9	1926.94	121.9	22.73	51.79	3.56	0	0	13.06
984.2	1934.02	99.67	28	43.24	2.9	0	0	14.24
576.5	1851.95	153.46	16.55	65.09	4.6	0	0	11.48
1086.9	1972.47	92.34	31.19	39.61	2.6	0	0	14.87
3143.7	2121.29	36.54	90.72	15.56	0.95	0	0	16.08
487.9	1810.78	174.09	13.97	73.52	5.36	0	0	10.69
532.2	1842.64	164.94	15.24	69.19	5	0	0	11.09
533.4	1842.66	164.56	15.28	69.06	4.99	0	0	11.1
2653.8	2097.14	43.47	75.39	18.51	1.18	0	0	16.67
871.7	1932.5	112.39	24.76	47.88	3.3	0	0	13.57
681.1	1883.13	136.04	19.43	58.15	4.05	0	0	12.25
663	1913.49	143.69	18.93	59.83	4.21	0	0	12.1
572.9	1865.57	158.82	16.34	66.83	4.77	0	0	11.35
782.2	1963.11	128.68	22.31	53.46	3.67	0	0	12.92
549.1	1854.78	163.63	15.66	68.76	4.94	0	0	11.16

828.2	1956.92	120.53	23.63	50.54	3.45	0	0	13.27
978.1	1970.15	103.02	27.94	43.57	2.94	0	0	14.25
1017.3	1994.78	101.96	29.03	42.87	2.87	0	0	14.4
1017.3	1994.78	101.96	29.03	42.87	2.87	0	0	14.4
927.6	1931.88	105.09	26.46	45.4	3.05	0	0	13.94
1213.6	2082.31	93.13	34.63	38.02	2.51	0	0	15.27
1130.8	2162.69	107.98	32.26	42.05	2.8	0	0	14.78
749.6	1938.22	130.85	21.38	54.82	3.78	0	0	12.71
749.6	1938.22	130.85	21.38	54.82	3.78	0	0	12.71
923.9	1955.54	108.1	26.35	46.05	3.1	0	0	13.88
842.4	1871.39	108.58	24.03	48.06	3.25	0	0	13.46
798.7	1895.9	117.31	22.79	50.74	3.47	0	0	13.15
798.7	1895.9	117.31	22.79	50.74	3.47	0	0	13.15
866.3	2032.93	124.35	24.72	50.23	3.43	0	0	13.43
984.6	2045.88	111.03	28.08	45.31	3.04	0	0	14.13
1055.6	2051.73	104.16	30.11	42.7	2.84	0	0	14.52
967.7	2067.07	115.33	27.6	46.43	3.13	0	0	14.01
967.7	2067.07	115.33	27.6	46.43	3.13	0	0	14.01
1301.1	2027.38	82.51	37.11	34.97	2.28	0	0	15.64
1037.8	2045.13	105.27	29.6	43.23	2.88	0	0	14.43
549.8	1874.42	166.89	15.68	69.28	4.99	0	0	11.14
713.8	1968.81	141.83	20.36	57.98	4.04	0	0	12.39
770	1922.86	125.16	21.97	53.03	3.65	0	0	12.9
770	1922.86	125.16	21.97	53.03	3.65	0	0	12.9
1347.8	2077.74	83.99	38.4	34.9	2.26	0	0	15.72
1160.7	2082.12	97.75	33.09	39.89	2.63	0	0	14.99
613.8	1913.43	156.11	17.5	64.56	4.57	0	0	11.63
763.8	1966.73	132.54	21.77	54.87	3.77	0	0	12.76
763.8	1966.73	132.54	21.77	54.87	3.77	0	0	12.76
551.7	1855.08	162.9	15.74	68.5	4.92	0	0	11.18
722.7	1934.54	135.25	20.61	56.52	3.92	0	0	12.51
808.6	1951.5	123.01	23.06	51.68	3.53	0	0	13.12
649.3	1949.54	152.57	18.53	62.07	4.39	0	0	11.92
712.1	1972.45	142.41	20.32	57.97	4.05	0	0	12.4
712.1	1972.45	142.41	20.32	57.97	4.05	0	0	12.4
670.8	1941	146.4	19.14	60.17	4.23	0	0	12.11
476.7	1810.85	179.66	13.6	75.69	5.56	0	0	10.53
510.3	1837.57	172.49	14.56	72.2	5.26	0	0	10.84
573.9	1898.78	164.07	16.37	67.59	4.84	0	0	11.32
675.8	1945.75	145.74	19.3	59.69	4.2	0	0	12.16
573.8	1892.62	162.38	16.38	66.9	4.81	0	0	11.37
711	1971.6	141.65	20.32	57.36	4.03	0	0	12.45
553.1	1869.53	163.72	15.81	67.76	4.92	0	0	11.24
567.1	1877.39	161.04	16.21	66.6	4.82	0	0	11.36
601.5	1871.26	150.84	17.19	63.23	4.53	0	0	11.67
542.5	1863.37	165.84	15.51	68.67	5	0	0	11.15
696.9	1931.72	138.44	19.93	57.12	4.03	0	0	12.41

990.7	2006.94	104.91	28.35	43.28	2.94	0	0	14.35
661	1909.84	144.41	18.84	60.55	4.23	0	0	12.03
640.4	1906.6	148.55	18.26	62.1	4.36	0	0	11.87
611.1	1873.98	150.08	17.43	63.43	4.49	0	0	11.68
634.4	1887.96	146.74	18.09	61.85	4.35	0	0	11.86
685.6	1912.94	139.4	19.56	58.56	4.08	0	0	12.25
658.1	1896.22	142.71	18.77	60.18	4.22	0	0	12.04
622	1871.73	146.81	17.75	62.2	4.4	0	0	11.79

O_Ca_CO2	O_Ar_CO2	xCO2_CO2	Temperatu	Pressure_d	pH_adj_CO	fCO2_adj_	pCO2_adj_	HCO3_adj_
4.18	2.75	511.31	16.42	0	8.088	348.54	349.8	1812.98
3.96	2.6	557.5	15.77	0	8.067	370.31	371.6	1841.02
3.71	2.44	609.88	14.5	0	8.053	384.66	386.1	1866.69
2.72	1.79	908.03	11.97	0	7.932	521.01	523	1952.47
4.15	2.73	510.49	15.2	0	8.106	330.58	331.8	1805.85
1.78	1.17	1511.9	11.98	0	7.713	892.35	895.7	2026.4
4.25	2.79	498.96	15.08	0	8.117	321.38	322.5	1804.3
4.1	2.69	526.55	16.17	0	8.081	355.35	356.6	1820.48
4.15	2.73	516.77	16	0	8.092	346.13	347.4	1818.48
2	1.31	1223.42	18.5	0	7.7	925.79	929	1941.07
2.06	1.36	1177.41	18.5	0	7.716	889.97	893.1	1933.67
3.81	2.5	584.83	15.6	0	8.05	386.08	387.5	1849.5
3.57	2.35	640.06	14.3	0	8.036	400.77	402.2	1876.14
3.83	2.52	576.96	14.6	0	8.07	365.07	366.4	1844.8
3.42	2.25	668.09	13.55	0	8.028	405.81	407.3	1875
2.61	1.72	965.71	13.65	0	7.883	595.79	598	1969.23
2.3	1.51	1137.23	13.47	0	7.823	690.09	692.6	1989.36
2.74	1.8	966.24	12.23	0	7.919	547.73	549.8	1990.27
2.29	1.51	1117.41	14.5	0	7.809	709.85	712.4	1967.67
3.31	2.17	720.24	13.7	0	8.006	434.25	435.8	1901.29
1.84	1.21	1427.33	14.05	0	7.711	897.31	900.6	1989.91
1	0.66	3097.65	11.95	0	7.414	1901.64	1908.8	2162.29
3.82	2.52	601.09	15.04	0	8.056	382.87	384.3	1866.55
0.9	0.59	3267.12	13	0	7.363	2098.66	2106.5	2106.69
2.73	1.8	943.58	12.64	0	7.917	548.96	551	1976.75
3.06	2.01	808.62	14.1	0	7.952	505.01	506.9	1950.88
3.95	2.6	566.04	15.23	0	8.072	366.53	367.9	1851.39
3.87	2.54	581.94	16.97	0	8.036	404.94	406.4	1857.88
2.42	1.59	1041.41	13.06	0	7.86	621.66	624	1958.13
0.96	0.63	3107.84	12.7	0	7.395	1961.92	1969.2	2123
2.47	1.62	1077.04	11.9	0	7.874	612.07	614.4	2008.52
0.88	0.58	3421.24	12.73	0	7.35	2206.9	2215.1	2151.52
3.66	2.41	635.25	15.63	0	8.023	420.39	421.9	1891.47
4.05	2.67	550.7	17.95	0	8.043	397.58	399	1844.4
0.8	0.52	3985.8	14.65	0	7.27	2738.78	2748.8	2190.34
3.87	2.54	597.27	18.45	0	8.012	431.08	432.6	1854.05
2.91	1.92	885.73	12.45	0	7.952	500.92	502.8	1959.04
2.53	1.66	955.52	16	0	7.855	626.19	628.4	1901.51
2.86	1.88	876.98	12.95	0	7.94	514.94	516.9	1949.01
2.87	1.89	892.34	12.2	0	7.95	501.65	503.5	1957.26
2.72	1.79	938.23	13.9	0	7.901	569.91	572	1959.67
3.71	2.44	627.24	16.4	0	8.021	419.78	421.3	1868.62
3.05	2	769.71	15.4	0	7.945	504.98	506.8	1899.27
2.92	1.92	803.31	14.92	0	7.931	519.52	521.4	1900.72
3.54	2.32	644.77	14.94	0	8.024	413.13	414.6	1870.06
3.8	2.5	602.19	18.86	0	7.999	445.76	447.3	1854.03

2.85	1.87	865.16	12.38	0	7.948	501.97	503.9	1945.31
3.2	2.1	720.92	12.46	0	8.016	415.61	417.2	1880.18
3	1.97	830.64	15.4	0	7.928	534.65	536.6	1935.73
2.96	1.94	839.54	13.49	0	7.947	507.58	509.5	1947.32
3.1	2.03	789.67	13.5	0	7.971	478.65	480.4	1937.09
3.05	2	802.48	16.18	0	7.922	544.68	546.6	1936.64
3.37	2.21	713.02	16.07	0	7.974	476.44	478.1	1909.99
3.94	2.59	575.27	13.1	0	8.101	338.95	340.2	1859.88
2.56	1.68	986.62	14.9	0	7.857	635.46	637.8	1961.06
2.76	1.81	929.3	14.93	0	7.887	597.67	599.8	1975.33
3.65	2.4	646.95	13.1	0	8.061	377.03	378.4	1885.45
3.54	2.33	676.64	14.35	0	8.025	417.91	419.4	1904.21
4.1	2.7	546.05	14.65	0	8.101	338.63	339.9	1834.52
2.92	1.92	884.21	12.8	0	7.944	515.76	517.7	1975.85
3.25	2.14	757.62	12.8	0	8.003	439.71	441.3	1930.17
2.68	1.76	903.64	14.17	0	7.898	561.8	563.9	1915.84
4.07	2.68	535.1	14.3	0	8.107	329.68	330.9	1818.08
4.2	2.76	519.15	14.46	0	8.118	323.13	324.3	1822.96
3.49	2.3	679.95	15.18	0	8.006	435.08	436.7	1890.64
1.83	1.21	1515.32	12.37	0	7.719	893.61	897	2048.09
2.54	1.67	1004.98	12.39	0	7.888	584.56	586.7	1973.84
4.13	2.72	533.68	15.77	0	8.089	349.77	351	1828.43
3.69	2.43	642.56	16.5	0	8.014	428.42	429.9	1877.15
3.94	2.59	586.86	15.68	0	8.061	377.44	378.8	1854.42
4.16	2.75	552.08	18.13	0	8.055	384.66	386	1829.36
4.2	2.77	541.64	17	0	8.075	364.08	365.4	1829.86
3.21	2.11	756.59	11.6	0	8.02	418.48	420.1	1923.31
1.04	0.69	2812.97	14.6	0	7.412	1896.36	1903.3	2107.87
3.42	2.25	709.46	14.6	0	8.002	443.39	445	1913.38
3.98	2.61	560.4	17.55	0	8.043	395.91	397.3	1839.52
4.12	2.71	538.13	17.2	0	8.064	374.92	376.2	1834.08
1.5	0.99	2075.78	17.11	0	7.536	1507.61	1512.9	2183.83
1.23	0.81	2361.37	15.46	0	7.481	1622.86	1628.7	2100
4.31	2.83	494.66	17.52	0	8.085	353.29	354.5	1811.18
3.98	2.62	564.81	16.98	0	8.049	390.87	392.3	1848.34
4.18	2.75	528.29	16.9	0	8.074	364.92	366.2	1832.85
1.79	1.18	1664	17.12	0	7.625	1199.72	1204	2136.69
1.76	1.16	1689.7	17.12	0	7.616	1225.25	1229.6	2138
4.36	2.87	502.51	15.3	0	8.123	319.44	320.6	1813.04
4.21	2.77	531.8	17.4	0	8.07	371.02	372.3	1836.06
1.79	1.18	1665.6	15.94	0	7.643	1139.17	1143.3	2129.76
1.02	0.67	2916.36	14.98	0	7.392	2022.35	2029.7	2140.36
3.25	2.13	735.61	14.99	0	7.975	472.34	474.1	1910.15
1.16	0.76	2509.91	12.2	0	7.494	1550.67	1556.5	2116.49
2.79	1.83	906.96	12.2	0	7.936	520.89	522.8	1965.84
4.06	2.67	533.9	17.18	0	8.062	374.34	375.7	1822.04
2.16	1.42	1119.24	17.18	0	7.755	798.95	801.8	1921.28

3.71	2.44	622.15	18.6	0	7.987	462.14	463.7	1874.01
3.62	2.38	644.75	18.6	0	7.975	476.58	478.2	1882.2
3.64	2.39	628.96	15.4	0	8.029	411.04	412.5	1875.42
4.13	2.72	526.61	17.34	0	8.068	369.58	370.9	1820.24
3.96	2.6	559.63	16.15	0	8.062	375.02	376.4	1840.42
3.12	2.05	774.37	14.79	0	7.958	492.57	494.4	1918.84
7.07	4.65	211.2	17.2	0	8.389	145.05	145.6	1499.95
5.98	3.93	274.78	17.2	0	8.295	189.8	190.5	1578.73
3.29	2.16	732.18	16.12	0	7.963	489.96	491.7	1911.03
2.27	1.49	1077.14	16.13	0	7.793	733.17	735.8	1933.72
3.9	2.56	579.66	16.43	0	8.046	392.73	394.1	1854.53
3.87	2.54	585.55	16.43	0	8.043	396.3	397.7	1855.78
3.99	2.62	559.55	16.42	0	8.061	377.62	379	1842.83
4.07	2.67	543.55	16.47	0	8.071	366.97	368.3	1831.35
3.82	2.51	593.49	15.92	0	8.045	394.29	395.7	1860.59
3.68	2.42	618.67	15.08	0	8.039	398.34	399.8	1866.62
3.69	2.42	619.49	15.46	0	8.034	404.76	406.2	1868.43
2.63	1.73	918.21	13.56	0	7.899	559.89	562	1921.56
3.79	2.49	582.93	13.56	0	8.083	351.57	352.9	1841.74
3.82	2.51	593.66	15.27	0	8.055	383.79	385.2	1860.72
3.36	2.21	703.45	13.89	0	8.009	431.5	433.1	1903.56
3.57	2.35	649.5	14.57	0	8.03	409.19	410.7	1884.31
3.24	2.13	675.88	14.2	0	8.006	416.77	418.3	1823.34
4.12	2.71	541.63	14.2	0	8.109	332.62	333.8	1843.48
3.59	2.36	641.03	14.61	0	8.034	406.22	407.7	1884.83
3.42	2.24	687.2	14.4	0	8.01	432.52	434.1	1903.49
3.82	2.5	581.68	15.41	0	8.057	381.13	382.5	1853.08
3.85	2.52	577.77	15.67	0	8.056	382.18	383.6	1852.79
3.12	2.05	747.22	14.04	0	7.976	464.42	466.1	1894.59
3.31	2.17	709.42	14.04	0	8	440.12	441.7	1900.86
4.36	2.86	490.65	13.43	0	8.153	293.99	295.1	1813.84
4.99	3.27	397.61	13.08	0	8.236	233.84	234.7	1747.03
2.97	1.95	824.37	13.2	0	7.954	494.3	496.1	1934.59
2.43	1.6	1015.59	13.2	0	7.862	614.36	616.6	1942.1
3.74	2.46	594.55	14.18	0	8.063	372.93	374.3	1858.14
2.25	1.48	1120.91	13.75	0	7.813	704.79	707.4	1980.29
0.89	0.58	3240.75	13.75	0	7.351	2192.92	2201	2129.68
4.25	2.79	503.24	17.5	0	8.078	360.27	361.5	1814.85
4.03	2.65	548.94	16.15	0	8.068	371.88	373.2	1847.61
4.02	2.64	550.21	16.9	0	8.055	384.61	386	1847.19
1.06	0.7	2738.87	15.19	0	7.415	1889.23	1896.1	2105.34
2.74	1.8	899.63	15.19	0	7.889	585.3	587.4	1939.12
3.31	2.18	702.67	18.77	0	7.93	530.39	532.2	1886.94
3.51	2.3	684.01	17.64	0	7.966	492.58	494.3	1918.01
3.87	2.54	591.06	17.25	0	8.025	417.94	419.4	1870.07
3.14	2.06	806.96	15.9	0	7.93	542.8	544.7	1969.03
3.99	2.62	566.5	15.15	0	8.073	366.65	368	1860.45

2.94	1.93	854.38	15.8	0	7.905	573.4	575.5	1962.99
2.52	1.65	1009.08	16.1	0	7.829	689.25	691.7	1976.33
2.49	1.63	1049.48	16.1	0	7.816	717.52	720.1	2001.1
2.49	1.63	1049.48	16.1	0	7.816	717.52	720.1	2001.1
2.56	1.68	956.94	15.7	0	7.849	642.42	644.7	1938.16
2.27	1.49	1252.05	15.23	0	7.769	831.1	834.1	2089.77
2.63	1.73	1166.64	13.1	0	7.85	706.11	708.7	2171.73
3.19	2.1	773.29	13.37	0	7.982	467.71	469.4	1945.61
3.19	2.1	773.29	13.37	0	7.982	467.71	469.4	1945.61
2.63	1.73	953.18	12	0	7.912	548.72	550.8	1964.26
2.65	1.74	869.11	12.6	0	7.925	512.14	514.1	1879.3
2.86	1.88	823.93	13.5	0	7.941	502.74	504.6	1903.21
2.86	1.88	823.93	13.5	0	7.941	502.74	504.6	1903.21
3.03	1.99	893.72	13.2	0	7.941	538.41	540.4	2040.94
2.71	1.78	1015.75	12.5	0	7.896	597.41	599.6	2054.68
2.54	1.67	1089	12	0	7.873	629.37	631.7	2061.04
2.81	1.85	998.3	12.7	0	7.906	591.26	593.5	2075.75
2.81	1.85	998.3	12.7	0	7.906	591.26	593.5	2075.75
2.01	1.32	1342.28	14.1	0	7.741	855.87	859	2035.63
2.56	1.69	1070.6	13.1	0	7.863	647.26	649.7	2053.64
4.07	2.67	567.25	14	0	8.095	349.58	350.9	1880.82
3.46	2.27	736.39	15.6	0	7.976	487.91	489.7	1974.79
3.05	2.01	794.38	15.2	0	7.938	519.26	521.1	1929.12
3.05	2.01	794.38	15.2	0	7.938	519.26	521.1	1929.12
2.04	1.34	1390.47	12.9	0	7.753	845.21	848.4	2087.07
2.38	1.56	1197.42	12.1	0	7.835	697.94	700.6	2091.69
3.8	2.5	633.22	15.1	0	8.038	409.67	411.1	1919.4
3.23	2.12	787.92	15.9	0	7.941	529.61	531.5	1972.63
3.23	2.12	787.92	15.9	0	7.941	529.61	531.5	1972.63
3.97	2.61	569.21	17.8	0	8.031	411.51	413	1859.21
3.3	2.17	745.56	16.8	0	7.945	519.58	521.4	1939.72
3	1.97	834.21	16.2	0	7.908	568.78	570.8	1957.27
3.72	2.44	669.9	16.9	0	7.995	467.5	469.1	1954.53
3.47	2.28	734.65	16.5	0	7.965	505.19	507	1977.86
3.47	2.28	734.65	16.5	0	7.965	505.19	507	1977.86
3.57	2.35	692	17.4	0	7.971	493.39	495.1	1945.72
4.38	2.88	491.8	19.2	0	8.063	376.04	377.3	1813.99
4.21	2.76	526.41	18.5	0	8.051	391.31	392.7	1841.19
4	2.63	592.08	19.8	0	7.994	464.69	466.3	1901.81
3.56	2.34	697.17	17.5	0	7.967	499.15	500.9	1950.41
3.96	2.6	591.99	15.8	0	8.053	393.88	395.3	1898.02
3.46	2.27	733.54	14.7	0	7.993	467.98	469.7	1978.13
4	2.63	570.6	18.5	0	8.023	424.5	426	1873.25
3.94	2.58	585	18.1	0	8.02	428.24	429.7	1881.38
3.69	2.42	620.49	17.4	0	8.003	441.81	443.4	1875.72
4.05	2.66	559.63	17.8	0	8.041	404.39	405.8	1867.47
3.39	2.22	719	17.8	0	7.946	521.56	523.4	1936.21

2.57	1.69	1022.12	14.3	0	7.858	648.55	650.9	2014.42
3.52	2.31	681.92	16.2	0	7.988	462.79	464.4	1915.24
3.62	2.38	660.69	16.6	0	7.995	455.56	457.2	1911.69
3.66	2.4	630.48	16.8	0	8.005	438.1	439.7	1878.85
3.58	2.35	654.49	15.9	0	8.006	438.37	439.9	1893.43
3.4	2.23	707.31	14.2	0	8.003	441.96	443.6	1919.61
3.48	2.29	678.88	16.1	0	7.988	458.86	460.5	1901.64
3.58	2.35	641.68	14.8	0	8.027	410.37	411.9	1877.81

CO3_adj_C	CO2_adj_C	B_Alk_adj_	OH_adj_CC	P_Alk_adj_	Si_Alk_adj_	Revelle_ad	O_Ca_adj_	O_Ar_adj_(
168.06	12.64	76.19	3.23	0	0	10.93	4.06	2.61
158.41	13.69	72.1	2.89	0	0	11.34	3.82	2.45
147.68	14.79	67.87	2.47	0	0	11.84	3.56	2.28
106.36	21.67	50.64	1.46	0	0	14.23	2.56	1.63
166.03	12.44	76.29	2.99	0	0	10.96	4.01	2.57
68.17	36.91	33.47	0.9	0	0	17.1	1.63	1.04
170.61	12.12	78.61	3.05	0	0	10.81	4.11	2.63
164.35	12.98	74.73	3.1	0	0	11.07	3.97	2.55
166.39	12.72	75.33	3.12	0	0	11.01	4.02	2.58
79.42	31.62	36.91	1.61	0	0	15.81	1.92	1.24
81.99	30.4	38.12	1.67	0	0	15.6	1.99	1.28
152.47	14.34	69.86	2.74	0	0	11.57	3.68	2.36
142.17	15.49	65.74	2.34	0	0	12.09	3.43	2.19
152.68	13.99	70.38	2.6	0	0	11.56	3.68	2.36
135.49	16.05	63.59	2.13	0	0	12.36	3.27	2.08
102.48	23.48	48.01	1.54	0	0	14.53	2.47	1.58
89.18	27.39	41.97	1.32	0	0	15.52	2.15	1.37
106.84	22.56	50.08	1.46	0	0	14.37	2.57	1.64
89.65	27.23	42.52	1.42	0	0	15.31	2.16	1.38
130.56	17.12	60.58	2.05	0	0	12.72	3.15	2.01
70.91	34.91	34.12	1.08	0	0	16.77	1.71	1.09
35.93	78.99	17.06	0.44	0	0	17.73	0.86	0.55
152.67	14.46	69.74	2.63	0	0	11.64	3.68	2.36
32.31	84.42	15.58	0.44	0	0	17.18	0.78	0.5
106.74	22.35	49.95	1.51	0	0	14.32	2.57	1.64
121.38	19.62	55.97	1.89	0	0	13.36	2.92	1.87
157.94	13.77	71.92	2.78	0	0	11.4	3.81	2.44
155.39	14.46	69.6	3.02	0	0	11.52	3.76	2.42
94.11	24.99	44.82	1.38	0	0	15.04	2.27	1.45
34.69	79.62	16.63	0.46	0	0	17.54	0.83	0.53
95.69	25.5	45.13	1.27	0	0	15.18	2.3	1.47
31.65	89.53	15	0.41	0	0	17.03	0.76	0.49
146.36	15.61	66.14	2.58	0	0	11.99	3.53	2.26
163.28	13.79	72.48	3.37	0	0	11.19	3.95	2.54
28.87	104.68	13.24	0.41	0	0	16.06	0.7	0.45
155.26	14.74	68.82	3.29	0	0	11.5	3.76	2.42
113.89	20.52	53.35	1.6	0	0	13.83	2.74	1.75
98.73	23.13	45.75	1.78	0	0	14.51	2.4	1.54
111.99	20.77	52.47	1.64	0	0	13.89	2.7	1.72
112.2	20.71	52.82	1.56	0	0	13.92	2.7	1.72
106.66	22.33	49.52	1.64	0	0	14.25	2.57	1.64
148.1	15.23	67.03	2.76	0	0	11.82	3.58	2.3
121.08	18.9	56.02	2.1	0	0	13.15	2.92	1.87
115.8	19.7	54.34	1.95	0	0	13.41	2.79	1.79
140.8	15.67	64.89	2.41	0	0	12.12	3.4	2.17
152.58	15.08	67.46	3.31	0	0	11.6	3.7	2.39

111.47	20.61	52.61	1.58	0	0	13.9	2.69	1.71
125.97	17.04	59.98	1.85	0	0	12.83	3.04	1.93
118.55	20.02	54.02	2.02	0	0	13.47	2.87	1.83
116.28	20.13	53.98	1.76	0	0	13.64	2.8	1.79
122.08	18.98	56.53	1.85	0	0	13.29	2.94	1.88
121.4	19.89	55.08	2.16	0	0	13.29	2.93	1.88
134.32	17.46	60.81	2.4	0	0	12.56	3.24	2.08
156.33	13.6	72.34	2.41	0	0	11.5	3.77	2.4
100.69	24.12	46.81	1.64	0	0	14.59	2.43	1.55
108.98	22.65	49.96	1.76	0	0	14.15	2.63	1.68
144.44	15.13	67.02	2.2	0	0	12.04	3.48	2.22
140.2	16.15	63.88	2.28	0	0	12.31	3.38	2.16
163.47	12.95	74.88	2.8	0	0	11.16	3.94	2.52
114.59	20.88	53.18	1.63	0	0	13.86	2.76	1.76
128.27	17.8	59.76	1.87	0	0	12.94	3.09	1.97
105.35	21.79	50.15	1.68	0	0	14.07	2.54	1.62
162.63	12.74	75.5	2.75	0	0	11.1	3.92	2.5
168.04	12.42	77.25	2.87	0	0	10.96	4.05	2.59
139.29	16.35	64.12	2.39	0	0	12.24	3.35	2.15
69.95	36.63	33.41	0.94	0	0	17.14	1.68	1.07
99.2	23.96	47.19	1.38	0	0	14.76	2.39	1.52
165.42	12.93	75.11	3.04	0	0	11.07	3.99	2.56
147.41	15.49	66.6	2.75	0	0	11.88	3.56	2.29
157.36	13.98	71.49	2.83	0	0	11.43	3.79	2.43
167.01	13.28	74.05	3.52	0	0	11.03	4.04	2.6
168.56	12.97	75.6	3.32	0	0	10.97	4.07	2.62
126.03	17.62	59.43	1.72	0	0	13.03	3.04	1.93
38.61	72.55	18.21	0.57	0	0	17.72	0.93	0.59
135.78	16.97	62.19	2.23	0	0	12.52	3.27	2.09
159.57	13.9	71.22	3.23	0	0	11.31	3.86	2.49
165.25	13.29	73.82	3.29	0	0	11.1	4	2.57
57.91	53.63	25.02	0.96	0	0	17.94	1.4	0.9
46.28	60.59	21.4	0.73	0	0	18.04	1.12	0.72
173.83	12.4	77.65	3.57	0	0	10.75	4.2	2.71
159.73	13.94	71.64	3.12	0	0	11.33	3.86	2.48
167.97	13.04	75.35	3.29	0	0	11	4.05	2.61
69.98	42.62	30.56	1.19	0	0	17.26	1.69	1.09
68.75	43.5	30.11	1.17	0	0	17.32	1.66	1.07
174.69	11.97	79.49	3.15	0	0	10.74	4.21	2.7
169.2	13.07	75.22	3.4	0	0	10.99	4.09	2.63
69.16	41.95	30.53	1.1	0	0	17.38	1.67	1.07
37.9	76.53	17.53	0.57	0	0	17.6	0.91	0.58
129.04	17.88	59.33	2.17	0	0	12.8	3.11	1.99
42.62	63.94	20.4	0.55	0	0	18.26	1.02	0.65
109.23	21.49	51.51	1.51	0	0	14.12	2.63	1.67
163.19	13.28	73.48	3.27	0	0	11.11	3.95	2.54
85.37	28.32	40.41	1.62	0	0	15.33	2.06	1.33

149.25	15.73	66.08	3.15	0	0	11.79	3.61	2.33
145.7	16.23	64.39	3.06	0	0	11.97	3.53	2.28
145.33	15.38	66.21	2.55	0	0	11.97	3.51	2.25
166.16	13.05	74.52	3.36	0	0	11.01	4.02	2.58
158.69	13.72	71.85	2.96	0	0	11.34	3.83	2.46
123.48	18.77	56.9	2.04	0	0	13.12	2.98	1.91
286.84	5.14	130	6.98	0	0	8.01	6.93	4.46
241.86	6.73	110.93	5.6	0	0	8.66	5.85	3.76
130.78	17.94	59.27	2.35	0	0	12.73	3.16	2.03
89.53	26.83	42.15	1.59	0	0	15.16	2.16	1.39
156.14	14.24	70.44	2.94	0	0	11.47	3.77	2.42
154.94	14.37	69.96	2.92	0	0	11.52	3.74	2.4
159.94	13.7	72.07	3.03	0	0	11.31	3.87	2.48
162.91	13.29	73.5	3.12	0	0	11.16	3.94	2.53
152.98	14.51	69.38	2.79	0	0	11.61	3.69	2.37
146.72	15.04	67.32	2.54	0	0	11.87	3.54	2.27
147.19	15.1	67.23	2.6	0	0	11.86	3.55	2.28
103.19	22.14	49.3	1.58	0	0	14.25	2.49	1.59
150.66	13.91	70.33	2.42	0	0	11.62	3.63	2.32
152.32	14.41	69.36	2.67	0	0	11.64	3.68	2.35
132.86	16.91	61.32	2.1	0	0	12.62	3.21	2.05
142.21	15.69	65.36	2.36	0	0	12.12	3.43	2.19
128.54	16.16	61.93	2.16	0	0	12.41	3.1	1.98
164.3	12.9	75.02	2.73	0	0	11.18	3.96	2.53
142.71	15.58	65.1	2.38	0	0	12.13	3.45	2.2
135.39	16.7	61.9	2.21	0	0	12.52	3.27	2.09
152.16	14.28	69.01	2.71	0	0	11.64	3.68	2.36
153.49	14.2	69.36	2.78	0	0	11.59	3.71	2.38
123.63	18.1	58.09	1.98	0	0	12.99	2.98	1.9
131.32	17.15	60.97	2.1	0	0	12.66	3.17	2.02
173.7	11.68	79.98	2.81	0	0	10.78	4.19	2.67
199.35	9.39	91.98	3.27	0	0	9.91	4.81	3.06
117.24	19.74	55.26	1.75	0	0	13.49	2.82	1.8
95.06	24.53	45.86	1.41	0	0	14.85	2.29	1.46
149.35	14.46	69.25	2.46	0	0	11.73	3.6	2.3
88.01	27.7	41.7	1.32	0	0	15.53	2.12	1.35
32.65	86.22	15.42	0.46	0	0	17.11	0.79	0.5
171.35	12.65	76.81	3.5	0	0	10.83	4.14	2.67
161.62	13.59	72.85	3	0	0	11.27	3.9	2.5
161.55	13.75	72.38	3.14	0	0	11.27	3.9	2.51
39.63	71.03	18.54	0.61	0	0	17.75	0.95	0.61
108.52	22.01	50.46	1.82	0	0	14	2.62	1.68
133.71	17.93	60.2	2.82	0	0	12.44	3.23	2.09
140.88	17.23	62.39	2.75	0	0	12.3	3.4	2.19
155.89	14.76	69.9	3.04	0	0	11.52	3.76	2.42
125.11	19.96	56.2	2.15	0	0	13.24	3.01	1.93
159.83	13.79	72.84	2.78	0	0	11.36	3.85	2.47

116.94	21.16	53.1	2	0	0	13.63	2.82	1.81
99.55	25.23	45.54	1.73	0	0	14.71	2.4	1.54
98.44	26.24	44.77	1.68	0	0	14.88	2.37	1.52
98.44	26.24	44.77	1.68	0	0	14.88	2.37	1.52
101.5	23.76	47.59	1.75	0	0	14.38	2.44	1.57
89.11	31.19	39.72	1.39	0	0	15.92	2.15	1.38
102.91	28.29	44.58	1.36	0	0	15.46	2.48	1.58
126.26	18.58	58.49	1.89	0	0	13.09	3.04	1.94
126.26	18.58	58.49	1.89	0	0	13.09	3.04	1.94
102.99	22.76	49.26	1.41	0	0	14.47	2.48	1.58
103.86	20.84	51.29	1.53	0	0	13.97	2.5	1.59
112.89	19.9	53.99	1.74	0	0	13.57	2.72	1.74
112.89	19.9	53.99	1.74	0	0	13.57	2.72	1.74
119.55	21.51	53.56	1.69	0	0	13.89	2.88	1.84
105.94	24.39	48.32	1.42	0	0	14.73	2.55	1.62
98.86	26.1	45.54	1.28	0	0	15.21	2.38	1.51
110.27	23.98	49.51	1.49	0	0	14.57	2.65	1.69
110.27	23.98	49.51	1.49	0	0	14.57	2.65	1.69
78.14	33.23	36.57	1.17	0	0	16.44	1.88	1.2
100.43	25.93	45.86	1.4	0	0	15.05	2.42	1.54
162.57	13.62	73.91	2.61	0	0	11.36	3.91	2.5
138.11	18.1	61.15	2.32	0	0	12.68	3.33	2.13
121.37	19.51	55.96	2.04	0	0	13.25	2.92	1.87
121.37	19.51	55.96	2.04	0	0	13.25	2.92	1.87
79.03	34.03	36.67	1.07	0	0	16.63	1.9	1.21
92.43	28.84	42.38	1.19	0	0	15.77	2.22	1.42
152.22	15.42	68.37	2.56	0	0	11.87	3.66	2.35
128.96	19.46	57.7	2.21	0	0	13.06	3.1	1.99
128.96	19.46	57.7	2.21	0	0	13.06	3.1	1.99
160.21	14.31	71.43	3.25	0	0	11.34	3.87	2.49
132.08	18.6	59.16	2.42	0	0	12.77	3.18	2.05
119.58	20.73	54.19	2.1	0	0	13.46	2.88	1.85
149.41	16.7	65.04	2.74	0	0	12.13	3.6	2.32
139.06	18.26	60.83	2.46	0	0	12.65	3.35	2.15
139.06	18.26	60.83	2.46	0	0	12.65	3.35	2.15
143.47	17.36	62.83	2.72	0	0	12.32	3.46	2.23
177.56	12.56	78.33	4	0	0	10.64	4.29	2.77
170.09	13.34	75.02	3.63	0	0	10.96	4.11	2.65
162.14	15.27	69.66	3.6	0	0	11.44	3.92	2.54
142.84	17.53	62.29	2.72	0	0	12.38	3.45	2.22
158.83	14.54	70.61	2.81	0	0	11.57	3.83	2.46
137.56	17.88	60.83	2.2	0	0	12.76	3.32	2.12
161.31	14.5	70.39	3.39	0	0	11.38	3.9	2.52
158.46	14.79	69.34	3.24	0	0	11.51	3.83	2.47
147.99	15.57	66.08	2.92	0	0	11.86	3.58	2.3
163.15	14.09	71.64	3.3	0	0	11.31	3.95	2.54
135.7	18.18	59.49	2.65	0	0	12.63	3.29	2.12

100.66	25.11	45.68	1.54	0	0	14.89	2.43	1.55
141.01	16.85	63.66	2.53	0	0	12.27	3.4	2.18
145.31	16.4	65.17	2.67	0	0	12.09	3.5	2.25
146.97	15.68	66.49	2.78	0	0	11.88	3.54	2.28
143.25	16.12	65.16	2.56	0	0	12.1	3.45	2.21
135.18	17.11	62.26	2.15	0	0	12.55	3.25	2.08
139.29	16.77	63.31	2.5	0	0	12.29	3.36	2.15
142.89	15.61	65.96	2.41	0	0	12.05	3.44	2.2

xCO2_adj_	pCO2_air_(	Windspeed	CO2_Flux_(	CO2_Flux_:	CO2_Const	KHSO4	pH_Scale	Air_Sea_Flu
356.23	0	0	0	0	"K1 K2 fro	"Dickson"	"Total scal	"Wanninkh
378.2	0	0	0	0	"K1 K2 fro	"Dickson"	"Total scal	"Wanninkh
392.34	0	0	0	0	"K1 K2 fro	"Dickson"	"Total scal	"Wanninkh
530.16	0	0	0	0	"K1 K2 fro	"Dickson"	"Total scal	"Wanninkh
337.42	0	0	0	0	"K1 K2 fro	"Dickson"	"Total scal	"Wanninkh
908.02	0	0	0	0	"K1 K2 fro	"Dickson"	"Total scal	"Wanninkh
327.99	0	0	0	0	"K1 K2 fro	"Dickson"	"Total scal	"Wanninkh
363.08	0	0	0	0	"K1 K2 fro	"Dickson"	"Total scal	"Wanninkh
353.6	0	0	0	0	"K1 K2 fro	"Dickson"	"Total scal	"Wanninkh
948.57	0	0	0	0	"K1 K2 fro	"Dickson"	"Total scal	"Wanninkh
911.87	0	0	0	0	"K1 K2 fro	"Dickson"	"Total scal	"Wanninkh
394.23	0	0	0	0	"K1 K2 fro	"Dickson"	"Total scal	"Wanninkh
408.69	0	0	0	0	"K1 K2 fro	"Dickson"	"Total scal	"Wanninkh
372.39	0	0	0	0	"K1 K2 fro	"Dickson"	"Total scal	"Wanninkh
413.52	0	0	0	0	"K1 K2 fro	"Dickson"	"Total scal	"Wanninkh
607.17	0	0	0	0	"K1 K2 fro	"Dickson"	"Total scal	"Wanninkh
703.16	0	0	0	0	"K1 K2 fro	"Dickson"	"Total scal	"Wanninkh
557.48	0	0	0	0	"K1 K2 fro	"Dickson"	"Total scal	"Wanninkh
724.01	0	0	0	0	"K1 K2 fro	"Dickson"	"Total scal	"Wanninkh
442.57	0	0	0	0	"K1 K2 fro	"Dickson"	"Total scal	"Wanninkh
914.8	0	0	0	0	"K1 K2 fro	"Dickson"	"Total scal	"Wanninkh
1935	0	0	0	0	"K1 K2 fro	"Dickson"	"Total scal	"Wanninkh
390.72	0	0	0	0	"K1 K2 fro	"Dickson"	"Total scal	"Wanninkh
2137.46	0	0	0	0	"K1 K2 fro	"Dickson"	"Total scal	"Wanninkh
558.93	0	0	0	0	"K1 K2 fro	"Dickson"	"Total scal	"Wanninkh
514.88	0	0	0	0	"K1 K2 fro	"Dickson"	"Total scal	"Wanninkh
374.12	0	0	0	0	"K1 K2 fro	"Dickson"	"Total scal	"Wanninkh
414.12	0	0	0	0	"K1 K2 fro	"Dickson"	"Total scal	"Wanninkh
633.19	0	0	0	0	"K1 K2 fro	"Dickson"	"Total scal	"Wanninkh
1997.64	0	0	0	0	"K1 K2 fro	"Dickson"	"Total scal	"Wanninkh
622.78	0	0	0	0	"K1 K2 fro	"Dickson"	"Total scal	"Wanninkh
2247.14	0	0	0	0	"K1 K2 fro	"Dickson"	"Total scal	"Wanninkh
429.28	0	0	0	0	"K1 K2 fro	"Dickson"	"Total scal	"Wanninkh
407.08	0	0	0	0	"K1 K2 fro	"Dickson"	"Total scal	"Wanninkh
2793.85	0	0	0	0	"K1 K2 fro	"Dickson"	"Total scal	"Wanninkh
441.66	0	0	0	0	"K1 K2 fro	"Dickson"	"Total scal	"Wanninkh
509.93	0	0	0	0	"K1 K2 fro	"Dickson"	"Total scal	"Wanninkh
639.7	0	0	0	0	"K1 K2 fro	"Dickson"	"Total scal	"Wanninkh
524.43	0	0	0	0	"K1 K2 fro	"Dickson"	"Total scal	"Wanninkh
510.56	0	0	0	0	"K1 K2 fro	"Dickson"	"Total scal	"Wanninkh
580.94	0	0	0	0	"K1 K2 fro	"Dickson"	"Total scal	"Wanninkh
429.03	0	0	0	0	"K1 K2 fro	"Dickson"	"Total scal	"Wanninkh
515.54	0	0	0	0	"K1 K2 fro	"Dickson"	"Total scal	"Wanninkh
530.11	0	0	0	0	"K1 K2 fro	"Dickson"	"Total scal	"Wanninkh
421.56	0	0	0	0	"K1 K2 fro	"Dickson"	"Total scal	"Wanninkh
456.94	0	0	0	0	"K1 K2 fro	"Dickson"	"Total scal	"Wanninkh

510.97	0	0	0	0	"K1 K2 froı	"Dickson"	"Total scal	"Wanninkł
423.09	0	0	0	0	"K1 K2 froı	"Dickson"	"Total scal	"Wanninkł
545.83	0	0	0	0	"K1 K2 froı	"Dickson"	"Total scal	"Wanninkł
517.2	0	0	0	0	"K1 K2 froı	"Dickson"	"Total scal	"Wanninkł
487.72	0	0	0	0	"K1 K2 froı	"Dickson"	"Total scal	"Wanninkł
556.54	0	0	0	0	"K1 K2 froı	"Dickson"	"Total scal	"Wanninkł
486.75	0	0	0	0	"K1 K2 froı	"Dickson"	"Total scal	"Wanninkł
345.25	0	0	0	0	"K1 K2 froı	"Dickson"	"Total scal	"Wanninkł
648.41	0	0	0	0	"K1 K2 froı	"Dickson"	"Total scal	"Wanninkł
609.87	0	0	0	0	"K1 K2 froı	"Dickson"	"Total scal	"Wanninkł
384.04	0	0	0	0	"K1 K2 froı	"Dickson"	"Total scal	"Wanninkł
426.18	0	0	0	0	"K1 K2 froı	"Dickson"	"Total scal	"Wanninkł
345.44	0	0	0	0	"K1 K2 froı	"Dickson"	"Total scal	"Wanninkł
525.2	0	0	0	0	"K1 K2 froı	"Dickson"	"Total scal	"Wanninkł
447.76	0	0	0	0	"K1 K2 froı	"Dickson"	"Total scal	"Wanninkł
572.82	0	0	0	0	"K1 K2 froı	"Dickson"	"Total scal	"Wanninkł
336.19	0	0	0	0	"K1 K2 froı	"Dickson"	"Total scal	"Wanninkł
329.57	0	0	0	0	"K1 K2 froı	"Dickson"	"Total scal	"Wanninkł
444.07	0	0	0	0	"K1 K2 froı	"Dickson"	"Total scal	"Wanninkł
909.62	0	0	0	0	"K1 K2 froı	"Dickson"	"Total scal	"Wanninkł
595.04	0	0	0	0	"K1 K2 froı	"Dickson"	"Total scal	"Wanninkł
357.23	0	0	0	0	"K1 K2 froı	"Dickson"	"Total scal	"Wanninkł
437.91	0	0	0	0	"K1 K2 froı	"Dickson"	"Total scal	"Wanninkł
385.44	0	0	0	0	"K1 K2 froı	"Dickson"	"Total scal	"Wanninkł
393.94	0	0	0	0	"K1 K2 froı	"Dickson"	"Total scal	"Wanninkł
372.36	0	0	0	0	"K1 K2 froı	"Dickson"	"Total scal	"Wanninkł
425.7	0	0	0	0	"K1 K2 froı	"Dickson"	"Total scal	"Wanninkł
1934.39	0	0	0	0	"K1 K2 froı	"Dickson"	"Total scal	"Wanninkł
452.28	0	0	0	0	"K1 K2 froı	"Dickson"	"Total scal	"Wanninkł
405.17	0	0	0	0	"K1 K2 froı	"Dickson"	"Total scal	"Wanninkł
383.53	0	0	0	0	"K1 K2 froı	"Dickson"	"Total scal	"Wanninkł
1542.07	0	0	0	0	"K1 K2 froı	"Dickson"	"Total scal	"Wanninkł
1656.89	0	0	0	0	"K1 K2 froı	"Dickson"	"Total scal	"Wanninkł
361.54	0	0	0	0	"K1 K2 froı	"Dickson"	"Total scal	"Wanninkł
399.75	0	0	0	0	"K1 K2 froı	"Dickson"	"Total scal	"Wanninkł
373.17	0	0	0	0	"K1 K2 froı	"Dickson"	"Total scal	"Wanninkł
1227.16	0	0	0	0	"K1 K2 froı	"Dickson"	"Total scal	"Wanninkł
1253.27	0	0	0	0	"K1 K2 froı	"Dickson"	"Total scal	"Wanninkł
326.08	0	0	0	0	"K1 K2 froı	"Dickson"	"Total scal	"Wanninkł
379.63	0	0	0	0	"K1 K2 froı	"Dickson"	"Total scal	"Wanninkł
1163.66	0	0	0	0	"K1 K2 froı	"Dickson"	"Total scal	"Wanninkł
2063.71	0	0	0	0	"K1 K2 froı	"Dickson"	"Total scal	"Wanninkł
482.01	0	0	0	0	"K1 K2 froı	"Dickson"	"Total scal	"Wanninkł
1578.21	0	0	0	0	"K1 K2 froı	"Dickson"	"Total scal	"Wanninkł
530.14	0	0	0	0	"K1 K2 froı	"Dickson"	"Total scal	"Wanninkł
382.93	0	0	0	0	"K1 K2 froı	"Dickson"	"Total scal	"Wanninkł
817.27	0	0	0	0	"K1 K2 froı	"Dickson"	"Total scal	"Wanninkł

473.57	0	0	0	0	"K1 K2 froı	"Dickson"	"Total scal	"Wanninkł
488.37	0	0	0	0	"K1 K2 froı	"Dickson"	"Total scal	"Wanninkł
419.63	0	0	0	0	"K1 K2 froı	"Dickson"	"Total scal	"Wanninkł
378.13	0	0	0	0	"K1 K2 froı	"Dickson"	"Total scal	"Wanninkł
383.17	0	0	0	0	"K1 K2 froı	"Dickson"	"Total scal	"Wanninkł
502.54	0	0	0	0	"K1 K2 froı	"Dickson"	"Total scal	"Wanninkł
148.38	0	0	0	0	"K1 K2 froı	"Dickson"	"Total scal	"Wanninkł
194.16	0	0	0	0	"K1 K2 froı	"Dickson"	"Total scal	"Wanninkł
500.6	0	0	0	0	"K1 K2 froı	"Dickson"	"Total scal	"Wanninkł
749.09	0	0	0	0	"K1 K2 froı	"Dickson"	"Total scal	"Wanninkł
401.39	0	0	0	0	"K1 K2 froı	"Dickson"	"Total scal	"Wanninkł
405.04	0	0	0	0	"K1 K2 froı	"Dickson"	"Total scal	"Wanninkł
385.94	0	0	0	0	"K1 K2 froı	"Dickson"	"Total scal	"Wanninkł
375.08	0	0	0	0	"K1 K2 froı	"Dickson"	"Total scal	"Wanninkł
402.76	0	0	0	0	"K1 K2 froı	"Dickson"	"Total scal	"Wanninkł
406.53	0	0	0	0	"K1 K2 froı	"Dickson"	"Total scal	"Wanninkł
413.25	0	0	0	0	"K1 K2 froı	"Dickson"	"Total scal	"Wanninkł
570.54	0	0	0	0	"K1 K2 froı	"Dickson"	"Total scal	"Wanninkł
358.26	0	0	0	0	"K1 K2 froı	"Dickson"	"Total scal	"Wanninkł
391.76	0	0	0	0	"K1 K2 froı	"Dickson"	"Total scal	"Wanninkł
439.84	0	0	0	0	"K1 K2 froı	"Dickson"	"Total scal	"Wanninkł
417.39	0	0	0	0	"K1 K2 froı	"Dickson"	"Total scal	"Wanninkł
424.96	0	0	0	0	"K1 K2 froı	"Dickson"	"Total scal	"Wanninkł
339.15	0	0	0	0	"K1 K2 froı	"Dickson"	"Total scal	"Wanninkł
414.37	0	0	0	0	"K1 K2 froı	"Dickson"	"Total scal	"Wanninkł
441.11	0	0	0	0	"K1 K2 froı	"Dickson"	"Total scal	"Wanninkł
389.1	0	0	0	0	"K1 K2 froı	"Dickson"	"Total scal	"Wanninkł
390.28	0	0	0	0	"K1 K2 froı	"Dickson"	"Total scal	"Wanninkł
473.47	0	0	0	0	"K1 K2 froı	"Dickson"	"Total scal	"Wanninkł
448.7	0	0	0	0	"K1 K2 froı	"Dickson"	"Total scal	"Wanninkł
299.55	0	0	0	0	"K1 K2 froı	"Dickson"	"Total scal	"Wanninkł
238.18	0	0	0	0	"K1 K2 froı	"Dickson"	"Total scal	"Wanninkł
503.53	0	0	0	0	"K1 K2 froı	"Dickson"	"Total scal	"Wanninkł
625.84	0	0	0	0	"K1 K2 froı	"Dickson"	"Total scal	"Wanninkł
380.25	0	0	0	0	"K1 K2 froı	"Dickson"	"Total scal	"Wanninkł
718.32	0	0	0	0	"K1 K2 froı	"Dickson"	"Total scal	"Wanninkł
2235.03	0	0	0	0	"K1 K2 froı	"Dickson"	"Total scal	"Wanninkł
368.67	0	0	0	0	"K1 K2 froı	"Dickson"	"Total scal	"Wanninkł
379.96	0	0	0	0	"K1 K2 froı	"Dickson"	"Total scal	"Wanninkł
393.3	0	0	0	0	"K1 K2 froı	"Dickson"	"Total scal	"Wanninkł
1928.29	0	0	0	0	"K1 K2 froı	"Dickson"	"Total scal	"Wanninkł
597.4	0	0	0	0	"K1 K2 froı	"Dickson"	"Total scal	"Wanninkł
543.63	0	0	0	0	"K1 K2 froı	"Dickson"	"Total scal	"Wanninkł
504.16	0	0	0	0	"K1 K2 froı	"Dickson"	"Total scal	"Wanninkł
427.56	0	0	0	0	"K1 K2 froı	"Dickson"	"Total scal	"Wanninkł
554.45	0	0	0	0	"K1 K2 froı	"Dickson"	"Total scal	"Wanninkł
374.22	0	0	0	0	"K1 K2 froı	"Dickson"	"Total scal	"Wanninkł

585.63	0	0	0	0	"K1 K2 froı	"Dickson"	"Total scal	"Wanninkh
704.19	0	0	0	0	"K1 K2 froı	"Dickson"	"Total scal	"Wanninkh
733.07	0	0	0	0	"K1 K2 froı	"Dickson"	"Total scal	"Wanninkh
733.07	0	0	0	0	"K1 K2 froı	"Dickson"	"Total scal	"Wanninkh
656.05	0	0	0	0	"K1 K2 froı	"Dickson"	"Total scal	"Wanninkh
848.32	0	0	0	0	"K1 K2 froı	"Dickson"	"Total scal	"Wanninkh
719.23	0	0	0	0	"K1 K2 froı	"Dickson"	"Total scal	"Wanninkh
476.52	0	0	0	0	"K1 K2 froı	"Dickson"	"Total scal	"Wanninkh
476.52	0	0	0	0	"K1 K2 froı	"Dickson"	"Total scal	"Wanninkh
558.37	0	0	0	0	"K1 K2 froı	"Dickson"	"Total scal	"Wanninkh
521.42	0	0	0	0	"K1 K2 froı	"Dickson"	"Total scal	"Wanninkh
512.27	0	0	0	0	"K1 K2 froı	"Dickson"	"Total scal	"Wanninkh
512.27	0	0	0	0	"K1 K2 froı	"Dickson"	"Total scal	"Wanninkh
548.47	0	0	0	0	"K1 K2 froı	"Dickson"	"Total scal	"Wanninkh
608.18	0	0	0	0	"K1 K2 froı	"Dickson"	"Total scal	"Wanninkh
640.44	0	0	0	0	"K1 K2 froı	"Dickson"	"Total scal	"Wanninkh
602.02	0	0	0	0	"K1 K2 froı	"Dickson"	"Total scal	"Wanninkh
602.02	0	0	0	0	"K1 K2 froı	"Dickson"	"Total scal	"Wanninkh
872.6	0	0	0	0	"K1 K2 froı	"Dickson"	"Total scal	"Wanninkh
659.29	0	0	0	0	"K1 K2 froı	"Dickson"	"Total scal	"Wanninkh
356.38	0	0	0	0	"K1 K2 froı	"Dickson"	"Total scal	"Wanninkh
498.21	0	0	0	0	"K1 K2 froı	"Dickson"	"Total scal	"Wanninkh
530	0	0	0	0	"K1 K2 froı	"Dickson"	"Total scal	"Wanninkh
530	0	0	0	0	"K1 K2 froı	"Dickson"	"Total scal	"Wanninkh
860.75	0	0	0	0	"K1 K2 froı	"Dickson"	"Total scal	"Wanninkh
710.27	0	0	0	0	"K1 K2 froı	"Dickson"	"Total scal	"Wanninkh
418.1	0	0	0	0	"K1 K2 froı	"Dickson"	"Total scal	"Wanninkh
540.97	0	0	0	0	"K1 K2 froı	"Dickson"	"Total scal	"Wanninkh
540.97	0	0	0	0	"K1 K2 froı	"Dickson"	"Total scal	"Wanninkh
421.26	0	0	0	0	"K1 K2 froı	"Dickson"	"Total scal	"Wanninkh
531.26	0	0	0	0	"K1 K2 froı	"Dickson"	"Total scal	"Wanninkh
581.17	0	0	0	0	"K1 K2 froı	"Dickson"	"Total scal	"Wanninkh
478.06	0	0	0	0	"K1 K2 froı	"Dickson"	"Total scal	"Wanninkh
516.37	0	0	0	0	"K1 K2 froı	"Dickson"	"Total scal	"Wanninkh
516.37	0	0	0	0	"K1 K2 froı	"Dickson"	"Total scal	"Wanninkh
504.83	0	0	0	0	"K1 K2 froı	"Dickson"	"Total scal	"Wanninkh
385.64	0	0	0	0	"K1 K2 froı	"Dickson"	"Total scal	"Wanninkh
400.93	0	0	0	0	"K1 K2 froı	"Dickson"	"Total scal	"Wanninkh
476.95	0	0	0	0	"K1 K2 froı	"Dickson"	"Total scal	"Wanninkh
510.8	0	0	0	0	"K1 K2 froı	"Dickson"	"Total scal	"Wanninkh
402.28	0	0	0	0	"K1 K2 froı	"Dickson"	"Total scal	"Wanninkh
477.41	0	0	0	0	"K1 K2 froı	"Dickson"	"Total scal	"Wanninkh
434.95	0	0	0	0	"K1 K2 froı	"Dickson"	"Total scal	"Wanninkh
438.56	0	0	0	0	"K1 K2 froı	"Dickson"	"Total scal	"Wanninkh
452.06	0	0	0	0	"K1 K2 froı	"Dickson"	"Total scal	"Wanninkh
413.97	0	0	0	0	"K1 K2 froı	"Dickson"	"Total scal	"Wanninkh
533.93	0	0	0	0	"K1 K2 froı	"Dickson"	"Total scal	"Wanninkh

661.36	0	0	0	0	"K1 K2 froı	"Dickson"	"Total scal	"Wanninkł
472.87	0	0	0	0	"K1 K2 froı	"Dickson"	"Total scal	"Wanninkł
465.7	0	0	0	0	"K1 K2 froı	"Dickson"	"Total scal	"Wanninkł
447.95	0	0	0	0	"K1 K2 froı	"Dickson"	"Total scal	"Wanninkł
447.77	0	0	0	0	"K1 K2 froı	"Dickson"	"Total scal	"Wanninkł
450.64	0	0	0	0	"K1 K2 froı	"Dickson"	"Total scal	"Wanninkł
468.8	0	0	0	0	"K1 K2 froı	"Dickson"	"Total scal	"Wanninkł
418.69	0	0	0	0	"K1 K2 froı	"Dickson"	"Total scal	"Wanninkł

Windspeed_units
"m/sec"
"m/sec"
"m/sec"
"m/sec"
"m/sec"
"m/sec"
"m/sec"
"m/sec"
"m/sec"
"m/sec"
"m/sec"
"m/sec"
"m/sec"
"m/sec"
"m/sec"
"m/sec"
"m/sec"
"m/sec"
"m/sec"
"m/sec"
"m/sec"
"m/sec"
"m/sec"
"m/sec"
"m/sec"
"m/sec"
"m/sec"
"m/sec"
"m/sec"
"m/sec"
"m/sec"
"m/sec"
"m/sec"
"m/sec"
"m/sec"
"m/sec"
"m/sec"
"m/sec"
"m/sec"
"m/sec"
"m/sec"
"m/sec"
"m/sec"
"m/sec"
"m/sec"
"m/sec"

"m/sec"
"m/sec"
"m/sec"
"m/sec"
"m/sec"
"m/sec"
"m/sec"
"m/sec"
"m/sec"
"m/sec"
"m/sec"
"m/sec"
"m/sec"
"m/sec"
"m/sec"
"m/sec"
"m/sec"
"m/sec"
"m/sec"
"m/sec"
"m/sec"
"m/sec"
"m/sec"
"m/sec"
"m/sec"
"m/sec"
"m/sec"
"m/sec"
"m/sec"
"m/sec"
"m/sec"
"m/sec"
"m/sec"
"m/sec"
"m/sec"
"m/sec"
"m/sec"
"m/sec"
"m/sec"
"m/sec"
"m/sec"
"m/sec"
"m/sec"
"m/sec"
"m/sec"
"m/sec"
"m/sec"

"m/sec"
"m/sec"
"m/sec"
"m/sec"
"m/sec"
"m/sec"
"m/sec"
"m/sec"
"m/sec"
"m/sec"
"m/sec"
"m/sec"
"m/sec"
"m/sec"
"m/sec"
"m/sec"
"m/sec"
"m/sec"
"m/sec"
"m/sec"
"m/sec"
"m/sec"
"m/sec"
"m/sec"
"m/sec"
"m/sec"
"m/sec"
"m/sec"
"m/sec"
"m/sec"
"m/sec"
"m/sec"
"m/sec"
"m/sec"
"m/sec"
"m/sec"
"m/sec"
"m/sec"
"m/sec"
"m/sec"
"m/sec"
"m/sec"
"m/sec"
"m/sec"
"m/sec"
"m/sec"
"m/sec"

"m/sec"
"m/sec"
"m/sec"
"m/sec"
"m/sec"
"m/sec"
"m/sec"
"m/sec"
"m/sec"
"m/sec"
"m/sec"
"m/sec"
"m/sec"
"m/sec"
"m/sec"
"m/sec"
"m/sec"
"m/sec"
"m/sec"
"m/sec"
"m/sec"
"m/sec"
"m/sec"
"m/sec"
"m/sec"
"m/sec"
"m/sec"
"m/sec"
"m/sec"
"m/sec"
"m/sec"
"m/sec"
"m/sec"
"m/sec"
"m/sec"
"m/sec"
"m/sec"
"m/sec"
"m/sec"
"m/sec"
"m/sec"
"m/sec"
"m/sec"
"m/sec"
"m/sec"
"m/sec"
"m/sec"

"m/sec"
"m/sec"
"m/sec"
"m/sec"
"m/sec"
"m/sec"
"m/sec"
"m/sec"

PROCEEDINGS OF THE ROYAL SOCIETY B BIOLOGICAL SCIENCES

Limacina helicina shell dissolution as an indicator of declining habitat suitability owing to ocean acidification in the California Current Ecosystem

N. Bednarsek, R. A. Feely, J. C. P. Reum, B. Peterson, J. Menkel, S. R. Alin and B. Hales

Proc. R. Soc. B 2014 **281**, 20140123, published 30 April 2014

PROCEEDINGS OF THE ROYAL SOCIETY B

rspb.royalsocietypublishing.org

Research

Cite this article: Bednaršek N, Feely RA, Reum JCP, Peterson B, Menkel J, Alin SR, Hales B. 2014 *Limacina helicina* shell dissolution as an indicator of declining habitat suitability owing to ocean acidification in the California Current Ecosystem. *Proc. R. Soc. B* **281**: 20140123.
http://dx.doi.org/10.1098/rspb.2014.0123

Received: 17 January 2014
Accepted: 2 April 2014

Subject Areas:
environmental science, ecology

Keywords:
pteropods, ocean acidification, dissolution, aragonite undersaturation, habitat reduction

Author for correspondence:
N. Bednaršek
e-mail: nina.bednarsek@noaa.gov

Electronic supplementary material is available at http://dx.doi.org/10.1098/rspb.2014.0123 or via http://rspb.royalsocietypublishing.org.

Royal Society Publishing

Limacina helicina shell dissolution as an indicator of declining habitat suitability owing to ocean acidification in the California Current Ecosystem

N. Bednaršek[1], R. A. Feely[1], J. C. P. Reum[2], B. Peterson[3], J. Menkel[4], S. R. Alin[1] and B. Hales[5]

[1]National Oceanic and Atmospheric Administration (NOAA), Pacific Marine Environmental Laboratory (PMEL), 7600 Sand Point Way NE, Seattle, WA 98115, USA
[2]Conservation Biology Division, Northwest Fisheries Science Center, National Marine Fisheries Service, National Oceanic and Atmospheric Administration (NOAA), 2725 Montlake Boulevard East, Seattle, WA 98112, USA
[3]NOAA NMFS NW Fisheries Science Center, 2030 SE Marine Science Drive, Newport, OR 97365, USA
[4]Oregon State University, Cooperative Institute for Marine Resources Studies, Hatfield Marine Science Center, 2030 SE Marine Science Drive, Newport, OR 97365, USA
[5]College of Earth, Ocean, and Atmospheric Sciences, Oregon State University, Corvallis, OR 97331, USA

Few studies to date have demonstrated widespread biological impacts of ocean acidification (OA) under conditions currently found in the natural environment. From a combined survey of physical and chemical water properties and biological sampling along the Washington–Oregon–California coast in August 2011, we show that large portions of the shelf waters are corrosive to pteropods in the natural environment. We show a strong positive correlation between the proportion of pteropod individuals with severe shell dissolution damage and the percentage of undersaturated water in the top 100 m with respect to aragonite. We found 53% of onshore individuals and 24% of offshore individuals on average to have severe dissolution damage. Relative to pre-industrial CO_2 concentrations, the extent of undersaturated waters in the top 100 m of the water column has increased over sixfold along the California Current Ecosystem (CCE). We estimate that the incidence of severe pteropod shell dissolution owing to anthropogenic OA has doubled in near shore habitats since pre-industrial conditions across this region and is on track to triple by 2050. These results demonstrate that habitat suitability for pteropods in the coastal CCE is declining. The observed impacts represent a baseline for future observations towards understanding broader scale OA effects.

1. Introduction

The release of carbon dioxide (CO_2) into the atmosphere from fossil fuel burning, cement production and deforestation processes has resulted in atmospheric CO_2 concentrations that have increased about 40% since the beginning of the industrial era [1,2]. The oceans have taken up approximately 28% of the total amount of CO_2 produced by human activities over this time-frame [1–3], causing a variety of chemical changes known as ocean acidification (OA). The process of OA has reduced the average surface ocean pH by about 0.1 and is expected to reduce average pH by another 0.3 units by the end of this century [4,5]. The rapid change in ocean chemistry is faster than at any time over the past 50 Myr [6]. This CO_2 uptake will lead to a reduction in the saturation state of seawater with respect to calcite and aragonite, which are the two most common polymorphs of calcium carbonate ($CaCO_3$) formed by marine organisms [5,7].

High-latitude areas of the open ocean will be the most affected by OA owing to the high solubility of CO_2 in cold waters [8–10]; however, the California Current Ecosystem (CCE) is already experiencing CO_2 concentrations similar to the projections for high-latitude regions, pointing towards enhanced vulnerability to OA [11–14]. This is, in part, owing to the natural process of upwelling, which

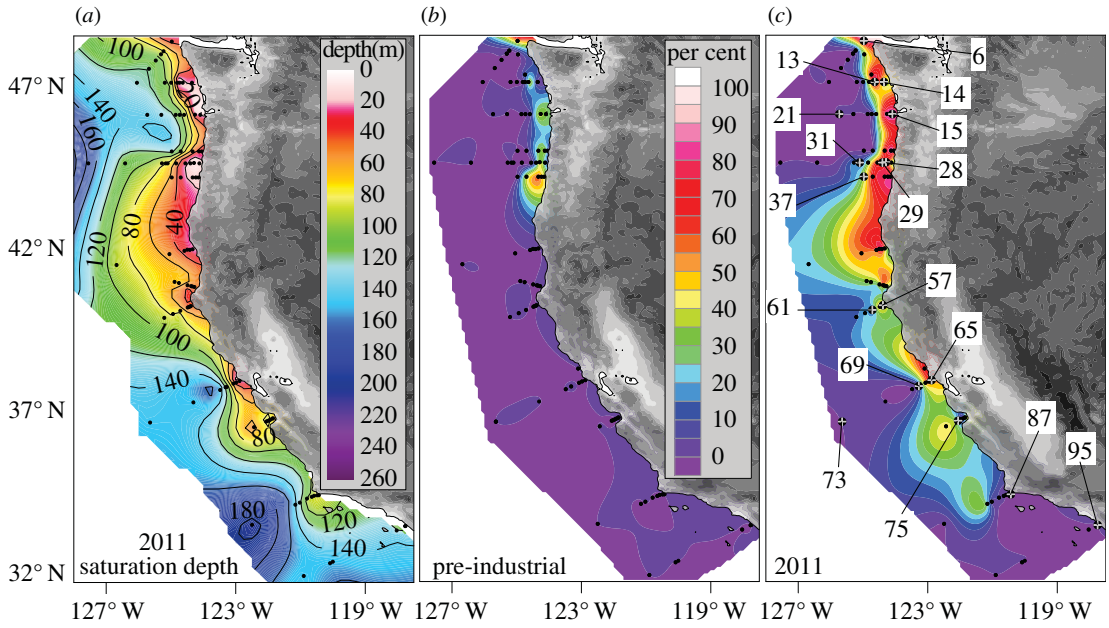

Figure 1. Planview maps. (*a*) Depth of the aragonite saturation horizon along the US West Coast. (*b*) Per cent of upper 100 m of the water column in the CCE estimated to be undersaturated during the (*b*) pre-industrial time and (*c*) the August–September 2011 time period. Pteropod station locations are indicated by numbers within the squares (*c*) and are referred to in figure 3.

brings already CO_2-rich waters from the ocean interior to the shelf environment and adds to the anthropogenic CO_2 contribution. These combined processes result in the greater frequency of thermodynamically unfavourable conditions [14,15], enhancing dissolution of $CaCO_3$ in the water column [16]. The term that quantifies the thermodynamic tendency towards dissolution or precipitation is the saturation state, or Ω_{ar} (omega); for a given $CaCO_3$ mineral, e.g. aragonite, $\Omega_{ar} = [Ca^{2+}][CO_3^{2-}]/K'_{spar}$, where $[Ca^{2+}]$ and $[CO_3^{2-}]$ are concentrations of calcium and carbonate ion, respectively, and K'_{spar} is the apparent solubility product for aragonite. When omega is greater than 1, precipitation is thermodynamically favoured, and when omega is less than 1, there is a thermodynamic tendency towards dissolution. Because of the combined effects of pressure and organic matter remineralization at depth, Ω_{ar} is typically lower at greater depths. The depth at which $\Omega_{ar} = 1$, known as the aragonite saturate horizon, has shoaled by as much as 25–40 m in upwelling shelf waters and approximately 40–100 m in offshore regions of the CCE [11,14]. The CCE is characterized by strong spatial (both horizontal and vertical) and temporal gradients in Ω_{ar} [11,14], with the aragonite saturation shoaling closest to the surface during the summer upwelling season in the Washington–Oregon coastal regions and off northern California. Based on both discrete observations and model calculations, it has been suggested that the upwelled undersaturated source-waters were present 10% of the time at the shelf break in the pre-industrial era, and contemporary ocean source-waters are undersaturated approximately 30% of the time during the upwelling season at the shelf break [12–14]. The upwelled undersaturated waters reach their shallowest depths close to the coast where they occasionally reach the surface [4,11,14]. The results for the 2011 cruise (figure 1*a*,*c*), which are representative of summertime conditions for the last few years, show evidence for corrosive water shoaling along the bottom to depths of about 20–50 m in the coastal waters off Washington, Oregon and northern California, and to depths of 60–120 m off southern California. The Washington–Oregon results are consistent with time-series measurements off Newport, Oregon, which provide evidence for increased fluctuations in Ω_{ar} (range: 0.8–3.8) on time-scales of weeks and very low saturation state waters during the upwelling season from June through to October [14,16]. From the moored saturation state and temperature observations from 2007 through to 2011, it is evident that the upwelling events primarily occur in the summer and early autumn months and last for approximately one to five weeks [14,16]. During this period, offshore surface waters generally have higher aragonite saturation states than the onshore waters (figure 1*a*,*c*). After the upwelling season has ended in November, the surface Ω_{ar} values average about 2.0 (range: 1.8–2.3) and show little variability during the winter and early spring months [14]. The anthropogenic component of the increased dissolved inorganic carbon (DIC) in the upwelled water contributes approximately 10–20% of the total change in Ω_{ar} during the upwelling season [14,16].

For the southern California region, the 2011 Ω_{ar} data in figure 1*a*,*c* are also consistent with the proxy-based 2005–2011 time series of Ω_{ar} data of Alin *et al.* [17] for the CalCOFI region off southern California, which suggest that the aragonite saturation horizon generally varies between depths of about 50–200 m and shows more spatial variability during the summer upwelling season. This makes the CCE an ideal ecosystem to study seasonally persistent OA conditions for better informed predictions of future impacts, especially for species that might be most vulnerable to more intensified and prolonged exposure to OA [18–20].

Pteropods are ubiquitous holoplanktonic calcifiers that are particularly important for their role in carbon flux and energy transfer in pelagic ecosystems. From an evolutionary perspective, a progressively thinner and lighter shell might have

provided pteropods with a competitive advantage for conquering new niches within the pelagic realm [21]. They build shells of aragonite, a more soluble form of $CaCO_3$, and contribute 20–42% towards global carbonate production [22], with higher biomasses in polar areas [23,24] as well as on the continental shelves and areas of high productivity [22]. The CCE includes shelf waters that are among the most biologically productive in the world [25], where the most ubiquitous pteropod species, *Limacina helicina*, can attain high abundances [26] and represent an important prey group for ecologically and economically important fishes, bird and whale diets [27]. Their spatial habitat stretches along the CCE and their vertical habitat encompasses the upper 75–150 m during day and night, with some healthy individuals capable of vertically migrating much deeper [28,29].

The CCE is a major upwelling region that is already experiencing 'acidified' conditions [11–14] under which thin pteropod shells are vulnerable to dissolution [30–32], even by short-term exposures (4–14 days) to near-saturated waters ($\Omega_{ar} \sim 1$), which makes them a suitable indicator for monitoring small-scale changes in the carbonate chemistry environment [30]. The existence of strong vertical gradients in aragonite saturation in the first 100 m of the CCE further accelerated by anthropogenic OA, where undersaturation protrudes into the pteropod vertical habitat provided a setting for estimating quantitative relationships between *in situ* undersaturation and shell dissolution. These quantitative relationships can further be used to evaluate potential changes in reduction of vertical habitat suitability for pteropods over time owing to OA.

2. Material and methods

(a) Carbonate chemistry sampling and analytical methods

For the 2011 West Coast OA (WCOA) cruise, samples were analysed for DIC, total alkalinity (TA) and hydrographic data along 13 cross-shelf transects (figure 1*a*), from 11 August to 3 September 2011. The conditions observed during the 2011 WCOA summer cruise were consistent with other observations and model results for the last several years during the upwelling season [11–17]. Water samples were collected from modified Niskin-type bottles and analysed for DIC, TA, oxygen, nutrients and dissolved and particulate organic carbon. The DIC concentration was determined by gas extraction and coulometry using a modified Single Operator Multi-parameter Metabolic Analyser, with a precision of ± 1.5 µmol kg^{-1}. Seawater TA was measured by acidimetric titration, employing the open-cell method described by Dickson *et al.* [33,34]. The precision for TA was ± 2.0 µmol kg^{-1}. Replicate samples were typically taken for two sample depths at each station. The replicate samples were interspersed throughout station depth for quality assurance. No systematic differences between the replicates were observed. Data accuracy was confirmed by regular analyses of certified reference materials [33].

Using the programme of Lewis & Wallace [35], carbonate ion concentration was calculated using carbonic acid dissociation constants of Lueker *et al.* [36]. The *in situ* degree of saturation of seawater with respect to aragonite and calcite is the ion product of the concentrations of calcium and carbonate ions, at the *in situ* temperature, salinity and pressure, divided by the apparent stoichiometric solubility product (K'_{spar}) for those conditions, where Ca^{2+} concentrations are estimated from the salinity, and carbonate ion concentrations are calculated from the DIC and TA data. The temperature and salinity effect on the solubility is estimated from the equation of Mucci [37] and includes the adjustments to the constants recommended by Millero [38].

(b) Physical–chemical background calculations

We used carbonate chemistry measurements obtained from discrete water samples to develop a linear model for estimating aragonite saturation state (Ω_{ar}) values across depths at each sampling station, based on conductivity, temperature and depth (CTD) depth profiles of oxygen concentrations and temperature. Although predictive algorithms of Ω_{ar} have been developed for the CCE using these variables [17,39], they are not valid for near-surface waters (less than 15 m) and were therefore not applied to our dataset. In preliminary models of Ω_{ar}, we evaluated multiple regression models where temperature and oxygen were included as predictor variables, but we observed residual error structure at the station level. To accommodate this issue and achieve better predictive performance, we fitted a mixed effects model for both variables (temperature (°C) and oxygen (µmol kg^{-1})). We used ln-transformed Ω_{ar} and O_2 to improve normality in the residual error. We evaluated model fit based on the proportion of variance explained by both the fixed and random effects (i.e. the 'conditional r^2') [40] and the root mean square error (RMSE). The final model had a conditional r^2 of 0.99 and a RMSE (based on the original Ω_{ar} scale) of 0.0016, indicating a strong fit to the data, and was subsequently used to predict Ω_{ar} across all depths (0–100 m) with corresponding CTD temperature and oxygen concentration measurements. The model was fitted using the 'nlme' statistical library and implemented in the 'R' statistical software package [41].

(c) Biological sampling

Sampling stations were located from 31 to 48° N and from 122 to 126° W (figure 1*a*,*c*). The survey encompassed three broad regions typified by regional differences in wind and temperature patterns that potentially affect the dynamics of Ω_{ar} [42]. The region north of Cape Mendocino (40.5° N) was denoted as the northern region, between Cape Mendocino and Point Conception (34.5° N) as the central region, and southward from Point Conception (32.4° N) as the southern region (figure 1*c*). Because each transect was conducted in a perpendicular orientation to the coastline, the stations farthest offshore along some transects may cross these boundaries. Onshore and offshore regions were delineated by the 200 m shelf break isobath. Pteropods were sampled using a 1 m diameter Bongo net with a 333 µm mesh net usually towed at a speed of two to three knots for approximately 30 min. As the upper 100 m of the water column is pteropod vertical migration habitat [29], sampling strategy was aimed at vertically integrating the first 100 m of water column. While different pteropod species were caught, only individuals of *L. helicina* were preserved and were subsequently counted and analysed for evidence of dissolution. To estimate abundance in the upper 100 m, the subsample (N) was taken from the original sample reporting counts as depth-integrated abundance (ind m^{-2}) (electronic supplementary material, table S1). For the purpose of the dissolution study, only live individuals were preserved in buffered formalin with pH ~ 8.4, which protected shells from further dissolution; 10 individuals on average were randomly picked from each preserved sample where *L. helicina* individuals were found, usually in the form of juveniles and subadults ranging in lengths from 0.5 to 2.5 mm. The analysed samples contained only forma *Limacina helicina helicina* f. *pacifica*, while f. *acuta* was excluded from analyses in order to not mix potentially genetically different populations. Upon visual inspection with a light microscope, we discarded the shells that were mechanically broken. In the process of shell preparation (described below), some of the shells are usually mechanically destroyed or damaged. Those were discarded and only intact shells were deemed suitable for scanning electron microscopy (SEM) shell analyses.

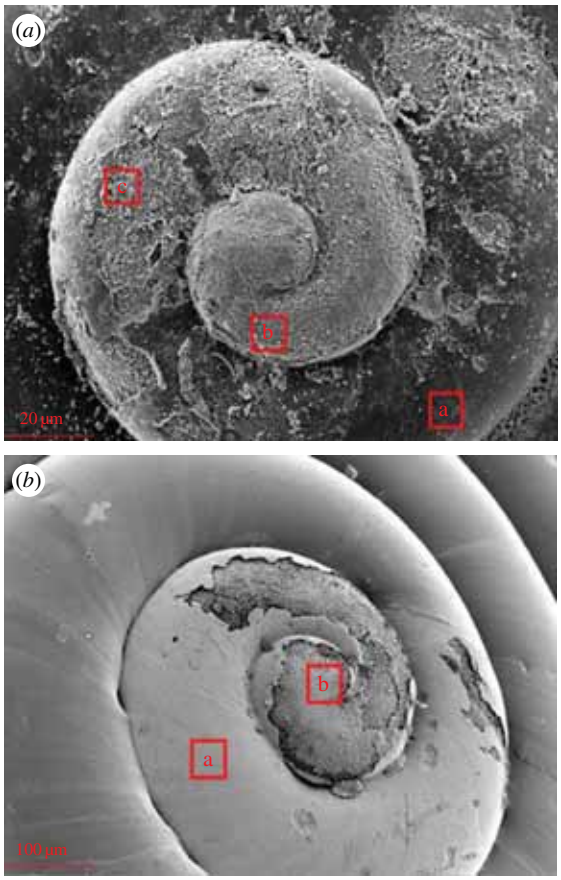

Figure 2. SEM images of shells of the pteropod *Limacina helicina helicina* f. *pacifica* sampled during the 2011 cruise showing signs of *in situ* dissolution from (*a*) an onshore station, with the entire shell affected by dissolution, and (*b*) from the offshore region, with only the protoconch (first whorl) affected. Indicated in the figure are: a, intact surface; b, Type I dissolution; and c, severe dissolution (Type II or Type III): see Material and methods for description of dissolution types. (Online version in colour.)

(d) Shell preparation

We used a non-invasive preparation method on preserved specimens to examine shell surfaces using SEM. A two-step preparation method of dehydration and drying is necessary in order to not introduce methodological artefacts of shell damage created by sheer forces under vacuum inside the SEM. Previous work demonstrated that the chemical treatments do not introduce any additional shell dissolution [30]. Second, plasma etching was applied to remove upper organic layers and expose the structural elements of the shell.

We categorized shell dissolution into three types based on the depth within the crystalline layer to which dissolution extended, following Bednaršek *et al.* [30]. Dissolution characterized by Type II and Type III damage impacts shell fragility [30], and we therefore referred to this kind of damage as severe (figure 2*a*).

(e) Statistical analysis

We evaluated whether the fraction of undersaturated waters in the top 100 m of the water column (as inferred from our model-based estimation of Ω_{ar}) was associated with the incidence of severe shell damage (Type II or Type III damage) in this natural habitat of pteropods. At onshore stations where bottom depths were shallower than 100 m, we estimated the fraction of the total water column that was undersaturated. We modelled the probability of observing severe shell damage using logistic regression where the response variable (severe damage present/not present) was treated as binomial (coded as 1 and 0, respectively) and the predictor variable (per cent undersaturation of the water column) was related to the response variable using a logit link function [43]. We tested whether the model containing the per cent undersaturation term was a significant improvement over the null model (intercept only) using a likelihood ratio test (see equation (3.1) in Results and discussion).

(f) Sensitivity study

We conducted a sensitivity study to evaluate potential differences in Ω_{ar} between present-day conditions and those assuming DIC levels corresponding to pre-industrial and future (2050) atmospheric CO_2 levels. For pre-industrial and future estimates, we assumed that the source-water DIC responded to air–sea CO_2 equilibrium conditions at the time of its last contact with the atmosphere, following Harris *et al.* [14]. Using a modified version of the Feely *et al.* [11] method for calculating Ω_{ar}, Harris *et al.* [14] (see the electronic supplementary material) calculated anthropogenic contribution to DIC to be approximately 53 µmol kg^{-1} during the summer upwelling time. To calculate Ω_{ar} values corresponding to pre-industrial DIC levels, we simply subtracted 53 µmol kg^{-1} from our *in situ* measurements of DIC and recalculated the carbonate system. This carries the implicit assumption that source-water alkalinity has been time-invariant, and that the respiratory modification of TA and DIC have also been constant over time. We estimated a potential anthropogenic contribution of 1.19 µmol kg^{-1} yr^{-1} to DIC or 46.4 µmol kg^{-1} increases in source-water DIC for 2050 based on an assumed continuation of an increasing trend in North Pacific surface water DIC [44]. This value was added to the 2011 DIC observations, and the Ω_{ar} values were calculated from those values and the 2011 TA. For both pre-industrial and future estimates of Ω_{ar}, we fit linear mixed effects models to predict values across depths based on CTD temperature and oxygen concentrations. From the predicted Ω_{ar} values, we estimated the percentage of the top 100 m of the water column that was undersaturated for comparison to present-day estimates. The linear mixed effects models of pre-industrial and 2050 Ω_{ar} fitted the data well (conditional r^2: 0.99 for both models) and exhibited low residual error (RMSE: 0.0013 and 0.0021, respectively).

3. Results and discussion

We collected and analysed samples originating from the National Oceanographic and Atmospheric Administration (NOAA) 2011 WCOA cruise, from northern Washington State to southern California from 11 August to 3 September 2011 (figure 1*a*). There is a large degree of variability of aragonite saturation state across regions within the CCE (figure 1*c*). Co-varying trends in temperature, salinity, oxygen and carbonate chemistry determine the depth of the aragonite saturation horizon ($\Omega_{ar} = 1$), represented as the depth of the undersaturated water (figure 1*a*) and the percentage of water undersaturated with respect to aragonite in the upper 100 m (figure 1*c*). To estimate the aragonite saturation state across the full water column, we used the fitted model to predict Ω_{ar} at all depths based on CTD temperature, salinity and oxygen sensor measurements, from which we calculated the vertically integrated percentage of undersaturation in the first 100 m based on the depth at which the aragonite saturation horizon occurred.

The coastal waters of the North American West Coast experience larger variability in carbonate chemistry as a result of several interacting processes, including seasonal upwelling, uptake of anthropogenic CO_2 and local respiratory

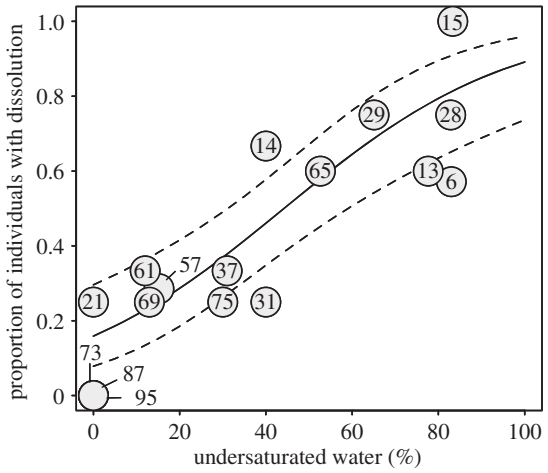

Figure 3. Proportion of pteropods with severe shell dissolution as a function of the percentage of the water column in the upper 100 m that is undersaturated with respect to aragonite. Station locations from figure 1*c* are shown with each symbol. The fitted regression line (solid line) and 95% prediction confidence band (dashed lines) are overlaid.

processes in water masses below the photic zone and nutrient overloads [45]. The seasonal upwelling along with bathymetric characteristics, such as wider shelves of the northern and central CCE, result in steep Ω_{ar} gradients across short depth intervals, though the gradients are much less pronounced over the narrow shelves in the southern CCE (figure 1*c*). Along the West Coast, low Ω_{ar} occurs in the late spring through to early autumn months, primarily from the seasonal upwelling of high CO_2 water from depths of about 80–200 m. By August, we observed, on average, 30% of the upper 100 m of the water column to be undersaturated, with a greater percentage of undersaturation occurring onshore relative to offshore stations (48% versus 13%, respectively; see Material and methods; figure 1*a*,*c* and table 1). The upwelled undersaturated waters reach their shallowest depths close to the coast [11,14] and undersaturated waters can exceed 50% of the upper 100 m of the water column (figure 1*c*). This general spatial pattern was evident throughout most of the CCE, except for onshore stations south of approximately 34° N that were generally supersaturated in the top 100 m and differed little from offshore stations (figure 1*c*; electronic supplementary material, figure S1). Electronic supplementary material, figure S1, shows the station-by-station profiles of Ω_{ar} with depth. In the northern and central onshore CCE stations (stations 6, 13, 14, 15, 28, 29, 57, 65, 87 and 95), the aragonite saturation horizon is located within the upper 20–50 m, while in the offshore stations (stations 21, 31 37, 57, 61 and 69), this occurs at about 80 m or deeper. Southern CCE offshore stations are similar to the northern and central offshore CCE stations in that the depth of undersaturation generally occurs below 80 m (stations 73 and 75), while in the southern onshore CCE stations, supersaturated conditions persist throughout the shallow water column (electronic supplementary material, figure S1), consistent with the Alin *et al.* [17] time-series results.

At the investigated stations, depth-integrated pteropod abundance and dissolution were determined. Pteropod populations show a considerable degree of regional variability in abundance, with depth-integrated abundances increasing from the southern part of the northern stations (see

Table 1. Mean percentage of the water column that was undersaturated with respect to aragonite and mean proportion of individuals with severe shell dissolution across all stations sampled during the 2011 West Coast survey under present-day conditions (2011) and assuming reductions (pre-industrial) and increases (2050) to *in situ* measurements of DIC. (The relationship estimated in figure 3 was used to estimate the probability of observing severe shell damage under *in situ* DIC concentrations measured in August 2011. Proportions were converted to percentages for clarity.)

	pre-industrial	2011	2050
percentage of undersaturated water (100 m)			
all stations	4	29	53
bottom depth < 200 m	8	48	72
bottom depth > 200 m	0	13	38
mean proportion of ind. with severe shell dissolution			
all stations	18	38	57
bottom depth < 200 m	21	53	71
bottom depth > 200 m	16	24	45

classifications of regions in Material and methods) to central onshore stations, where they can reach up to 14 000 ind m^{-2} (electronic supplementary material, table S1). Although the sampled stations were biased towards onshore stations, *L. helicina* was often present in high numbers in the offshore stations, as previously reported by Mackas & Galbraith [29].

In situ shell dissolution of *L. helicina* was the predominant feature observed in the live samples collected with a 333 µm mesh Bongo net at the peak of summer upwelling in August 2011. Shell dissolution was examined and demonstrated on preserved specimens using SEM after initial steps of dehydration and chemical drying. We observed shell dissolution at 14 out of 17 sites, i.e. 82% of all the investigated stations sampled along the CCE. The signatures of dissolution ranged from increased porosity and upper crystalline layer erosion (Type I) to severe types of dissolution affecting lower crystalline layers (Type II and Type III; see Material and methods). The latter dissolution types were considered severe as shell integrity was compromised and a fragile shell is more prone to damage (figure 2*a*).

Shell dissolution of *L. helicina* closely corresponded to carbonate chemistry conditions. We observed a strong positive relationship between the proportion of pteropods with severe dissolution and the percentage of undersaturated habitat in the top 100 m of the water column (log likelihood ratio test: $L = 23.1$, d.f. $= 1$, $p < 0.001$; figure 3). The fitted model (original response scale) took the form

$$y = \frac{e^{3.67(\pm 0.82)x - 1.66 \pm 0.40}}{1 + e^{3.67(\pm 0.82)x - 1.66 \pm 0.40}}, \quad (3.1)$$

where y is the proportion of individuals with severe shell dissolution, and x is the percentage of undersaturated waters in the top 100 m.

At stations where none of the top 100 m of the water column was undersaturated, almost no evidence of severe

dissolution was present (with the exception of station 21 where undersaturation started at 111 m). By contrast, higher percentages of water column undersaturation corresponded to an increase in the proportion of individuals with severe dissolution (figure 3), making this habitat less favourable for pteropods as it increases the tendency of their shell dissolution. Consequently, with further shoaling of the depth of undersaturation in the upper 100 m, pteropod vertical habitat suitability declines. Comparing the stations between offshore and onshore, we found 53% of onshore individuals and 24% of offshore individuals on average to have severe dissolution (table 1). *Limacina helicina* from onshore regions showed dissolution that was evenly spread over the entire surface of shells (figure 2*a*), while in offshore regions only the first whorl (protoconch) showed evidence of dissolution (figure 2*b*). This suggests that less corrosive offshore conditions only affected pteropods during early stages, while prolonged exposure to more severe undersaturated conditions in onshore regions resulted in dissolution covering the whole shell.

We used equation (3.1) to predict the proportion of individuals with severe shell dissolution under various proportions of undersaturated ($\Omega_{ar} < 1$) conditions, corresponding to the pre-industrial era and the years 2011 and 2050 across all stations in the survey, always referring to the conditions during the peak of the upwelling season in summer. For pre-industrial conditions, we assumed that the source-water DIC responded to air–sea CO_2 differences following Harris *et al.* [14], and subtracted 53 $\mu mol\ kg^{-1}$ from our year 2011 *in situ* DIC measurements. For the year 2050, the calculated 46 $\mu mol\ kg^{-1}$ increase in source-water DIC was based on an assumed continuation of an increasing trend in DIC in north Pacific surface water [44], which is consistent with the recent modelling results for this region [12,13].

Our estimates suggest a naturally occurring baseline of severe shell dissolution in approximately 20% of pteropod individuals in the CCE during the upwelling season under pre-industrial conditions. However, relative to pre-industrial CO_2 concentrations, the modern volume of undersaturated waters in the top 100 m of the water column has increased over sixfold along the CCE (figure 1*b*,*c* and table 1). Increased occurrence of undersaturated waters in 2011 is thus thought to correspond to higher severe shell dissolution relative to pre-industrial conditions, especially in the onshore regions of the CCE during the upwelling season. Onshore, 53% of pteropod individuals on average were affected by severe shell dissolution in August 2011; more than double the proportion calculated for the pre-industrial era (table 1). With the projected increase in anthropogenic CO_2 uptake by 2050 (see sensitivity study in Material and methods), we estimate that 72% of the top 100 m water column in onshore stations will be undersaturated. Our undersaturation-dissolution model suggests that progressive shoaling of the aragonite undersaturation horizon may result in 70% of individuals being affected by severe shell dissolution in 2050, or about a tripling of severe damage relative to the pre-industrial era throughout most of the coastal region (table 1).

Significant increases in vertical and spatial extent of conditions favouring pteropod shell dissolution are expected to make this habitat potentially unsuitable for pteropods. Although pteropods have been exposed to high CO_2 from seasonally persistent upwelling through evolution, we have not found any evidence of resilience to counteract the scale of dissolution observed currently. While dissolution in juvenile bivalves has been a significant factor for increased mortality [46], the link between undersaturation and dissolution-driven mortality in pteropods has not been directly confirmed. However, with the occurrence of high CO_2, increased dissolution combined with increased frailty [30–32,47] might compromise shell integrity to the extent where indirect effects of bacterial infection and acid–base balance would induce increased acute mortality [46]. The first bottleneck would primarily affect veligers and larvae, life stages where complete shell dissolution in the larvae can occur within two weeks upon exposure to undersaturation [48]. The lack of shell would lessen an individual's defence against predators, and the shell also plays an essential role in feeding, buoyancy control and pH regulation [49]. The shell is of particular importance later during the reproductive stage, when sperm are exchanged between individuals and need to be stored before fertilizing an egg [21], thus shell compromised by dissolution may hinder reproductive success.

Besides mechanistic explanations for dissolution-driven mortality, higher energy expenditure can come at a cost to the individual's energy budget, although this is also dependent on food availability and life stage [32,50]. Undersaturated conditions are known to elicit repair-calcification and changes in metabolic processes [51–53], with potentially long-term implications for growth, fecundity and fitness [54]. Evidence suggests that exceeding an individual's energy budget can change a pteropod's swimming behaviour, reduce their wing beat frequency and cause increased mortality owing to combined exposure to lower pH and salinity [55].

Therefore, the recent observed decline in *L. helicina* populations on the continental shelf of Vancouver Island [29], where we demonstrated high occurrence of severe shell dissolution, calls for more in-depth characterization of possible dissolution-related mortality [46]. Given the multitude of biological processes at important pteropod life stages that are potentially affected by increased shell dissolution, we suggest that dissolution provides an insight as a potential causal pathway for the observed pteropod decline. On the other hand, no population decline has been detected in the southern CCE [56], where our data indicate that extensive dissolution is lacking and reflect predominantly supersaturated conditions in comparison with the northern CCE, which is not specific only for this cruise survey period.

Biogeochemically, increased dissolution will reduce the ballasting effect of settling particles [57] and downward carbon fluxes [58] but increase TA in the upper water column [7]. By 2050, tripling in the costal regions of pteropod shell dissolution is expected to drive twice as much $CaCO_3$ dissolution, with potentially significant increases in TA within the upper water column. Use of pteropods as a sentinel species can prove to be indispensable for understanding future changes in the ocean carbon chemistry.

The decline of suitable habitat and demonstrable dissolution of biogenic carbonates as a response to the changes in the CCE is expected to have large and profound implications for the long-term biological and biogeochemical effects of CO_2 in the coastal waters of the Pacific northwest [12,13,20,59]. Dissolution impacts observed along the CCE are much more extensive spatially than previously reported for the Southern Ocean pteropods [31] and represent a baseline for future observations, where pteropod shell dissolution observations could have direct implications for understanding broader scale OA effects.

4. Conclusion

The highly productive CCE region provides an environment where *L. helicina* can occasionally reach high abundances [26], both offshore [29] and onshore. Prevalence of juveniles indicate coastal regions to also be their reproductive habitats (electronic supplementary material, table S1). This makes CCE a core habitat for sustainability of pteropod population, reflecting their importance in food webs as well as the regional biogeochemical carbonate cycle in the coastal waters of the CCE. However, these new results are among the first clearly indicating a direction towards declining habitat suitability for pteropods in the natural environment of the CCE owing to OA. This study demonstrates a strong positive relationship between the proportion of pteropods affected by severe dissolution and the percentage of undersaturated water in the upper 100 m of the water column. Our estimates suggest that the incidence of severe shell dissolution has already more than doubled relative to pre-industrial conditions and could increase to as much as 70% by 2050 along the northern and central onshore CCE. While pteropod populations might still thrive in offshore regions in the near future, continuous reduction of habitat availability in the onshore shelf regions will put pteropods at risk, with strong implications for their sustainability.

Acknowledgements. We would like to thank Jennifer Fisher and Cynthia Peacock for collecting samples during the cruise, as well as the officers and crew of the R/V *Wecoma*. Our thanks also go to Dana Greeley and Sandra Bigley for their help with the manuscript figures and editing.

Funding statement. This research was supported by the NOAA Ocean Acidification Program and the Pacific Marine Environmental Laboratory.

References

1. Sabine CL *et al*. 2004 The oceanic sink for anthropogenic CO_2. *Science* **305**, 367–371. (doi:10.1126/science.1097403)
2. Canadell JG *et al*. 2007 Contributions to accelerating atmospheric CO_2 growth from economic activity, carbon intensity, and efficiency of natural sinks. *Proc. Natl Acad. Sci. USA* **104**, 18 866–18 870. (doi:10.1073/pnas.0702737104)
3. Feely RA *et al*. 2013 Global ocean carbon cycle, in *State of the Climate in 2012*, Global Oceans. *Bull. Am. Meteorol. Soc.* **94**, S72–S75.
4. Feely RA, Doney SC, Cooley SR. 2009 Ocean acidification: present conditions and future changes in a high-CO_2 world. *Oceanography* **22**, 36–47. (doi:10.5670/oceanog.2009.95)
5. Doney SC, Fabry VJ, Feely RA, Kleypas JA. 2009 Ocean acidification: the other CO_2 problem. *Annu. Rev. Mar. Sci.* **1**, 169–192. (doi:10.1146/annurev.marine.010908.163834)
6. Hönisch B *et al*. 2012 The geological record of ocean acidification. *Science* **335**, 1058–1063. (doi:10.1126/science.1208277)
7. Feely RA *et al*. 2004 Impact of anthropogenic CO_2 on the $CaCO_3$ system in the oceans. *Science* **305**, 362–366. (doi:10.1126/science.1097329)
8. Orr JC *et al*. 2005 Anthropogenic ocean acidification over the twenty-first century and its impact on calcifying organisms. *Nature* **437**, 681–686. (doi:10.1038/nature04095)
9. Steinacher M, Joos F, Frolicher TL, Plattner G-K, Doney SC. 2009 Imminent ocean acidification in the Arctic projected with the NCAR global coupled carbon cycle-climate model. *Biogeosciences* **6**, 515–533. (doi:10.5194/bg-6-515-2009)
10. McNeil BI, Matear RJ. 2008 Southern ocean acidification: a tipping point at 450-ppm atmospheric CO_2. *Proc. Natl Acad. Sci. USA* **105**, 18 860–18 864. (doi:10.1073/pnas.0806318105)
11. Feely RA, Sabine CL, Hernández-Ayón JM, Ianson D, Hales B. 2008 Evidence for upwelling of corrosive 'acidified' water onto the continental shelf. *Science* **320**, 1490–1492. (doi:10.1126/science.1155676)
12. Hauri C *et al*. 2013 Spatiotemporal variability and long-term trends of ocean acidification in the California Current System. *Biogeosciences* **10**, 193–216. (doi:10.5194/bg-10-193-2013)
13. Gruber N *et al*. 2012 Rapid progression of ocean acidification in the California Current System. *Science* **337**, 220–223. (doi:10.1126/science.1216773)
14. Harris KE, DeGrandpre MD, Hales B. 2013 Aragonite saturation state dynamics in a coastal upwelling zone. *Geophys. Res. Lett.* **40**, 2720–2725. (doi:10.1002/grl.50460)
15. Juranek LW *et al*. 2009 A novel method for determination of aragonite saturation state on the continental shelf of central Oregon using multi-parameter relationships with hydrographic data. *Geophys. Res. Lett.* **36**, L24601. (doi:10.1029/2009GL040778)
16. Evans W, Hales B, Strutton PG. 2011 Seasonal cycle of surface ocean pCO_2 on the Oregon shelf. *J. Geophys. Res.* **116**, C05012. (doi:10.1029/2010JC006625)
17. Alin SR *et al*. 2012 Robust empirical relationships for estimating the carbonate system in the southern California Current System and application to CalCOFI hydrographic cruise data (2005–2011). *J. Geophys. Res.* **117**, C05033. (doi:10.1029/2011JC007511)
18. Fabry VJ, Seibel BA, Feely RA, Orr JC. 2008 Impacts of ocean acidification on marine fauna and ecosystem processes. *Ices J. Mar. Sci.* **65**, 414–432. (doi:10.1093/icesjms/fsn048)
19. Kroeker KJ *et al*. 2013 Impacts of ocean acidification on marine organisms: quantifying sensitivities and interaction with warming. *Global Change Biol.* **19**, 1884–1896. (doi:10.1111/gcb.12179)
20. Barton A, Hales B, Waldbusser GG, Langdon C, Feely RA. 2012 The Pacific oyster, *Crassostrea gigas*, shows negative correlation to naturally elevated carbon dioxide levels: Implications for near-term ocean acidification effects. *Limnol. Oceanogr.* **57**, 698–710. (doi:10.4319/lo.2012.57.3.0698)
21. Lalli CM, Gilmer RW. 1989 *Pelagic snails: the biology of holoplanktonic gastropod mollusks*. Stanford, CA: Stanford University Press.
22. Bednaršek N, Možina J, Vogt M, O'Brien C, Tarling GA. 2012 The global distribution of pteropods and their contribution to carbonate and carbon biomass in the modern ocean. *Earth Syst. Sci. Data* **4**, 167–186. (doi:10.5194/essd-4-167-2012)
23. Accornero A, Manno C, Esposito F, Gambi MC. 2003 The vertical flux of particulate matter in the polynya of Terra Nova Bay. Part II. Biological components. *Antarctic Sci.* **15**, 175–188. (doi:10.1017/S0954102003001214)
24. Bathmann UV, Noji TT, von Bodungen B. 1991 Sedimentation of pteropods in the Norwegian Sea in autumn. *Deep Sea Res. Part A* **38**, 1341–1360. (doi:10.1016/0198-0149(91)90031-A)
25. Muller-Karger FE *et al*. 2005 The importance of continental margins in the global carbon cycle. *Geophys. Res. Lett.* **32**, L01602. (doi:10.1029/2004GL021346)
26. McGowan JA. 1967 *Distributional atlas of pelagic molluscs in the California Current region*. CalCOFI Atlas no. 6. La Jolla, CA: Scripps Institution of Oceanography.
27. Armstrong JL *et al*. 2005 Distribution, size, and interannual, seasonal and diel food habits of northern Gulf of Alaska juvenile pink salmon, *Oncorhynchus gorbuscha*. *Deep Sea Res. Part II* **52**, 247–265. (doi:10.1016/j.dsr2.2004.09.019)
28. Mackas DL, Galbraith MD. 2001 Zooplankton distribution and dynamics in a North Pacific eddy of coastal origin. 1. Transport and loss of continental margin species. *Jpn J. Oceanogr.* **58**, 725–738. (doi:10.1023/A:1022802625242)
29. Mackas DL, Galbraith MD. 2012 Pteropod time-series from the NE Pacific. *Ices J. Mar. Sci.* **69**, 448–459. (doi:10.1093/icesjms/fsr163)

30. Bednaršek N *et al*. 2012 Description and quantification of pteropod shell dissolution: a sensitive bioindicator of ocean acidification. *Glob. Change Biol.* **18**, 2378–2388. (doi:10.1111/j.1365-2486.2012.02668.x)
31. Bednaršek N *et al*. 2012 Extensive dissolution of live pteropods in the Southern Ocean. *Nat. Geosci.* **5**, 881–885. (doi:10.1038/ngeo1635)
32. Lischka S, Riebesell U. 2012 Synergistic effects of ocean acidification and warming on overwintering pteropods in the Arctic. *Glob. Change Biol.* **18**, 3517–3528. (doi:10.1111/gcb.12020)
33. Dickson AG, Afgan JD, Anderson GC. 2003 Reference materials for oceanic CO_2 analysis: a method for the certification of total alkalinity. *Mar. Chem.* **80**, 185–197. (doi:10.1016/S0304-4203(02)00133-0)
34. Dickson AG, Sabine CL, Christian JR. (eds) 2007 Guide to best practices for ocean CO_2 measurements. PICES Special Publication 3, IOCCP Report No 8. Sidney, BC: North Pacific Marine Science Organization.
35. Lewis E, Wallace DWR. 1998 Program developed for CO_2 system calculations. Technical Report ORNL/CDIAC-105. Carbon Dioxide Information Analysis Center, Oak Ridge National Laboratory, US Department of Energy, Oak Ridge, TN, USA.
36. Lueker TJ, Dickson AG, Keeling CD. 2000 Ocean pCO_2 calculated from dissolved inorganic carbon. *Mar. Chem.* **70**, 105–119. (doi:10.1016/S0304-4203(00)00022-0)
37. Mucci A. 1983 The solubility of calcite and aragonite in seawater at various salinities, temperatures, and one atmosphere total pressure. *Am. J. Sci.* **283**, 781–799. (doi:10.2475/ajs.283.7.780)
38. Millero FJ. 1995 Thermodynamics of the carbon dioxide system in the oceans. *Geochim. Cosmochim. Acta* **59**, 661–677. (doi:10.1016/0016-7037(94)00354-O)
39. Willette TM *et al*. 2001 Ecological processes influencing mortality of juvenile pink salmon (*Oncorhynchus gorbuscha*) in Prince William Sound, Alaska. *Fish. Oceanogr.* **10**, 14–41. (doi:10.1046/j.1054-6006.2001.00043.x)
40. Nakagawa S, Schielzeth H. 2013 A general and simple method for obtaining R^2 from generalized linear mixed-effects models. *Methods Ecol. Evol.* **4**, 133–142. (doi:10.1111/j.2041-210x.2012.00261.x)
41. R Development Core Team. 2008 *R: a language and environment for statistical computing*. Vienna, Austria: R Foundation for Statistical Computing.
42. Dorman CE, Winant CD. 1995 Buoy observation of the atmosphere along the west coast of the United States, 1981–1990. *J. Geophys. Res.* **100**, 16 029–16 044. (doi:10.1029/95JC00964)
43. Kutner M, Nachtsheim C, Neter J, Li W. 2004 *Applied linear statistical models*. New York, NY: McGraw-Hill/Irwin.
44. Dore JE, Lukas R, Sadler DW, Karl DM. 2003 Climate-driven changes to the atmospheric CO_2 sink in the subtropical North Pacific Ocean. *Nature* **424**, 754–757. (doi:10.1038/nature01885)
45. Feely RA *et al*. 2012 Decadal changes in the aragonite and calcite saturation state of the Pacific Ocean. *Glob. Biogeochem. Cycles* **26**, GB3001. (doi:10.1029/2011GB004157)
46. Green MA, Waldbusser GG, Reilly SL, Emerson K, O'Donnell S. 2009 Death by dissolution: sediment saturation state as a mortality factor for juvenile bivalves. *Limnol. Oceanogr.* **54**, 1037–1047. (doi:10.4319/lo.2009.54.4.1037)
47. Comeau S, Gorsky G, Jeffree R, Teyssié JL, Gattuso J-P. 2009 Impact of ocean acidification on a key Arctic pelagic mollusc (*Limacina helicina*). *Biogeosciences* **6**, 1877–1882. (doi:10.5194/bg-6-1877-2009)
48. Comeau S, Gorsky G, Alliouane S, Gattuso J-P. 2010 Larvae of the pteropod *Cavolinia inflexa* exposed to aragonite undersaturation are viable but shell-less. *Mar. Biol.* **157**, 2341–2345. (doi:10.1007/s00227-010-1493-6)
49. Simkiss K, Wilbur KM. 1989 *Biomineralization: cell biology and mineral deposition*. San Diego, CA: Academic Press.
50. Thomsen J, Casties I, Pansch C, Körtzinger A, Meltzner F. 2013 Food availability outweighs ocean acidification effects in juvenile *Mytilus edulis*: laboratory and field experiments. *Glob. Change Biol.* **19**, 1017–1027. (doi:10.1111/gcb.12109)
51. Seibel BA, Maas AE, Dierssen HM. 2012 Energetic plasticity underlies a variable response to ocean acidification in the pteropod, *Limacina helicina antarctica*. *PLoS ONE* **7**, e30464. (doi:10.1371/journal.pone.0030464)
52. Comeau S, Jeffree R, Teyssie JL, Gattuso J-P. 2010 Response of the Arctic pteropod *Limacina helicina* to projected future environmental conditions. *PLoS ONE* **5**, e11362. (doi:10.1371/journal.pone.0011362)
53. Lischka S, Büdenbender J, Boxhammer T, Riebesell U. 2011 Impact of ocean acidification and elevated temperatures on early juveniles of the polar shelled pteropod *Limacina helicina*: mortality, shell degradation, and shell growth. *Biogeosciences* **8**, 919–932. (doi:10.5194/bg-8-919-2011)
54. Wood HL, Spicer JI, Widdicombe S. 2008 Ocean acidification may increase calcification rates, but at a cost. *Proc. R. Soc. B* **275**, 1767–1773. (doi:10.1098/rspb.2008.0343)
55. Manno C, Morata N, Primicerio R. 2012 *Limacina retroversa's* response to combined effects of ocean acidification and sea water freshening. *Estuar. Coast. Shelf Sci.* **113**, 163–171. (doi:10.1016/j.ecss.2012.07.019)
56. Ohman MD, Lavaniegos BE, Townsend AW. 2009 Multi-decadal variations in calcareous holozooplankton in the California Current System: thecosome pteropods, heteropods, and foraminifera. *Geophys. Res. Lett.* **36**, L18608. (doi:10.1029/2009GL039901)
57. Klaas C, Archer DE. 2002 Association of sinking organic matter with various types of mineral ballast in the deep sea: implications for the rain ratio. *Global Biogeochem. Cycles* **16**, 63-1–63-14. (doi:10.1029/2001GB001765)
58. Betzer PR *et al*. 1984 The oceanic carbonate system: a reassessment of biogenic controls. *Science* **226**, 1074–1077. (doi:10.1126/science.226.4678.1074)
59. Waldbusser GG *et al*. 2013 A developmental and energetic basis linking larval oyster shell formation to acidification sensitivity. *Geophys. Res. Lett.* **40**, 2171–2176. (doi:10.1002/grl.50449)

nature climate change

ARTICLES

PUBLISHED ONLINE: 15 DECEMBER 2014 | DOI: 10.1038/NCLIMATE2479

Saturation-state sensitivity of marine bivalve larvae to ocean acidification

George G. Waldbusser[1]*, Burke Hales[1], Chris J. Langdon[2], Brian A. Haley[1], Paul Schrader[2], Elizabeth L. Brunner[1], Matthew W. Gray[2], Cale A. Miller[3] and Iria Gimenez[1]

Ocean acidification results in co-varying inorganic carbon system variables. Of these, an explicit focus on pH and organismal acid–base regulation has failed to distinguish the mechanism of failure in highly sensitive bivalve larvae. With unique chemical manipulations of seawater we show definitively that larval shell development and growth are dependent on seawater saturation state, and not on carbon dioxide partial pressure or pH. Although other physiological processes are affected by pH, mineral saturation state thresholds will be crossed decades to centuries ahead of pH thresholds owing to nonlinear changes in the carbonate system variables as carbon dioxide is added. Our findings were repeatable for two species of bivalve larvae could resolve discrepancies in experimental results, are consistent with a previous model of ocean acidification impacts due to rapid calcification in bivalve larvae, and suggest a fundamental ocean acidification bottleneck at early life-history for some marine keystone species.

Ocean acidification (OA) is described as an imbalance between the acidic influence of rapidly accelerating anthropogenic CO_2 emissions and the slow buffering response due to weathering of continental rock and carbonate marine sediment, causing increased acidity of marine waters[1,2]. The release of CO_2 from fossil fuel emissions and cement production, and decreasing uptake efficiency of CO_2 by land and sea has resulted in the fastest increase in p_{CO_2} (partial pressure of carbon dioxide) in the past 800,000 years[3]. Conversely the natural mechanisms that buffer acidic perturbations from increasing p_{CO_2} occur over timescales of hundreds of thousands to millions of years[1,2]. Modern anthropogenic changes in the open ocean have tightly coupled aqueous p_{CO_2}, pH and mineral solubility responses, but it was not always thus. Previous instances of elevated p_{CO_2} in the geologic record, such as the Cretaceous, seem to coincide with significantly elevated alkalinity[4], and were fairly benign with respect to OA, with elevated p_{CO_2} not indicative of low pH or mineral corrosivity. Throughout the geologic record and in many coastal habitats the marine carbonate system decouples, resulting in changes in pH, p_{CO_2} and saturation state that do not follow the co-variance assumed for modern open-ocean average surface waters[5].

Effects of ocean acidification on a suite of marine organisms have been the subject of significant recent work. Although many experimental results have shown equivocal impacts when taken in composite, the process of calcification has mostly exhibited negative sensitivity to OA (ref. 6). Physiological processes that may experience OA sensitivity occur across all taxa in nearly all natural waters; however, persistent calcified structures can elevate species that precipitate calcium carbonate to keystone status in marine waters. Bivalves, which provide a number of critical ecosystem services, have been noted as particularly sensitive to OA (refs 7–10). Some experiments have even found OA impacts at present-day, compared with pre-industrial, p_{CO_2} levels[11]. Marine bivalves seem to be sensitive to OA owing to the limited degree to which they regulate the ionic balance and pH of their haemolymph (blood)[12–15], and acute sensitivities at specific, short-lived, life-history stages that may result in carryover effects later in life[16–20]. Bivalve larvae are particularly sensitive to OA during the hours- to days-long bottleneck when initial shell (called prodissoconch I or PDI) is formed during embryogenesis[17]. Before PDI shell formation, larvae lack robust feeding and swimming appendages and must rely almost exclusively on maternal energy from eggs; and during calcification of PDI the calcification surfaces are in greater contact with ambient seawater than during following shell stages[17]. Failure of larvae to complete shell formation before exhausting maternal energy reserves leads to eventual mortality, as seen in well-documented oyster hatchery failures[18]. So far, the prevailing physiological mechanism identified for OA effects on organisms has been in their ability to regulate internal acid–base status; however, short-term exposure impacts and carryover effects documented in bivalve larvae[18–21] and greater exposure of PDI calcification to ambient seawater[17] points to another mechanism for the early larval sensitivity not captured by regulation of internal acid–base chemistry[22].

In most natural waters the dissolved inorganic carbon (DIC) system controls both pH and the thermodynamic mineral solubility (saturation state), but in different ways. pH is determined by the ratio of dissolved concentrations of CO_2 to carbonate ions, whereas saturation state is predominantly controlled by absolute carbonate ion concentration. The potential that organisms will respond differently to pH (ratio) or mineral saturation state (abundance), highlights how the decoupling of carbonate system variables in coastal zones[5] or geologic time[1,2] provides a formidable challenge in interpreting and predicting organismal responses to OA. The seemingly simple experimental perturbation of CO_2 bubbling results in the

[1]College of Earth, Ocean, and Atmospheric Sciences, Oregon State University, 104 COAS Admin. Bldg., Corvallis, Oregon 97331, USA. [2]Coastal Oregon Marine Experimental Station and Department of Fisheries and Wildlife, Hatfield Marine Science Center, Oregon State University, 2030 SE Marine Science Drive, Newport, Oregon 97365, USA. [3]Department of Fisheries and Wildlife, Oregon State University, 104 Nash Hall Oregon State University, Corvallis, Oregon 97331, USA. *e-mail: waldbuss@coas.oregonstate.edu

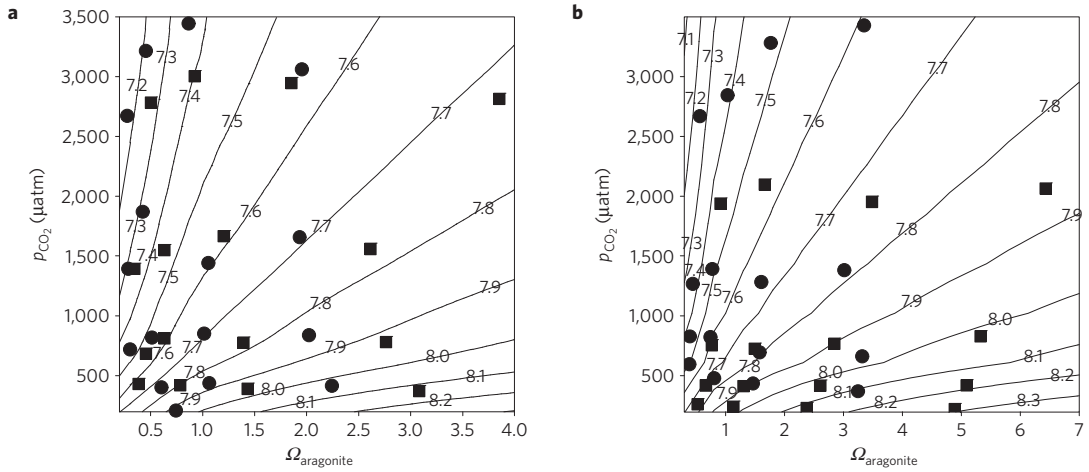

Figure 1 | Carbonate chemistry values for the 16 experimental treatments for each of the four experiments grouped by species, plotted against p_{CO_2} and saturation state, with isopleths of pH plotted in p_{CO_2}/saturation state space. a, Values for the two experiments on *Mytilus galloprovincialis*. **b**, Values for the two experiments on *Crassostrea gigas*. Circle and square symbols represent chemistry for the first and second experiments, respectively.

equilibrium redistribution of the acid–base species with pH, saturation state, p_{CO_2} and dissolved inorganic carbon (DIC) all changing simultaneously. The co-variance of carbonate parameters leaves interpretation of experimental responses unclear if organismal sensitivity to each parameter is physiologically distinct, particularly if the importance of each process varies across ontology (for example, respiration, shell formation, feeding rate). The underlying mechanisms of organismal sensitivity to OA may therefore not be constrainable without special experimental techniques.

We conducted series of experiments in which we applied a unique chemical manipulation approach to decouple the carbonate system parameter-covariance and evaluated larval growth and development of two bivalve species: the Pacific oyster, *Crassostrea gigas*, and the Mediterranean mussel, *Mytilus galloprovincialis*. Through simultaneous manipulation of DIC and alkalinity, we generated a 4×4 factorial design with aragonite saturation state (Ω_{ar}) and p_{CO_2}. Our experimental design separated Ω_{ar} and p_{CO_2} effects on larval responses; and responses to pH were evaluated by examining responses to pH within a p_{CO_2} and Ω_{ar} treatment level. Using this approach, we assessed which carbonate system parameter is most important to early larval shell development and growth: pH, p_{CO_2}, or Ω_{ar}.

Results

We successfully decoupled pH, p_{CO_2}, and Ω_{ar} experimentally to find Ω_{ar} as the primary variable affecting early larval shell development and growth in these two bivalve species. Below we describe why this direct sensitivity to Ω_{ar} demands a refinement of our current model of OA responses of calcifying organisms, and the environmental relevance of these results.

Chemistry manipulations. We simultaneously altered abundance and ratio of DIC and alkalinity to provide three orthogonal experimental axes in pH, p_{CO_2} and saturation state of the calcium carbonate mineral aragonite (Ω_{ar}) (Fig. 1 and Supplementary Table 1). The sensitivity of these parameters to DIC:alkalinity means that there is some variability within treatment suites, but that variability was far less than the differences among treatments. We were able to replicate treatment conditions via DIC and alkalinity, as evidenced by the concordance between expected versus measured values (Supplementary Fig. 1). At the termination of the 48 h incubation period we found p_{CO_2} generally increased by approximately 10–30% relative to initial conditions. The greatest p_{CO_2} increases were in treatments with the poorest larval development, probably due to elevated microbial respiration associated with larval mortality in these treatments.

Prodissoconch I shell development. The dominant effect of Ω_{ar} on proportion normal shell development (PNS) is immediately apparent in Fig. 2. The Ω_{ar} effect is clear for both species, with highly significant effects (Mussels $F_{3,15} = 105.53$, $p < 0.0001$, Oysters $F_{3,15} = 76.79$, $p < 0.0001$, Supplementary Table 2); Ω_{ar} explained 88% and 86% of the variance in proportion normal for the mussels and oysters, respectively. p_{CO_2} and the interaction between Ω_{ar} and p_{CO_2} were not significant (Supplementary Table 2). Experiment number was found to be statistically significant, but only explained 3% and 6% of the variance for the mussels and oysters, respectively (Supplementary Table 2). We fit a three-parameter logistic equation to the untransformed treatment means of PNS (Fig. 2) to determine the functional response of both species to saturation state. The fit was found to be highly significant for mussel ($F_{2,29} = 223.01$, $R^2 = 0.93$, $p < 0.0001$) and oyster larvae ($F_{2,29} = 72.61$, $R^2 = 0.83$, $p < 0.0001$).

Our results unequivocally show that saturation state is the primary carbonate system variable of importance for normal shell development for these two bivalve species; we will, however, further explore possible pH effects in our experiments, given its importance to physiological acidosis and the historical emphasis on pH in OA experiments. Because pH covaries with the primary factors in the analysis of variance (ANOVA), and a slight visual pattern is apparent (Fig. 2), we ran a series of regression analyses of PNS versus pH, within a saturation state treatment. Although we found some statistically significant slopes, generally in the low-Ω_{ar} treatments (Supplementary Table 3), the effect is equivocal and its magnitude markedly smaller than the Ω_{ar} effect. The largest effect we found was in the lowest saturation state treatment for oysters, with a 0.1 increase in PNS per 0.1 pH units from pH 7.27 to 7.51. Other significant slopes were less than half of this, 0.02 to 0.04 PNS per 0.1 pH unit within a Ω_{ar} treatment. The pH effect across the entire experimental range seen in Fig. 2 is, therefore, primarily an artefact of pH covariance with Ω_{ar}. Furthermore, at pH values of <7.6 and <7.4 in the mussel and oyster experiments respectively, we still see excellent PNS of >80% if Ω_{ar} is high. We therefore reiterate that Ω_{ar} is the primary carbonate system variable driving successful shell development of early larvae in these two species.

Shell growth. Even among larvae that seemed to develop normal shell morphology, Ω_{ar} was still the primary factor influencing growth (Fig. 3 and Supplementary Table 4). Ω_{ar} had statistically

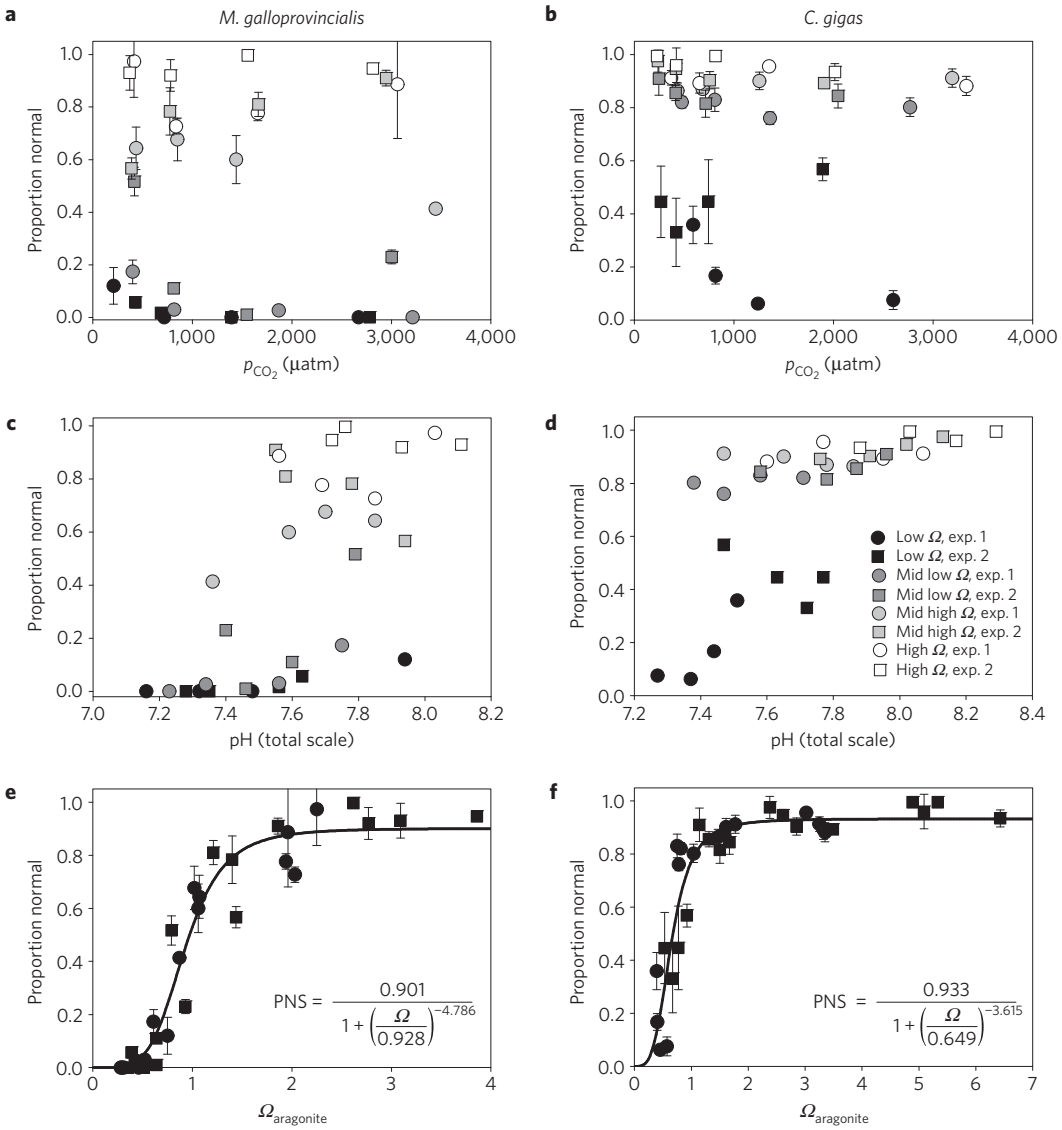

Figure 2 | Shell development in response to carbonate system variables for both species. Mean proportion of normal shell development (PNS) of D-hinge larvae for mussel (**a**,**c**,**e**) and oyster (**b**,**d**,**f**) experiments in response to p_{CO_2} (**a**,**b**), pH (**c**,**d**), and saturation state (**e**,**f**). Circles and squares are the first and second experiments, respectively. Fills from black to white represent increasing saturation state. Symbols are the mean values of the three replicate containers, each of which was sub-sampled three times (approximately 100–200 larvae per sub-sample). Error bars are standard deviations of mean replicate values per treatment. Error bars were excluded from the pH plot to allow easier visual interpretation.

significant effects on the mussels ($F_{2,24} = 707.63$, $p < 0.0001$) and oysters ($F_{3,9} = 219.29$, $p < 0.0001$), explaining 93% and 81% of the variance in normal shell length for each species. The lack of normally developed mussel larvae in the low-Ω_{ar} treatments prevented size estimates. Shell length decreased by nearly 25% and 10% with decreasing Ω_{ar} across our experimental range in the mussel and oyster larvae, respectively. p_{CO_2} had minor significant positive effects on mussel ($F_{3,24} = 5.83$, $p = 0.0039$) and oyster larvae shell length ($F_{3,32} = 27.64$, $p < 0.0001$), (Fig. 3 and Supplementary Table 4), explaining 1% and 10% of the variance in shell length. The interaction between Ω_{ar} and p_{CO_2} was also statistically significant for both species, but only explaining 5% of the shell growth variance for both species (Supplementary Table 4 and Fig. 2). The positive response to p_{CO_2} may seem counter-intuitive at first; however, within an Ω_{ar} treatment level, DIC concentrations are proportional to p_{CO_2} (Supplementary Table 1) and inversely proportional to pH. We did not evaluate pH effects on shell growth, given what seems to be a positive response to decreasing pH, and thus a probable response to increasing DIC concentrations (Fig. 3). We will argue below that shell growth is responding to DIC within an Ω_{ar} treatment level, but saturation state is again the dominant parameter affecting shell growth of these early larvae. Shell length continues to increase with increasing saturation state even at the highest values in our treatments, $\Omega_{ar} \sim 4$ and $\Omega_{ar} \sim 6.5$ for the mussel and oyster larvae, respectively. We therefore fitted a power function to the response of shell length to saturation state (Fig. 3). The fit of the model for both species was highly significant: mussel larvae ($F_{2,10} = 81.36$, $R^2 = 0.89$, $p < 0.0001$) and oyster larvae ($F_{2,14} = 103.22$, $R^2 = 0.88$, $p < 0.0001$).

Why saturation state matters to bivalve larvae

Our results initially seems contradictory to the physiological basis for understanding ocean acidification impacts on organisms; particularly the overarching role of seawater pH, acid–base regulation, and extracellular acidosis in marine organisms[12,13,22–24]. Specifically, we found that seawater pH seems to have little

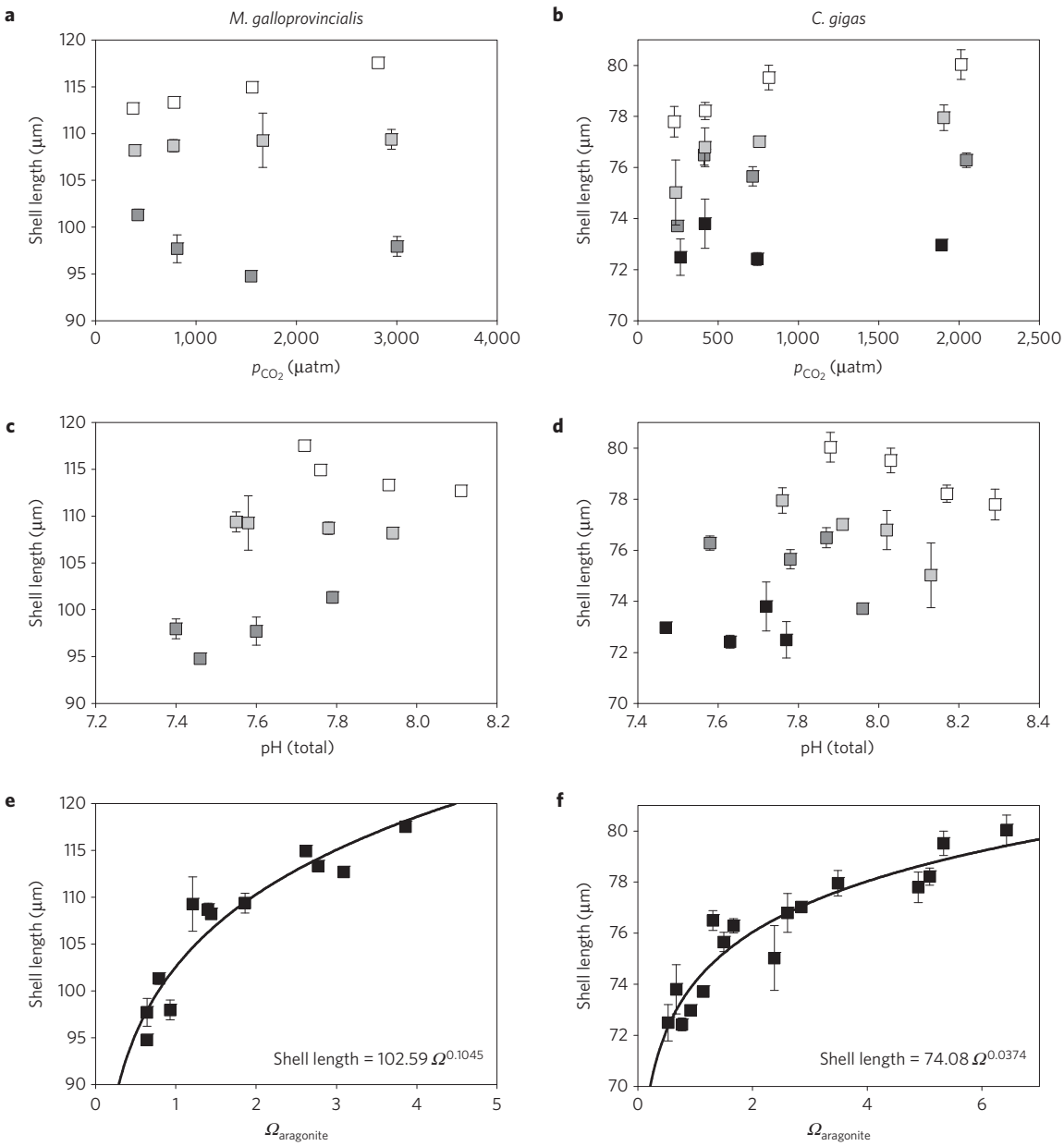

Figure 3 | Shell growth in response to carbonate system variables for both species. Mean shell length of normally developed larvae in response to p_{CO_2} (**a**,**b**), pH (**c**,**d**), and saturation state (**e**,**f**). The grey scale symbols are the same as used previously. Means and standard deviations are of replicate containers per treatment, as above. We lack larvae from low-Ω treatments owing to very poor development in the mussel experiments. The total number of normal larvae measured for shell length was 3,132 and 7,106 for the mussel and oyster experiments, respectively. Control shell lengths were 108.44 ± 2.57 µm and 78.78 ± 2.06 µm for the mussels and oysters, respectively.

to no measurable effect on early larval shell development and growth, except for the case where pH and Ω_{ar} are both very low (Figs 2 and 3). At these low levels, seawater pH probably becomes very important (particularly to bivalves, which show limited ability to regulate extracellular pH), as eukaryote intracellular pH typically ranges from 7.0 to 7.4 (ref. 25) and additional energy is needed to maintain physiochemical gradients crucial for passive and active cross-membrane ion transport[26] if extracellular pH approaches these values. Some species seem to be able to mitigate acidosis via bicarbonate accumulation; however, ability to do so is variable across taxa, and bicarbonate accumulation often requires several days to months[14,15,22]. During the transient (days) early larval stage it is unlikely that bivalve larvae have the time or physiological capacity to compensate for acidosis[22], with their limited energy budget and the embryological development taking place during this time period. Therefore, although seawater pH effects on organismal acidosis may also be at work during this early larval stage, we have experimentally shown that any pH effect is overwhelmed by the impact of saturation state during initial shell formation. The likelihood of organisms experiencing such low pH conditions without coinciding low-Ω conditions is also very unlikely (Fig. 1 and Supplementary Table 1). Therefore, the conclusions from this study do not contradict the importance of pH on marine bivalve larvae, but rather highlight the overwhelming significance of saturation state at this critical bottleneck for bivalve larvae.

We have previously argued[17] that during PDI shell formation in bivalve larvae the rapid rate of calcification (as shown in Fig. 4)

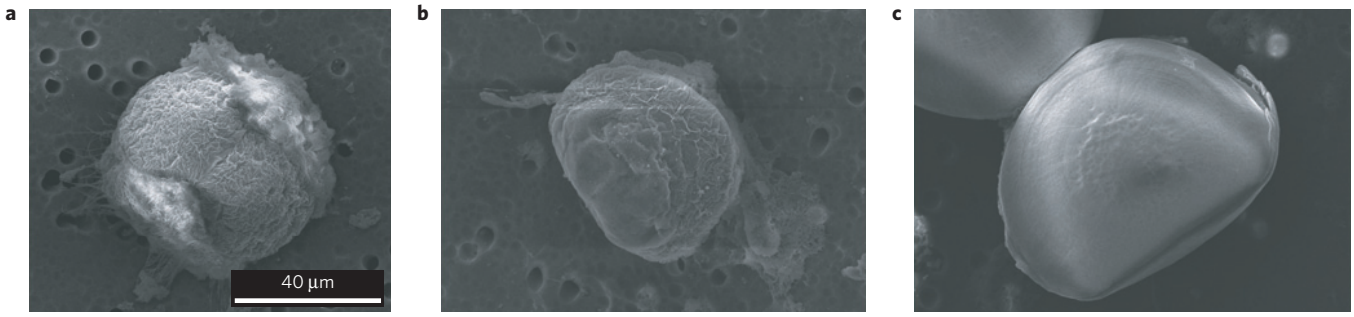

Figure 4 | Development of prodissoconch I shell in Pacific oyster larvae. Representative scanning electron micrographs of Pacific oyster larvae at 10 h (**a**), 14 h (**b**) and 16 h (**c**) post fertilization. Over the course of development from **a** to **c** the formation of the periostracum (wrinkled) is seen, followed by increasing amounts of hardening by calcium carbonate until, by 16 h, the prodissoconch I shell is formed and fully calcified and the periostracum is taut over the shell surface. Larvae were reared at 23 °C and salinity = 34, under atmospheric CO_2.

and increased exposure of crystal nucleation sites to seawater puts an important kinetic-energetic constraint on the larvae; thereby mandating an Ω_{ar} sensitivity (as in equation (1)). The classical representation of the calcification rate (r) following the standard empirical formulation is:

$$r = k(\Omega - 1) \quad (1)$$

The apparently predetermined amount of rapid calcification required to form the PDI shell and begin feeding requires the biocalcification rate constant (k) to be several orders of magnitude higher than inorganic precipitation[17]. This constraint also demands a rapidly accelerating biocalcification rate constant (k) as Ω approaches saturation (and thus $\Omega - 1$ approaches 0) to maintain the calcification rate necessary to complete the PDI shell without depleting maternal energy reserves. However, the logical extension of this argument that biocalcification is not possible below saturation is erroneous. Bivalve larvae clearly precipitate mineral when ambient conditions are undersaturated and must, therefore, create some level of supersaturation at crystal nucleation sites which are semi-exposed to the external environment. We suggest that larvae are both elevating Ω at the site of calcification and elevating k through physico-chemical changes at the organic–inorganic nucleation interface[17]. That is, the dependency on seawater Ω_{ar} in our experimental results (Fig. 2) supports the importance of this kinetic-energetic constraint; increasing seawater supersaturation lowers the energetic cost of shell building, increasing the scope for growth, as seen in the shell length response to Ω_{ar} (Fig. 3).

A curious pattern is observed in our shell length data. Figure 3 seems to indicate a minor (positive/negative) effect of p_{CO_2}/pH on shell growth. Within a Ω_{ar} treatment group, our experimental manipulations result in decreasing DIC with increasing pH (Supplementary Table 1). Previous studies in corals have suggested that total DIC (driven mostly by bicarbonate ion) is an important factor for calcification[27–29]. Alternatively, the ratio of DIC/[H^+] (which is in fact a proxy for carbonate ion and thus saturation state) due to the proton flux model[30] may be the controlling parameter for coral calcification. Given the differences in calcification mechanisms and shell morphology between larval prodissoconch I (PDI) and prodissoconch II (PDII; ref. 31), we postulate that any minor, secondary DIC effect may be acting during the latter PDII shell formation. In fact, a previous study[32] found that larval *C. gigas* shell size was not affected by elevated CO_2 at day one (PDI), but by three days post fertilization shells were significantly smaller in the high-CO_2 treatment (PDII). Larvae from our two-day experiments had already begun PDII shell formation; therefore, it seems plausible the impacts of Ω_{ar} (negative) and DIC (slightly positive) on shell length were acting on PDII. Conversely, the range of Ω_{ar} tested in this previous study[32] was roughly between 1 and 2 ($p_{CO_2} \sim 400$–$1{,}100\,\mu atm$), and may have resulted in undetectable PDI size differences over the smaller experimental range (highlighting the value of experimental treatments extending beyond open-ocean projections). The minor secondary positive effect of DIC (at supersaturation) seems consistent with previous studies. However, saturation state was still the dominant factor impacting the shell length of normally developed larvae. Although we cannot determine whether compensatory growth is possible if saturation state is improved later in larval life, the carry-over effects found on US West Coast oyster larvae indicate there is limited capacity to recover from OA exposure during the sensitive early larval stages[18–20].

Even the most critical of OA meta-analyses on organismal responses[6] note calcification as being the 'most sensitive' of responses to ocean acidification. For developing embryos of bivalve larvae, calcification is a process that determines whether larvae will survive or perish; without the development and calcification of the PDI shell, larvae probably lack a functional velum to support swimming and feeding owing to lack of muscular–skeletal attachment. Without an effective feeding mechanism, larvae will eventually exhaust endogenous energy reserves[17]. Although larvae may be able to support basal metabolism using dissolved organic matter (DOM; ref. 33), the velum is also responsible for DOM uptake[34]. Our results show that seawater Ω_{ar} directly affects shell development and growth, and this effect is not an indirect pH impact on internal acid–base status. Without shell development, or if it is too energetically expensive, there seems little opportunity for larvae to overcome OA during this early stage[17]. A previous study[35] suggested carbonate ion concentration, rather than saturation state, matters to larvae. Calcium addition was used to manipulate mineral solubility without a control for excess calcium at already supersaturated mineral solubility[35]. The addition of calcium to roughly twice that of seawater, as in ref. 35, at $\Omega_{ar} \sim 2.0$ (increasing Ω_{ar} to ~3.64) resulted in very poor shell development (PNS = 0.39 ± 0.8) and much smaller normal larvae (S.L. = 68.63 ± 3.22 µm) in *C. gigas*. This result is not surprising, given the role of calcium in cellular ion transport and immune response, and the lack of osmo-regulation in marine bivalves[14,36]. This is a minor point ultimately, because carbonate ion concentration usually controls saturation state in marine waters. Importantly, however, the carbonate in marine bivalve shell is derived from all forms of DIC, including respiratory carbon (ref. 17 and references therein); increased seawater saturation state seems to make the kinetics of shell formation less energetically expensive.

Environmental context

In marine waters, the increase of p_{CO_2} decreases saturation state and pH, but their declines approach potential thresholds differentially.

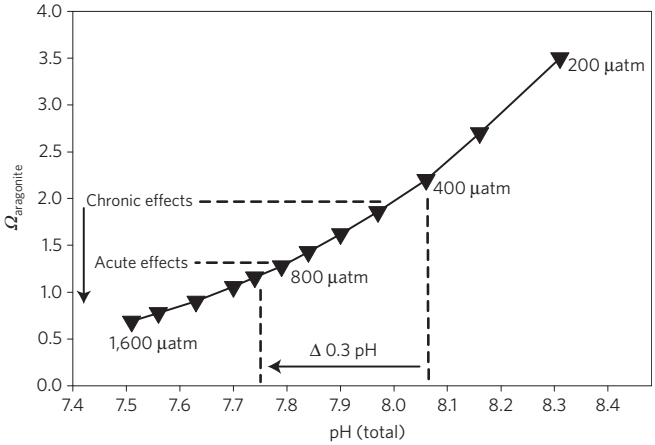

Figure 5 | Calculated response of pH and aragonite saturation state to increasing p_{CO_2} from 200 to 1,600 µatm (triangles) at typical upwelling conditions along the Oregon coast. Conditions calculated for total alkalinity = 2,300 µmol kg^{-1}, temperature = 13 °C, and salinity = 33. Symbols are values of p_{CO_2}. Chronic and acute effects due to saturation state decreases from experiments have been noted for bivalve larvae. The Δ 0.3 pH was previously noted as significant to many physiological processes in molluscs[8].

We have plotted the change in Ω_{ar} and pH as p_{CO_2} increases for typical upwelling conditions in Oregon's coastal waters (Fig. 5). We found acute responses of bivalve larvae begin to manifest at saturation states (Ω_{ar}) of ~1.2–1.5 (Figs 2 and 3). Other studies have documented sub-lethal chronic exposure effects in Pacific oyster larvae (~2.0: refs 18,35), Olympia oyster larvae (~1.4, ref. 19), Eastern oyster larvae (~1.9, ref. 11), and California mussel larvae (~1.8, ref. 37). Although far from an exhaustive list of experimental studies, placing these Ω_{ar} values in context of the present conditions in the California Current ecosystem illustrate two key points. First, there is limited remaining capacity for Oregon's coastal waters to absorb more CO_2 before sub-lethal Ω_{ar} thresholds are crossed for bivalve larvae. Increasing atmospheric CO_2 pushes saturation state across these thresholds more frequently and with greater magnitude in the California Current[38,39]. Second, these saturation state thresholds will be crossed long before recently documented pH changes found to be physiologically important in molluscs[8] (often >0.3 pH units). If transient conditions during spawning are unfavourable for bivalve larvae, in hatcheries or in the wild, then these impacts would result in diminished larval supply and recruitment to adult populations.

Larval supply and recruitment are vital to maintaining many benthic marine invertebrate populations[40]. Survival to metamorphosis requires normal development and rapid growth to limit larval predation[40]. Larger larval size indicates greater scope for growth and the repletion of energy stores needed to complete metamorphosis[41]; energy stores that are diminished under acidification stress[11]. Recruitment to adult populations can be highly variable year to year and often related to regional climatology[42,43]. The coastal zones where many ecologically and economically important marine calcifiers are found will not experience acidification gradually, as seen in the oligotrophic open ocean, but rather as increases in frequency, duration and magnitude of events that are unfavourable for specific life-history stages[5,38,44]. Our experimental work has shown that successful larval development and growth during rapid shell formation is dependent on seawater saturation state in temporal windows lasting two days or less (Fig. 4); thus providing increasing evidence for a mechanism by which transient, moderate acidification impacts[18] nearly resulted in collapse of the Pacific Northwest oyster industry[45]. These impacts occur on timescales relevant to changes already observed in coastal zones[5,18,46], regardless of future changes or direct cause, and thus decreases in saturation state can limit recruitment to present bivalve populations. Our experimental approach and findings shed new light on the organismal responses to OA, while indicating the importance of monitoring the complete carbonate chemistry system; without which successfully linking biological responses and chemical observations will prove exceptionally challenging.

Methods

Water collection and stripping dissolved inorganic carbon. For each experiment, 1 µm filtered seawater was collected from Yaquina Bay. The alkalinity was reduced by the addition of trace metal grade HCl in near-alkalinity equivalence, followed by bubbling with ambient air for 48 h to strip (DIC) as CO_2. The acidified, stripped seawater was then 0.22 µm-filtered, pasteurized, and stored at 2–5 °C. Before treatment manipulation, the seawater was bubbled with 0.2 µm-filtered outside air until atmospheric conditions were achieved, then carbonate DIC and alkalinity values were determined for manipulations.

Experimental manipulation. A 4×4 factorial experimental design was developed to target 16 total treatment combinations of p_{CO_2} and Ω_{ar} (saturation state with respect to aragonite; Fig. 1 and Supplementary Table 1), with triplicate 500 ml biological oxygen demand (BOD) bottles per treatment. Two separate experiments were conducted with each species. DIC and alkalinity concentrations were calculated for each of the 16 target treatment combinations (p_{CO_2} and Ω_{ar}). Experimental treatments were created by gravimetric addition of mineral acids and bases to the decarbonated seawater in gas-impermeable bags customized with Luer lock fittings. Aliquots of a concentrated, ambient-p_{CO_2}, solution of Na_2CO_3 and and $NaHCO_3$ were added to adjust DIC to target treatment levels followed by 0.1N HCl to adjust alkalinity. Immediately following chemical manipulation, the bags with treatment water were stored without head-space at 2–5 °C for up to several weeks before spawning broodstock. Antibiotics were added to BOD bottles (2 ppm chloramphenicol and 10 ppm ampicillin), which we found to have no negative effects on larvae or carbonate chemistry in previous trials. Controls were included to evaluate experimental manipulations and incubation conditions by hatching eggs in open culture containers, as well as by using stored seawater collected before decarbonation and not subjected to the chemical manipulations described in this study.

Carbonate chemistry measurements. Carbonate chemistry samples were collected from the treatment water bags just before stocking larvae in BOD bottles, and also from each BOD bottle at the end of the incubation period. Carbonate chemistry samples were collected in 350 ml amber glass bottles with polyurethane-lined crimp-sealed metal caps and preserved by the addition of 30 µl of saturated $HgCl_2$. Analyses of p_{CO_2} and DIC were carried out following the procedure of Bandstra *et al.*[47], modified for discrete samples as in Hales and colleagues[48]. Gas and liquid standards that bracketed the experimental range (Supplementary Table 1) were employed to ensure accuracy.

Larval rearing. Broodstock for mussel (*Mytilus galloprovincialis*) and oyster (*Crassostrea gigas*) experiments were obtained from Carlsbad Aquafarm, or from selected stocks of the Molluscan Broodstock Program (MBP; ref. 49), Yaquina Bay, respectively. Broodstock spawning was stimulated by a rapid increase of 10 °C in ambient seawater temperature. Gametes were collected from at least two male and two female parents, and the eggs fertilized in ambient seawater. Developing embryos were added at a density of 10 larvae ml^{-1} to triplicate BOD bottles per treatment after visual verification of successful fertilization. Sealed BOD bottles were oriented on their side and incubated for 48 h at culture temperature (18 °C for mussels and 22 °C and 25 °C for oyster trials 1 and 2, respectively). Larvae from each BOD bottle were concentrated after a filtered chemistry sample was collected, sampled in triplicate, and preserved in 10% formalin buffered to ~8.1–8.2.

Larval shell development and size. Larvae were examined microscopically to determine the proportion of normally and abnormally developed D-hinge (prodissoconch I) larvae as well as larval shell lengths. Normally developed larvae were characterized by a straight hinge, smooth curvature along the edge of the valve, and the appearance of tissue within the translucent shells[50]. Digital images were used to determine the shell length (longest axis perpendicular to the hinge) of normally developed larvae only. Images were analysed using ImageJ (V1.42).

Data analyses. Proportion normal data were scaled to the unmanipulated, seawater control for each experiment by dividing treatment values by control values. We used a two-way ANOVA, with p_{CO_2} and Ω_{ar} as the primary factors,

with experiment number as a blocking factor. Proportion normal data were square-root arcsine transformed. Assumptions of normality and homoscedasticity were checked, and any violations were managed as noted. Initial data analyses found unequal variance across treatment groups in the transformed proportion normal data, and mean values per treatment were used to improve heteroscedasticity as well as blocking by experiment. To evaluate pH effects on shell development we ran a series of regression analyses of transformed proportion normal regressed on pH, within each Ω_{ar} treatment and experiment. We then used a Bonferroni correction for multiple tests of significance to reduce Type 1 error. Analyses were conducted with the SAS software suite (v9.3). Nonlinear least-squares regression in Sigma-Plot (v12.5) was used to fit functional responses of development (logistic) and shell length (power).

Received 25 June 2014; accepted 25 November 2014; published online 15 December 2014

References

1. Archer, D., Kheshgi, H. & Maier-Reimer, E. Multiple timescales for neutralization of fossil fuel CO_2. *Geophys. Res. Lett.* **24,** 405–408 (1997).
2. Hönisch, B. *et al.* The geological record of ocean acidification. *Science* **335,** 1058–1063 (2012).
3. Luethi, D. *et al.* High-resolution carbon dioxide concentration record 650,000–800,000 years before present. *Nature* **453,** 379–382 (2008).
4. Zeebe, R. E. Seawater pH and isotopic paleotemperatures of Cretaceous oceans. *Palaeogeogr. Palaeoclimatol. Palaeoecol.* **170,** 49–57 (2001).
5. Waldbusser, G. G. & Salisbury, J. E. Ocean acidification in the coastal zone from an organism's perspective: Multiple system parameters, frequency domains, and habitats. *Ann. Rev. Mar. Sci.* **6,** 221–247 (2014).
6. Hendriks, I. E., Duarte, C. M. & Alvarez, M. Vulnerability of marine biodiversity to ocean acidification: A meta-analysis. *Estuar. Coast. Shelf Sci.* **86,** 157–164 (2010).
7. Parker, L. M. *et al.* Predicting the response of molluscs to the impact of ocean acidification. *Biology* **2,** 651–692 (2013).
8. Gazeau, F. *et al.* Impacts of ocean acidification on marine shelled molluscs. *Mar. Biol.* **160,** 2207–2245 (2013).
9. Wittmann, A. C. & Poertner, H. O. Sensitivities of extant animal taxa to ocean acidification. *Nature Clim. Change* **3,** 995–1001 (2013).
10. Kroeker, K. J. *et al.* Impacts of ocean acidification on marine organisms: Quantifying sensitivities and interaction with warming. *Glob. Change Biol.* **19,** 1884–1896 (2013).
11. Talmage, S. C. & Gobler, C. J. Effects of past, present, and future ocean carbon dioxide concentrations on the growth and survival of larval shellfish. *Proc. Natl Acad. Sci. USA* **107,** 17246–17251 (2010).
12. Thomsen, J. *et al.* Calcifying invertebrates succeed in a naturally CO_2-rich coastal habitat but are threatened by high levels of future acidification. *Biogeosciences* **7,** 3879–3891 (2010).
13. Melzner, F. *et al.* Food supply and seawater pCO(2) impact calcification and internal shell dissolution in the blue mussel *Mytilus edulis*. *PLoS ONE* **6,** e24223 (2011).
14. Shumway, S. E. Effect of salinity fluctuation on the osmotic pressure and Na^+, Ca^{2+}, and Mg^{2+} ion concentrations in the hemolymph of bivalve molluscs. *Mar. Biol.* **41,** 153–177 (1977).
15. Heinemann, A. *et al.* Conditions of *Mytilus edulis* extracellular body fluids and shell composition in a pH-treatment experiment: Acid–base status, trace elements and delta B-11. *Geochem. Geophys. Geosyst.* **13,** Q01005 (2012).
16. Waldbusser, G. G., Bergschneider, H. & Green, M. A. Size-dependent pH effect on calcification in post-larval hard clam Mercenaria spp. *Mar. Ecol. Prog. Ser.* **417,** 171–182 (2010).
17. Waldbusser, G. G. *et al.* A developmental and energetic basis linking larval oyster shell formation to acidification sensitivity. *Geophys. Res. Lett.* **40,** 2171–2176 (2013).
18. Barton, A., Hales, B., Waldbusser, G. G., Langdon, C. & Feely, R. A. The Pacific oyster, *Crassostrea gigas* shows negative correlation to naturally elevated carbon dioxide levels: Implications for near-term ocean acidification effects. *Limnol. Oceanogr.* **57,** 698–710 (2012).
19. Hettinger, A. *et al.* Persistent carry-over effects of planktonic exposure to ocean acidification in the Olympia oyster. *Ecology* **93,** 2758–2768 (2012).
20. Hettinger, A. *et al.* Larval carry-over effects from ocean acidification persist in the natural environment. *Glob. Change Biol.* **19,** 3317–3326 (2013).
21. Gobler, C. J. & Talmage, S. C. Short and long term consequences of larval stage exposure to constantly and ephemerally elevated carbon dioxide for marine bivalve populations. *Biogeosciences* **10,** 2241–2253 (2013).
22. Melzner, F. *et al.* Physiological basis for high CO_2 tolerance in marine ectothermic animals: Pre-adaptation through lifestyle and ontogeny? *Biogeosciences* **6,** 2313–2331 (2009).
23. Michaelidis, B., Ouzounis, C., Paleras, A. & Pörtner, H. O. Effects of long-term moderate hypercapnia on acid–base balance and growth rate in marine mussels *Mytilus galloprovincialis*. *Mar. Ecol. Prog. Ser.* **293,** 109–118 (2005).
24. Pörtner, H. O. Ecosystem effects of ocean acidification in times of ocean warming: A physiologist's view. *Mar. Ecol. Prog. Ser.* **373,** 203–217 (2008).
25. Madshus, I. H. Regulation of intracellular Ph in eukaryotic cells. *Biochem. J.* **250,** 1–8 (1988).
26. Walsh, P. J. & Milligan, C. L. Coordination of metabolism and intracellular acid–base status—ionic regulation and metabolic consequences. *Can. J. Zool. Rev. Can. Zool.* **67,** 2994–3004 (1989).
27. Jury, C. P., Whitehead, R. F. & Szmant, A. M. Effects of variations in carbonate chemistry on the calcification rates of *Madracis auretenra* (= *Madracis mirabilis* sensu Wells 1973): Bicarbonate concentrations best predict calcification rates. *Glob. Change Biol.* **16,** 1632–1644 (2010).
28. Ries, J. B. A physicochemical framework for interpreting the biological calcification response to CO_2-induced ocean acidification. *Geochim. Cosmochim. Acta* **75,** 4053–4064 (2011).
29. Comeau, S., Carpenter, R. C. & Edmunds, P. J Coral reef calcifiers buffer their response to ocean acidification using both bicarbonate and carbonate. *Proc. R. Soc. B* **280,** 1–8 (2013).
30. Jokiel, P. L. Coral reef calcification: Carbonate, bicarbonate and proton flux under conditions of increasing ocean acidification. *Proc. R. Soc. B* **280,** 1–4 (2013).
31. Kniprath, E. Ontogeny of the molluscan shell field—a review. *Zool. Scr.* **10,** 61–79 (1981).
32. Timmins-Schiffman, E., O'Donnell, M. J., Friedman, C. S. & Roberts, S. B. Elevated pCO(2) causes developmental delay in early larval Pacific oysters, *Crassostrea gigas*. *Mar. Biol.* **160,** 1973–1982 (2013).
33. Moran, A. L. & Manahan, D. T. Physiological recovery from prolonged 'starvation' in larvae of the Pacific oyster *Crassostrea gigas*. *J. Exp. Mar. Biol. Ecol.* **306,** 17–36 (2004).
34. Manahan, D. T. & Crisp, D. J. Autoradiographic studies on the uptake of dissolved amino-acids from sea-water by bivalve larvae. *J. Mar. Biol. Assoc. UK* **63,** 673–682 (1983).
35. Gazeau, F. *et al.* Effect of carbonate chemistry alteration on the early embryonic development of the Pacific oyster (*Crassostrea gigas*). *PLoS ONE* **6,** 1–8 (2011).
36. Bibby, R., Widdicombe, S., Parry, H., Spicer, J. & Pipe, R. Effects of ocean acidification on the immune response of the blue mussel Mytilus edulis. *Aquat. Biol.* **2,** 67–74 (2008).
37. Gaylord, B. *et al.* Functional impacts of ocean acidification in an ecologically critical foundation species. *J. Exp. Biol.* **214,** 2586–2594 (2011).
38. Hauri, C., Gruber, N., McDonnell, A. M. P. & Vogt, M. The intensity, duration, and severity of low aragonite saturation state events on the California continental shelf. *Geophys. Res. Lett.* **40,** 3424–3428 (2013).
39. Harris, K. E., DeGrandpre, M. D. & Hales, B. Aragonite saturation state dynamics in a coastal upwelling zone. *Geophys. Res. Lett.* **40,** 2720–2725 (2013).
40. Rumrill, S. S. Natural mortality of marine invertebrate larvae. *Ophelia* **32,** 163–198 (1990).
41. Ben Kheder, R., Quere, C., Moal, J. & Robert, R. Effect of nutrition on *Crassostrea gigas* larval development and the evolution of physiological indices Part B: Effects of temporary food deprivation. *Aquaculture* **308,** 174–182 (2010).
42. Kimmel, D. G. & Newell, R. I. E. The influence of climate variation on Eastern oyster (*Crassostrea virginica*) juvenile abundance in Chesapeake Bay. *Limnol. Oceanogr.* **52,** 959–965 (2007).
43. Dumbauld, B. R., Kauffman, B. E., Trimble, A. C. & Ruesink, J. L. The Willapa Bay oyster reserves in Washington state: Fishery collapse, creating a sustainable replacement, and the potential for habitat conservation and restoration. *J. Shellfish Res.* **30,** 71–83 (2011).
44. Gruber, N. *et al.* Rapid progression of ocean acidification in the California current system. *Science* **337,** 220–223 (2012).
45. Feely, R. A., Klinger, T., Newton, J. A. & Chadsey, M. *Scientific Summary of Ocean Acidification in Washington State Marine Waters* NOAA OAR Special Report No. 3934 (NOAA-OAR 2012).
46. White, M. M., McCorkle, D. C., Mullineaux, L. S. & Cohen, A. L. Early exposure of Bay Scallops (*Argopecten irradians*) to high CO_2 causes a decrease in larval shell growth. *PLoS ONE* **8,** e61065 (2013).
47. Bandstra, L., Hales, B. & Takahashi, T. High-frequency measurements of total CO_2: Method development and first oceanographic observations. *Mar. Chem.* **100,** 24–38 (2006).
48. Hales, B., Takahashi, T. & Bandstra, L. Atmospheric CO_2 uptake by a coastal upwelling system. *Glob. Biogeochem. Cycles* **19,** GB1009 (2005).

49. Langdon, C. J., Evans, F., Jacobson, D. & Blouin, M. Yields of cultured Pacific oysters *Crassostrea gigas* Thunberg improved after one generation of selection. *Aquaculture* **220,** 227–244 (2003).
50. American Society for Testing and Materials *Standard Guide for Conducting Static Acute Toxicity Tests Starting with Embryos of Four Species of Saltwater Bivalve Molluscs* E724-98 (ASTM International, 2012).

Acknowledgements

This work was supported by the National Science Foundation OCE CRI-OA #1041267 to G.G.W., B.H., C.J.L. and B.A.H. The authors would like to thank H. Bergschneider, R. Mabardy, J. Sun, G. Hutchinson and T. Klein for their dedicated efforts on the experimental work, S. Smith for sampling and imaging developing embryos, and J. Jennings for assistance and student training on carbonate analyses. G.G.W. would like to specifically thank T. Sawyer in the OSU Electron Microscope Laboratory for guidance on imaging bivalve embryos. Comments from A. Hettinger and S. E. Kolesar improved an earlier version of this manuscript.

Author contributions

G.G.W., B.H., C.J.L. and B.A.H. conceived and planned the research. G.G.W. designed and supervised experiments. G.G.W. and B.H. analysed data. P.S. organized study components and P.S., M.W.G., E.L.B., I.G. and C.A.M. developed and carried out the experiments. M.W.G., E.L.B., I.G. and C.A.M. analysed organism and chemistry samples. All authors contributed to writing the manuscript.

Additional information

Supplementary information is available in the online version of the paper. Reprints and permissions information is available online at www.nature.com/reprints. Correspondence and requests for materials should be addressed to G.G.W.

Competing financial interests

The authors declare no competing financial interests.